

IRIS

**UNAVCO, Inc** →

# 2003 JOINT WORKSHOP

JUNE 18-22, TENAYA LODGE, YOSEMITE



## Wednesday, June 18

3:00pm – 9:00pm      Workshop Registration  
4:00pm – 9:00pm      Poster room available for set-up

Meeting Foyer  
Salon II

# Thursday, June 19

8:15 – 9:00	Continental Breakfast	Meeting Foyer	
9:00 – 9:15	Welcome & Workshop Overview	Salon I	
	<i>Susan Beck, University of Arizona</i>		
	<i>Meghan Miller, Central Washington University</i>		
	<i>Gary Pavlis, Indiana University</i>		
	<i>Paul Silver, Carnegie Institution of Washington</i>		
	<i>Rob van der Hilst, Utrecht University</i>		
9:15 – 10:00	State of the Consortia		
	<i>Geoffrey Blewitt, University of Nevada, Chair, UNAVCO Inc. Board</i>		
	<i>Goran Ekstrom, Harvard University, Chair, IRIS Board</i>		
	<i>William Prescott, UNAVCO, Inc., President</i>		
	<i>David Simpson, IRIS, President</i>		
10:00 – 10:50	Plenary Science Session I: “Plate Boundary Processes” <i>Chairs: William Holt, Gary Pavlis</i>	Salon I	
	<i>“Plate Boundary Processes Along the Cascadia Convergent Margin: Recoverable and Permanent Deformation” – Meghan Miller, Central Washington University</i>		
	<i>“Rifting Issues in the Gulf of California” – Harold Magistrale, San Diego State University</i>		
10:50 – 11:10	Break		
	<i>“Kinematics and Dynamics of the San Andreas Fault System” – Brad Hager, Massachusetts Institute of Technology</i>		
	<i>“Tectonics of North America’s Highest Mountain Range: The St. Elias of southern Alaska” – Terry Pavlis, University of New Orleans</i>		
	<i>“The Alaska-Aleutians Subduction System” – Geoff Abers, Boston University</i>		
12:30 – 2:00	Lunch	Lawn Area	
2:00 – 6:00	Program Forums		
	2:00 – 2:50	• UNAVCO Project Support – <i>B. Johns</i> • IRIS DMS – <i>T. Ahern</i>	Salon V&VI Counties
	3:00 – 3:50	• IRIS PASSCAL – <i>J. Fowler</i> • UNAVCO Network Operations – <i>M. Jackson</i>	Salon V&VI Counties
	4:00 – 4:50	• UNAVCO Data – <i>F. Boler</i> • IRIS E&O – <i>J. Taber</i>	Salon V&VI Counties
	5:00 – 5:50	• IRIS GSN – <i>R. Butler</i> • UNAVCO E&O – <i>C. Meertens</i>	Salon V&VI Counties
7:00 – 10:00	Dinner	Lawn Area	
	EarthScope Review and Celebration		
	<i>Steve Hickman, Mike Jackson, David Simpson, Bob Smith, Greg van der Vink, Jim Whitcomb</i>		

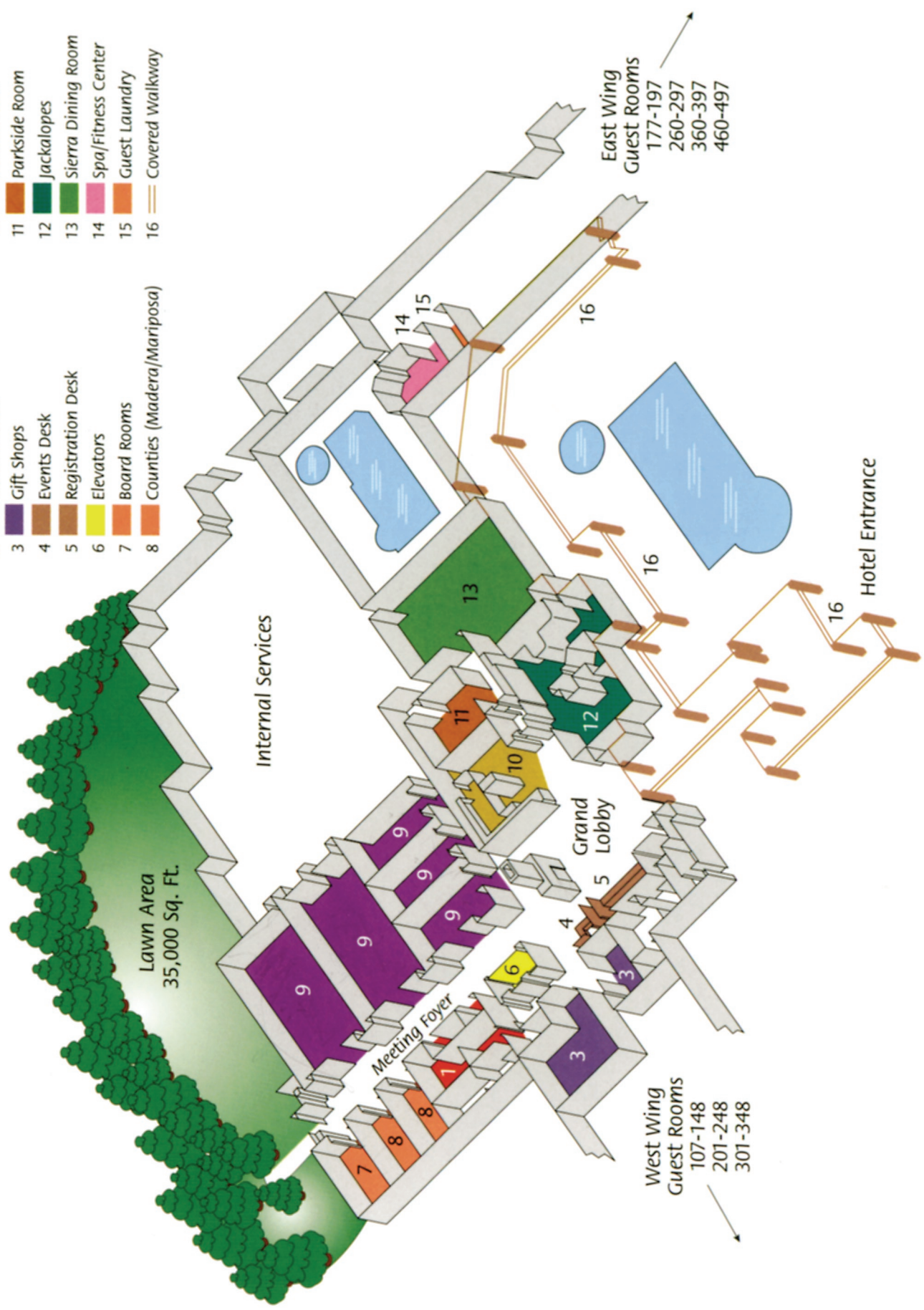
## Friday, June 20

8:15 – 9:00	Continental Breakfast	Meeting Foyer
9:00	Plenary Science Session II: “The Earthquake Problem” <i>Chairs: Paul Silver, Sue Beck</i>	Salon I
	<p><i>“Direct Observation of the San Andreas Fault at Seismogenic Depth: The SAFOD Project”</i> – Mark Zoback, Stanford University</p> <p><i>“The 2002 Denali Fault Earthquake: Insights from Geodesy and Seismology”</i> – Jeffrey Freymueller, University of Alaska, Fairbanks</p> <p><i>“Episodic Tremor and Slip (ETS) on the Cascadia Subduction Zone: The Chatter of Silent Slip”</i> – Herb Dragert and Garry Rogers, Geological Survey of Canada</p>	
10:15 – 10:30	Break	
	<p><i>“Temporal Variations of Seismogram Similarities: a new approach to the time-varying stress field”</i> – Fenglin Niu, Rice University and Paul Silver, Carnegie Institution of Washington</p> <p><i>“Geodetic Evidence of Slow Faulting During the 2001 Mw=8.4 Peru Earthquake Sequence”</i> – Timothy Melbourne, Central Washington University</p> <p><i>“Seismology with a Dense Seismic Network”</i> – Hiroo Kanamori, California Institute of Technology</p>	
12:00 – 1:30	Lunch	Lawn Area
1:30 – 4:50	Working Groups	
	<p>1:30 – 2:30</p> <ul style="list-style-type: none"> <li>• “Resolving Vertical Deformation with GPS” – Tom Herring, MIT</li> <li>• “Software Infrastructure for Seismology” – Colin Zelt, Rice University and Gary Pavlis, Indiana University</li> </ul> <p>2:40 – 3:40</p> <ul style="list-style-type: none"> <li>• “Stable North America Reference Frame” – Geoff Blewitt, University of Nevada, Reno</li> <li>• USArray Data Products – David James, Carnegie Institution</li> </ul> <p>3:50 – 4:50</p> <ul style="list-style-type: none"> <li>• EarthScope Data Management – Tim Ahern, IRIS, Fran Boler, UNAVCO</li> <li>• EarthScope Education and Outreach – Chuck Meertens, UNAVCO, John Taber, IRIS, Michelle Hall-Wallace, University of Arizona</li> </ul>	<p>Counties</p> <p>Salon V&amp;VI</p> <p>Salon V&amp;VI</p> <p>Counties</p> <p>Salon V&amp;VI</p> <p>Counties</p>
5:00 – 6:00	IRIS/SSA Distinguished Lecture Series, 2002/2003 Lecture <i>“The Discovery of the Earth: The Quest to Understand the Interior of Our Planet”</i> – Walter Mooney, U.S. Geological Survey	Salon I
6:00 – 7:30	Dinner w/ Jim Snyder, Historian, National Park Service	Lawn Area
7:30 – 9:30	UNAVCO Members Meeting	Salon V&VI
	Poster Session	Salon II

## Saturday, June 21

8:15 – 9:00	Continental Breakfast	Meeting Foyer
9:00 – 12:00	Plenary Science Session III: “Sampling across the Frequency Spectrum: Techniques Integration” <i>Chair: Meghan Miller</i>	Salon I
	<p>“Separating short-term (geodetic) and long-term (geodetic) effects in a subduction zone setting: some results from Costa Rica” – Tim Dixon, University of Miami</p> <p>“Comparing tidal, vertical GPS, and leveling records along the US Cascadia Margin” – Ray Weldon, Reed Burgette, and Noah Fay, University of Oregon, Eugene, and Meghan Miller, Central Washington University</p>	
10:15 – 10:30	Break	
	<p>“The Role of Aseismic Slip Along the San Andreas Fault System in Central California From GPS, InSAR and Seismology” – Roland Burgmann, University of California, Berkeley</p> <p>“Using 1 Hz GPS Data to Measure Permanent and Seismic Deformations Caused by the Denali Fault Earthquake” – Kristine Larson, University of Colorado, Boulder, Paul Bodin, University of Memphis, Joan Gomberg, USGS, Memphis, Herb Dragert, Geological Survey of Canada, and Andria Bilich, University of Colorado, Boulder</p> <p>“Tilt and broadband analysis of the February 1996 inflation episode of Kilauea, Hawaii” – Sharon Kedar, Jet Propulsion Laboratory, California Institute of Technology</p>	
12:00 – 1:30	Lunch	Lawn Area
1:30 – 4:30	<i>ad hoc</i> Meetings	
	<p>1:30 – 2:30</p> <ul style="list-style-type: none"> <li>• “Getting the most out of SAFOD: down-hole and near-field science and instrumentation needs” – Steve Hickman, William Ellsworth, USGS, Menlo Park</li> <li>• “Sharing Software in Geophysics” – Mike Bevis, University of Hawaii</li> </ul>	Salon V&VI Counties
	<p>2:30 – 3:30</p> <ul style="list-style-type: none"> <li>• “Theoretical Imaging Techniques for EarthScope” – Alan Levander, Rice University, Gary Pavlis, Indiana University</li> <li>• “Optimal Siting of Geodetic Instrumentation” – Paul Segall, Stanford University</li> <li>• “SAC and Beyond SAC” – Guust Nolet, Princeton University, Peter Goldstein, LLNL</li> </ul>	Salon V&VI Counties Salon I
	<p>3:30 – 4:30</p> <ul style="list-style-type: none"> <li>• “Intraplate Earthquakes: What we know and don’t know” – Sue Hough, USGS Pasadena, Paul Segall, Stanford</li> <li>• “US Educational Seismology Network: Next Steps” – Michael Hamburger, Indiana University</li> <li>• “PBO Design Standards: Antennas and Monuments” – Tom Herring, MIT, John Langbein, USGS</li> </ul>	Salon V&VI Counties Salon I
4:30 – 5:00	Field Trip Lectures	Salon V&VI
	“Crustal production and loss in continental magmatic arcs: Evidence from the Sierra Nevada, California” – Mihai Ducea, University of Arizona, Jason Saleeby, Caltech	
5:00 – 7:00	Dinner	Lawn Area

- 1 Business Center
- 2 Guest Phones
- 3 Gift Shops
- 4 Events Desk
- 5 Registration Desk
- 6 Elevators
- 7 Board Rooms
- 8 Counties (Madera/Mariposa)
- 9 Grand Ballroom
- 10 Parkside Deli
- 11 Parkside Room
- 12 Jackalopes
- 13 Sierra Dining Room
- 14 Spa/Fitness Center
- 15 Guest Laundry
- 16 Covered Walkway



West Wing  
Guest Rooms  
107-148  
201-248  
301-348

East Wing  
Guest Rooms  
177-197  
260-297  
360-397  
460-497

Lawn Area  
35,000 Sq. Ft.

Internal Services

Meeting Foyer

Grand Lobby

Hotel Entrance

# Joint Workshop

Tenaya Lodge, Yosemite

June 18-22, 2003

## Participants

### Geoffrey Abers

Earth Sciences Department  
Boston University  
685 Commonwealth Avenue  
Boston, MA 02215  
(617) 353-2616 (617) 353-3290  
abers@bu.edu

### Duncan Agnew

Scripps Inst Of Ocean/IGPP0225  
University of California, San Diego  
9500 Gilman Drive  
La Jolla, CA 92014-0225  
(858) 534-2590 (858) 534-5332  
dagnew@ucsd.edu

### Timothy K. Ahern

IRIS  
1408 NE 45th Street Suite 201  
Seattle, WA 98105  
(206) 547-0393 (206) 547-1093  
tim@iris.washington.edu

### Marcos Alvarez

PASSCAL Instrument Center  
New Mexico Tech  
100 East Road  
Socorro, NM 87801  
(505) 835-5070 (505) 835-5079  
alvarez@passcal.nmt.edu

### Charles J. Ammon

Department of Geosciences  
Penn State University  
440 Deike Building  
University Park, PA 16802  
(814) 865-2310 (814) 863-8750  
cammon@geosc.psu.edu

### Kent Anderson

US Geological Survey/Field Operations  
Albuquerque Seismological Lab  
801 University Blvd SE Suite 300  
Albuquerque, NM 87106-4345  
(505) 462-3204 (505) 462-3299  
kent@asl.cr.usgs.gov

### Greg Anderson

Western Earthquake Hazards Team  
US Geological Survey, Pasadena  
525 South Wilson Avenue  
Pasadena, CA 91106-3212  
(626) 583-6799 (626) 583-7827  
ganderson@usgs.gov

### Gene Arnn

UNAVCO  
3360 Mitchell Lane Suite C  
Boulder, CO 80301  
(720) 565-5984 (720) 565 5992  
arnn@unavco.org

### Richard Aster

Dept of Earth & Environmental Sciences  
New Mexico Tech  
801 Leroy Place  
Socorro, NM 87801  
(505) 835-5924 (505) 835-6436  
aster@ees.nmt.edu

### Shirley Baher

US Geological Survey  
645 Middlefield Road  
Menlo Park, CA 94025  
(650) 329-4878 (650) 329-5163  
sbaher@usgs.gov

### Calvin Barnes

Department Of Geosciences  
Texas Tech University  
Box 1050  
Lubbock, TX 79409-1053  
(806) 742-3106 (806) 742-0100  
cal.barnes@ttu.edu

### Mauricio Battaglia

Seismological Laboratory  
University of California, Berkeley  
215 McCone Hall  
Berkeley, CA 94720-4760  
(510) 642-8374  
battag@seismo.berkeley.edu

**Susan Beck**

Department Of Geosciences  
University Of Arizona  
Gould Simpson Building  
Tucson, AZ 85721  
(520) 621-4827 (520) 621-2672  
beck@geo.arizona.edu

**Rick Bennett**

Radio & Geoastronomy Division  
Harvard-Smithsonian Center for Astrophysics  
60 Garden Street MS 42  
Cambridge, MA 02138  
(617) 495-7453 (617) 495-7345  
rbennett@cfa.harvard.edu

**Mark Benthien**

Communication, Education & Outreach  
Southern California Earthquake Center  
3651 Trousdale Pkwy Suite 169  
Los Angeles, CA 90089  
(213) 740-0323 (213) 740-0011  
benthien@usc.edu

**Jonathan Berger**

Scripps Inst Of Ocean/IGPP0225  
University of California, San Diego  
9500 Gilman Drive  
La Jolla, CA 92093-0225  
(858) 534-2889 (858) 534-6354  
jberger@ucsd.edu

**Gregory Beroza**

Department Of Geophysics  
Stanford University  
Mitchell Bldg Panama Mall Room 397  
Stanford, CA 94305-2215  
(650) 723-4958 (650) 725-7344  
beroza@geo.stanford.edu

**Michael Bevis**

Pacific GPS Facility  
University of Hawaii  
1680 East West Rd HIGP (POST Ste 602)  
Honolulu, HI 96822  
(808) 956-7864 (808) 956-3188  
bevis@hawaii.edu

**Glenn Biasi**

Seismological Laboratory  
University Of Nevada, Reno  
Mail Stop 174  
Reno, NV 98557  
(775) 784-4576 (775) 784-4165  
glenn@seismo.unr.edu

**Susan Bilek**

Department of Geology  
University of Michigan  
2534 CC Little Bldg 425 E Univ. Ave  
Ann Arbor, MI 48109  
(734) 615-4076 (734) 763-4690  
sbilek@umich.edu

**Andria Bilich**

Aerospace Engineering Sciences  
University of Colorado, Boulder  
429 UCB  
Boulder, CO 8030-0429  
(303) 492-3489  
andria.bilich@colorado.edu

**Geoffrey Blewitt**

Nevada Bureau of Mines and Geology  
University of Nevada, Reno  
1664 N Virginia Street, Mail Stop 178  
Reno, NV 89557  
(775) 784-6691 (775) 784-1709  
gblewitt@unr.edu

**Yehuda Bock**

Scripps Inst Of Ocean/IGPP0225  
University of California, San Diego  
9500 Gilman Drive  
La Jolla, CA 92093-0225  
(858) 534-5292 (858) 534-9873  
ybock@ucsd.edu

**Paul Bodin**

Center for Earthquake Res & Information  
The University of Memphis  
3876 Central Avenue Suite 1  
Memphis, TN 38152-6590  
(901) 678-4845 (901) 678-4734  
bodin@ceri.memphis.edu

**Fran Boler**

Data Management & Archiving Group  
UNAVCO  
3340 Mitchell Lane  
Boulder, CO 80301  
(303) 497-8051 (303) 497-8028  
fboler@unavco.ucar.edu

**Harold Bolton**

Albuquerque Seismological Lab  
US Geological Survey  
801 University Blvd SE Suite 300  
Albuquerque, NM 87106-4345  
(505) 462-3211 (505) 462-3299  
bolton@asl.cr.usgs.gov

**Naomi Boness**

Geophysics Department  
Stanford University  
Mitchell Building  
Stanford, CA 94305  
(650) 723-3464  
nboness@stanford.edu

**Tom Brocher**

Western Earthquake Hazards Team  
US Geological Survey  
345 Middlefield Road MS 977  
Menlo Park, CA 94030  
(650) 329-4737 (650) 329-5163  
brocher@usgs.gov

**Roland Burgmann**

Dept of Earth & Planetary Science  
University of California, Berkeley  
307 McCone Hall  
Berkeley, CA 94720  
(510) 643-9545 (510) 643-9980  
burgmann@seismo.berkeley.edu

**Rhett Butler**

IRIS  
1200 New York Avenue NW Suite 800  
Washington, DC 20005  
(202) 682-2220 (202) 682-2444  
rhett@iris.edu

**Rufus Catchings**

US Geological Survey, Menlo Park  
345 Middlefield Road MS 977  
Menlo Park, CA 94025  
(650) 329-4749 (650) 329-5163  
catching@usgs.gov

**C. David Chadwell**

Scripps Institution of Oceanography  
University of California, San Diego  
9500 Gilman Drive  
La Jolla, CA 92093-0205  
(858) 534-2663 (858) 534-6849  
cchawell@ucsd.edu

**J. Andres Chavarria**

Dept of Earth & Ocean Sciences  
Duke University  
Old Chemistry Building 90229  
Durham, NC 27708  
(919) 681-4427 (919) 684-5833  
jac4@duke.edu

**Miranda Chin**

Geosciences Research Division  
National Geodetic Survey  
SSMC 4 Sta 9114, 1315 East West Hwy  
Silver Spring, MD 20910  
(301) 713-2840 (301) 713-4475  
miranda.chin@noaa.gov

**Douglas Christensen**

Geophysical Institute  
University Of Alaska, Fairbanks  
903 Koyukuk Drive PO Box 757320  
Fairbanks, AK 99775-7320  
(907) 474-7426 (907) 474-5618  
doug@giseis.alaska.edu

**Michael Cline**

Spatial Reference System Division  
National Geodetic Survey, NOAA  
SSMC 3,N/NGS22 Sta 9123,  
1315 East West Hwy  
Silver Spring, MD 20910  
(301) 713-3202 ext 146 (301) 713-4324  
mike.cline@noaa.gov

**Geoff Clitheroe**

Institute of Geological & Nuclear Sciences  
41A Bell Road  
Lower Hutt, Wellington, 6315  
NEW ZEALAND  
+ 5704702 + 5704616  
g.clitheroe@gns.cri.nz

**John Collins**

Dept Of Geology & Geophysics  
Woods Hole Oceanographic Institution  
MS 24 Clark South  
Woods Hole, MA 02543-1541  
(508) 289-2733 (508) 457-2150  
jcollins@whoi.edu

**Vernon Cormier**

Dept Of Geology & Geophysics  
University Of Connecticut U-2045  
345 Mansfield Road Room 207  
Storrs, CT 06269-2045  
(860) 486-1391 (860) 486-1383  
cormier@geol.uconn.edu

**Michael Craymer**

Geodetic Survey Division  
Natural Resources Canada  
615 Booth Street  
Ottawa, Ontario K1A 0E9  
CANADA  
(613) 947-1829 (613) 992-6628  
craymer@nrcan.gc.ca

**Philip Crotwell**

Dept Of Geological Sciences  
University Of South Carolina  
701 Sumter Street EWSC-617  
Columbia, SC 29208  
(803) 777-0955 (803) 777-0906  
crotwell@seis.sc.edu

**Colleen Dalton**

Dept of Earth & Planetary Sciences  
Harvard University  
20 Oxford Street  
Cambridge, MA 02138  
(617) 868-8801  
cdalton@fas.harvard.edu

**James Davis**

Smithsonian Astrophysical Observatory  
Harvard University  
60 Garden Street MS 42  
Cambridge, MA 02138  
(617) 496-7640 (617) 495-7345  
jdavis@cfa.harvard.edu

**Peter Davis**

Scripps Inst Of Ocean/IGPPA025  
University of California, San Diego  
9500 Gilman Drive  
La Jolla, CA 92093-0225  
(858) 534-2839 (858) 534-6354  
pdavis@ucsd.edu

**Phil Dawson**

Volcano Hazards Team  
US Geological Survey  
345 Middlefield Road MS-910  
Menlo Park, CA 94025  
(650) 329-4751 (650) 329-5203  
dawson@usgs.gov

**Thomas de la Torre**

University of Colorado, Boulder  
2200 Colorado Blvd Campus Box 399  
Boulder, CO 80309  
(303) 492-7296  
tomd@lithos.colorado.edu

**Tim Dixon**

MGG  
University of Miami  
4600 Rickenbacker Cswy  
Miami, FL 33149  
(305) 361-4660  
tdixon@rsmas.miami.edu

**Doug Dodge**

Lawrence Livermore National Lab  
7000 East Avenue L205  
Livermore, CA 94550  
(925) 423-4951  
dodge1@llnl.gov

**Herb Dragert**

Pacific Geosciences Centre  
Geological Survey of Canada  
9860 West Saanich Road  
Sidney  
BC, V8L 4B2  
CANADA  
(250) 363-6447 (250) 363-6565  
dragert@pgc.nrcan.gc.ca

**Mihai Ducea**

Department of Geosciences  
University of Arizona  
1040 E Fourth Street  
Tucson, AZ 85721  
(520) 621-5171 (520) 621-2671  
ducea@geo.arizona.edu

**Adam Dziewonski**

Dept Of Earth & Planetary Science  
Harvard University  
20 Oxford Street  
Cambridge, MA 02138  
(617) 495-2510 (617) 495-0635  
dziewons@eps.harvard.edu

**Jennifer Eakins**

IGPP  
University of California, San Diego  
9500 Gilman Drive MC 0225  
La Jolla, CA 92093-0225  
(650) 855-9605  
jeakins@ucsd.edu

**Paul Earle**

US Geological Survey, Denver  
MS 966 Box 25046 DFC  
Denver, CO 80401-1865  
(303) 273-8417 +1 (303) 273-8600  
pearle@usgs.gov

**Göran Ekström**

Dept Of Earth & Planetary Science  
Harvard University  
20 Oxford Street  
Cambridge, MA 02138  
(617) 496-8276 (617) 495-8839  
ekstrom@eps.harvard.edu

**William L. Ellsworth**

Branch Of Seismology  
US Geological Survey, Menlo Park  
345 Middlefield Road MS 977  
Menlo Park, CA 94025  
(650) 329-5020 (650) 329-5617  
ellsworth@usgs.gov

**Noah Fay**

Department of Geological Sciences  
University of Oregon  
1272 University of Oregon  
Eugene, OR 97405  
(541) 346-4653 (541) 346-4692  
nfay@newberry.uoregon.edu

**Karl Feaux**

UNAVCO  
3340 Mitchell Lane  
Boulder, CO 80301  
(303) 497-8037  
kfeaux@unavco.ucar.edu

**John Filson**

Earthquake Hazards Program  
US Geological Survey, National Center  
12201 Sunrise Valley Drive MS 905  
Reston, VA 20192  
(703) 648-6785 (703) 648-6592  
jfilson@usgs.gov

**Delphine Fitzenz**

Earthquake Hazards Team  
US Geological Survey  
345 Middlefield Road MS-977  
Menlo Park, CA 94025  
(650) 329-5533 (650) 329-5143  
fitzenz@usgs.gov

**Lucy Flesch**

Department of Terrestrial Magnetism  
Carnegie Institution of Washington  
5241 Broad Branch Road NW  
Washington, DC 20015  
(202) 478-8841 (202) 478-8821  
flesch@dtm.ciw.edu

**Jon Fletcher**

US Geological Survey  
345 Middlefield Road  
Menlo Park, CA 94025  
(650) 329-5628 (650) 329-5163  
jfletcher@usgs.gov

**Mathew J. Fouch**

Dept of Geological Sciences  
Arizona State University  
Box 871404  
Tempe, AZ 85287-1404  
(480) 965-9292 (480) 965-8102  
fouch@asu.edu

**Gillian Foulger**

US Geological Survey  
345 Middlefield Road MS 910  
Menlo Park, CA 94025  
(650) 329-4143  
foulger@usgs.gov

**James Fowler**

IRIS  
100 East Road  
Socorro, NM 87801  
(505) 835-5072 (505) 835-5079  
jim@iris.edu

**Jeff Freymuller**

Geophysical Institute  
University Of Alaska, Fairbanks  
903 Koyukuk Drive  
Fairbanks, AK 99775  
(907) 474-7286 (907) 474-5618  
jeff@giseis.alaska.edu

**Paul Friberg**

Software Development & Systems Integration  
ISTI  
70 Cereus Way  
New Paltz, NY 12561  
(845) 256-9290 (845) 256-9299  
p.friberg@isti.com

**Gary Fuis**

EGK Hazards Mail Stop 977  
US Geological Survey  
345 Middlefield Road  
Menlo Park, CA 94025  
(650) 329-4758 (650) 329-5163  
fuis@usgs.gov

**James Gaherty**

School Of Earth & Atmospheric Sciences  
Georgia Tech  
424 West End Ave Apt 2J  
New York, NY 10024  
(845) 365-8427  
gaherty@eas.gatech.edu

**Abhijit Gangopadhyay**

Department of Geological Sciences  
University of South Carolina  
701 Sumter Street EWSC Building  
Columbia SC 29028  
(803) 777-4528 (803) 7776610  
abhijit@seis.sc.edu

**Fuchun Gao**

Department of Earth Sciences  
Rice University  
6100 Main Street  
Houston, TX 77005  
(713) 348-2847 (713) 348-5024  
fcgao@rice.edu

**Lind Gee**

Seismological Laboratory  
University of California, Berkeley  
215 McCone Hall  
Berkeley, CA 94720-4760  
(510) 643-9449 (510) 643-5811  
lind@seismo.berkeley.edu

**Hersh Gilbert**

Department of Geosciences  
University of Arizona  
1040 E 4th Street  
Tucson, AZ 85721  
(520) 621-7378  
hgilbert@geo.arizona.edu

**Ken Gledhill**

Institute of Geological & Nuclear Sciences  
41A Bell Road  
Lower Hutt  
Wellington 6315  
NEW ZEALAND  
+ 5704788 + 5704616  
k.gledhill@gns.cri.nz

**Joan Gomberg**

CERI, University Of Memphis  
US Geological Survey  
3876 Central Avenue  
Memphis, TN 65211  
(901) 678-4858 (901) 678-4897  
gomberg@usgs.gov

**Francisco Gomez**

Department of Geological Sciences  
University of Missouri  
101 Geological Sciences Bldg  
Columbia, MO 65211  
(573) 882-9744 (573) 882-5458  
fgomez@missouri.edu

**Stephen Grand**

Dept Of Geological Sciences  
University of Texas  
C1100  
Austin, TX 78712  
(512) 471-3005 (512) 471-9425  
steveg@maestro.geo.utexas.edu

**Patricia Griego**

New Mexico Tech  
PASSCAL Instrument Center  
100 East Road  
Socorro, NM 87801  
(505) 835-5070 (505) 835-5079  
pgilbert@passcal.nmt.edu

**Bradford Hager**

Dept Of Earth Atmos & Planetary Sciences  
Massachusetts Institute of Technology  
77 Massachusetts Ave Rm 54-622  
Cambridge, MA 02139  
(617) 253-0126 (617) 253-1699  
bhhager@mit.edu

**Michelle Hall-Wallace**

Department Of Geosciences  
University of Arizona  
1040 E 4th Street  
Tucson, AZ 85721-0077  
(520) 621-9993 (520) 621-2672  
hall@geo.arizona.edu

**Michael Hamburger**

Department Of Geological Sciences  
Indiana University  
1005 E 10th Street  
Bloomington, IN 47405  
(812) 855-2934 (812) 855-7899  
hamburg@indiana.edu

**Roger Hansen**

Geophysical Institute  
University Of Alaska, Fairbanks  
907 Koyukuk Drive PO Box 757320  
Fairbanks, AK 99775-7320  
(907) 474-5533 (907) 474-5618  
roger@giseis.alaska.edu

**Jeanne Hardebeck**

US Geological Survey  
345 Middlefield Road, MS 977  
Menlo Park, CA 94025  
(650) 329-4711  
jhardebeck@usgs.gov

**Ruth Harris**

US Geological Survey  
345 Middlefield Road, MS 977  
Menlo Park, CA 94025  
(650) 329-4842  
harris@usgs.gov

**Ron Harris**

Department of Geology  
Brigham Young University  
S-349 Esc.  
Provo, UT 84602-4606  
(801) 422-9264  
rharris@byu.edu

**Danny Harvey**

Boulder Real Time Technology  
2045 Broadway Street Suite 400  
Boulder, CO 80302  
(303) 442-4946 (270) 907-0096  
danny@brtt.com

**Chris Hayward**

Department of Geosciences  
Southern Methodist University  
3225 Daniel Ave. Heroy Bldg Room 210  
Dallas, TX 75275  
(214) 768-3031 (214) 768-4291  
hayward@smu.edu

**Sidney Hellman**

Instrumental Software Technologies, Inc.  
77 Van Dam Street Suite 10  
Saratoga Springs, NY 12866  
(518) 602-0001 (518) 602-0002  
s.hellman@isti.com

**Donald Helmberger**

Division of Geology & PI Sciences  
1200 California Blvd MC 252-21  
Pasadena, CA 91125  
(626) 395-6998 (626) 564-0715  
helm@gps.caltech.edu

**Christel Hennet**

IRIS  
1200 New York Avenue NW  
Suite 800  
Washington, DC 20005  
(202) 682-2222 (202) 682-2444  
christel@iris.edu

**Thomas Henyey**

Department Of Earth Sciences  
University Of Southern California  
University Park  
Los Angeles, CA 90089-0740  
(213) 740-5832 (213) 740-0011  
henyey@usc.edu

**Thomas Herring**

Dept Of Earth Atmos. & Planetary Sciences  
Massachusetts Institute Of Technology  
77 Massachusetts Ave Room 54-618  
Cambridge, MA 02139  
(617) 253-5941 (617) 253-1699  
tah@mit.edu

**Stephen Hickman**

Branch Of Seismology  
US Geological Survey, Menlo Park  
345 Middlefield Road MS 977  
Menlo Park, CA 94025  
(650) 329-4807 (650) 329-5163  
hickman@usgs.gov

**John A. Hole**

Department of Geological Sciences  
Virginia Tech  
4044 Derring Hall  
Blacksburg, VA 24061-0420  
(540) 231-3858 (540) 231-3386  
hole@vt.edu

**William Holt**

Department of Geosciences  
SUNY, Stony Brook  
Stony Brook, 11794-2100  
(631) 632-8215 (631) 632-8240  
wholt@mantle.geo.sunysb.edu

**Susan Hough**

US Geological Survey, Pasadena  
525 S Wilson Avenue  
Pasadena, CA 91106  
(626) 583-7224 (626) 583-7827  
hough@gps.caltech.edu

**Sigrun Hreinsdottir**

University of Alaska, Fairbanks  
903 Koyukuk Dr PO box 757320  
Fairbanks, AK 9775-4345  
(907) 4745517 (907) 474-5618  
sigrun@giseis.alaska.edu

**Michael Hubenthal**

IRIS  
1200 New York Avenue NW  
Suite 800  
Washington, DC 20005  
(202) 682-2222 (202) 682-2444  
hubenth@iris.edu

**Kenneth Hudnut**

Earthquake Hazards Team  
US Geological Survey, Pasadena  
525 S Wilson Avenue  
Pasadena, CA 91106  
(626) 583-7232 (626) 583-7827  
hudnut@usgs.gov

**Eugene Humphreys**

Department of Geological Sciences  
University of Oregon  
Eugene, OR 97403  
(541) 346-5575 (541) 346-4692  
gene@newberry.uoregon.edu

**Jih-hao Hung**

Earth Sciences Department  
National Central University  
Chungli, Taiwan 32054  
CHINA  
+ 886.3.4275564  
jhung@earth.ncu.edu.tw

**Charles Hutt**

Albuquerque Seismological Lab  
US Geological Survey  
801 University Blvd SE Suite 300  
Albuquerque, NM 87106-4345  
(505) 462-3201 (505) 462-3299  
bhutt@usgs.gov

**Shane Ingate**

IRIS  
1200 New York Avenue NW  
Suite 800  
Washington, DC 20005  
(202) 682-2222 (202) 682-2444  
shane@iris.edu

**Michael Jackson**

UNAVCO  
3340 Mitchell Lane  
Boulder, CO 80301  
(303) 497-8008 (303) 497-8028  
mikej@unavco.ucar.edu

**David James**

Dept Of Terrestrial Magnetism  
Carnegie Institution Of Washington  
5241 Broad Branch Rd NW R-159  
Washington, DC 20015  
(202) 478-8838 (202) 478-8821  
james@dtm.ciw.edu

**Bjorn Johns**

UNAVCO  
3340 Mitchell Lane  
Boulder, CO 80301  
(303) 497-8034 (303) 497-8028  
bjorn@unavco.ucar.edu

**Daniel Johnson**

Department of Geology  
Central Washington University  
1636 NE 97th Street  
Seattle, WA 98115  
(206) 523-2778  
dan@geology.cwu.edu

**Leonard Johnson**

Division of Earth Sciences  
National Science Foundation  
4201 Wilson Boulevard Room 785  
Arlington, VA 22230  
(703) 292-4749 (703) 292-9025  
lejohnson@nsf.gov

**Cecil Jones**

UNAVCO  
3360 Mitchell Lane Suite C  
Boulder, CO 80301  
(720) 565-5984 (720) 565-5992  
jones@unavco.org

**Craig Jones**

CIRES  
University of Colorado, Boulder  
Campus Box 399  
Boulder, CO 80309-0399  
(303) 492-6994 (303) 492-2606  
cjones@cires.colorado.edu

**Thomas Jordan**

Department Of Earth Sciences  
University Of Southern California  
3651 Trousdale Parkway  
Los Angeles, CA 90089-0740  
(213) 821-1237 (213) 740-0011  
tjordan@usc.edu

**Jordi Julia**

Geosciences Department  
Penn State University  
405 Deike Building  
University Park, PA 16802  
(814) 865-4279  
jordi@essc.psu.edu

**Bruce Julian**

US Geological Survey  
345 Middlefield Road MS 977  
Menlo Park, CA 94025  
(650) 329-4797 (650) 329-5163  
julian@usgs.gov

**Linus Kamb**

IRIS  
1408 NE 45th Street Suite201  
Seattle, WA 98105  
(206) 547-0393 (206) 547-1093  
linus@iris.washington.edu

**Hiroo Kanamori**

Seismological Laboratory  
California Institute Of Technology  
1200 E California Boulevard  
Pasadena, CA 91125  
(626) 395-6914 (626) 564-0715  
hiroo@gps.caltech.edu

**Sharon Kedar**

NASA/ Jet Propulsion Laboratory  
4800 Oak Grove Drive  
Pasadena, CA 91109  
(818) 393-6808 (818) 393-4965  
sharon.kedar@jpl.nasa.gov

**Robert King**

Dept of Earth, Atmos & Planetary Science  
Massachusetts Institute Of Technology  
77 Massachusetts Avenue Room 54-620  
Cambridge, MA 02139  
(617) 253-7064 (617) 253-1699  
rwk@chandler.mit.edu

**Nancy King**

US Geological Survey  
525 S Wilson Avenue  
Pasadena, CA 91106  
(626) 583-7815 (626) 583-7827  
nking@usgs.gov

**Mikhail Kogan**

Lamont-Doherty Earth Observatory  
Columbia, University  
61 Route 9W  
Palisades NY 10964  
(845) 365-8882 (845) 365-8150  
kogan@ldeo.columbia.edu

**Keith Koper**

Dept of Earth & Atmospheric Sciences  
Saint Louis University  
3507 Laclede Avenue  
St Louis, MO 63103  
(314) 977-3197 (314) 977-3117  
koper@eas.slu.edu

**Minoo Kosarian**

Department of Geosciences  
Penn State University  
439 Deike Building University Park  
State College, PA 16802  
(814) 235-1190 (814) 863-7823  
muk115@psu.edu

**Charles Kurnik**

UNAVCO  
6640 Mitchell Lane  
Boulder, CO 80301  
(303) 497-8003  
ckurnik@unavco.ucar.edu

**David Lambert**

Divison Of Earth Sciences GEO/EAR  
National Science Foundation  
4201 Wilson Boulevard Room 785 S  
Arlington, VA 22230  
(703) 292-4736 (703) 292-9025  
dlambert@nsf.gov

**John Langbein**

Department of Earthquake Studies  
US Geological Survey  
345 Middlefield Road MS 977  
Menlo Park, CA 94025  
(650) 329-4853 (650) 329-5163  
langbein@usgs.gov

**Charles Langston**

CERI  
University of Memphis  
3876 Central Avenue Suite 1  
Memphis, TN 38152-3050  
(901) 678-4869 (901) 678-4734  
clangstn@memphis.edu

**Chris Larsen**

Geophysical Institute  
University of Alaska  
903 Koyukuk Drive  
Fairbanks, AK 99775  
(907) 474-5661  
chris@giseis.alaska.edu

**Kristine Larson**

Aerospace Engineering Sciences  
University of Colorado  
University Campus Box 429  
Boulder, CO 80309  
(303) 492-6583 (303) 492-7881  
kristine.larson@colorado.edu

**Angela Marie Larson**

Virginia Tech  
PO Box 66  
Ellinston, VA 24087-0066  
(540) 231-8827  
alarson@vt.edu

**David Lavallee**

Nevada Bureau of Mines & Geology  
University of Nevada, Reno  
Mail Stop 178  
Reno, NV 89557  
(775) 784-6691 (784) 784-1709  
lavallee@unr.edu

**Thorne Lay**

Department Of Earth Sciences  
University Of California, Santa Cruz  
1156 High Street Earth & Marine Sciences Bldg  
Santa Cruz, CA 95064  
(831) 459-3164 (831) 459-3074  
tlay@es.ucsc.edu

**Alena Leeds**

Field Operations for National  
Seismic Network  
US Geological Survey  
1711 Illinois Street  
Golden, Colorado 80401  
(303) 273-8462 (303) 887-8743  
aleeds@usgs.gov

**William Leith**

Earthquake Hazards Program  
US Geological Survey  
905 National Center  
Reston, VA 20192  
(703) 648-6786 (703) 648-6953  
wleith@usgs.gov

**Arthur Lerner-Lam**

Lamont-Doherty Earth Observatory  
Columbia University  
61 Rout 9 W box  
1000 Seismology Bldg 226  
Palisades, NY 10964  
(845) 365-8356 (845) 365-8150  
lerner@ldeo.columbia.edu

**Alan Levander**

Dept Of Earth Sciences  
Rice University  
6100 Main Street MS 126  
Houston, TX 63103  
(713) 348-6064 (713) 348-5214  
alan@esci.rice.edu

**Jim Lewkowicz**

Weston Geophysical Corporation  
57 Bedford Street Suite  
Lexington, MA 02420  
(781) 860-0127 (781) 860-0160  
jiml@westongeophysical.com

**Felipe Leyton**

Dept of Earth & Atmospheric Sciences  
Saint Louis University  
3507 Laclede Avenue  
Saint Louis, MO 63103  
(314) 977-3130 (314) 977-3117  
leyton@eas.slu.edu

**Yong-Gang Li**

Department of Earth Sciences  
University of Southern California  
University Park  
Los Angeles, CA 90089-0740  
(213) 740-3556 (213) 740-8801  
ygli@terra.usc.edu

**Koi Ling Lim**

US Geological Survey  
345 Middlefield Road MS 977  
Menlo Park, CA 94025  
(650) 329-4758  
fuis@usgs.gov

**Michael Lisowski**

Cascades Volcano Observatory  
US Geological Survey  
1300 SE Cardinal Ct # 100  
Vancouver, WA 98663  
(360) 993-8933 (360) 993-8982  
misowski@usgs.gov

**Leland Long**

Dept Of Earth & Atmos Sciences  
Georgia Institute of Technology  
311 Ferst Avenue  
Atlanta, GA 30332-0340  
(404) 894-2860 (404) 853-0232  
tim.long@eas.gatech.edu

**Alberto López**

Dept of Geological Sciences  
Northwestern University  
1915 Maple Avenue Apt 222  
Evanston, IL 60201  
(847) 491-5379 (847) 491-8060  
alberto@earth.northwestern.edu

**John Louie**

Seismological Lab 174  
University of Nevada, Reno  
1664 N Virginia Street  
Reno, NV 89557-0141  
(775) 784-4219 (775) 784-1833  
louie@seismo.unr.edu

**Kuo-Fong Ma**

Institute of Geophysics, NCU  
300 Jung-Da Road  
Jung-Li Taiwan, ROC 320-54  
+ 886.3.4227151x5634 +886.3.4222044  
kuofongm@yahoo.com.tw

**Harold Magistrale**

Dept of Geological Sciences  
San Diego State University  
5500 Campanile Drive  
San Diego, CA 92182-1020  
(619) 594-6741 (619) 594-6741  
harold@hal.sdsu.edu

**Jason Mallett**

IRIS  
1200 New York Avenue NW  
Suite 800  
Washington, DC 20005  
(202) 682-2222 (202) 682-2444  
Jason@iris.edu

**Michael Mayhew**

Division of Earth Sciences  
National Science Foundation  
4201 Wilson Boulevard  
Arlington, VA 22230  
(703) 292-4744 (703) 292-9025  
mmayhew@nsf.gov

**Art McGarr**

Branch Of Seismology  
US Geological Survey  
345 Middlefield Road MS977  
Menlo Park, CA 94025  
(650) 329-5645 (650) 329-5163  
mcgarr@usgs.gov

**Daniel McNamara**

US Geological Survey, Golden  
1711 Illinois Road  
Golden, CO 80401  
(303) 273-8550 (303) 273-8600  
mcnamara@usgs.gov

**Sara McNamara**

New Mexico Tech  
PO Box 2555  
Socorro, NM 87801  
(505) 835-5418  
mcnamara@ees.nmt.edu

**Darcy McPhee**

US Geological Survey  
MS 989 345 Middlefield Road  
Menlo Park, CA 94025  
(650) 329-4173 (650) 329-5133  
dmcphee@usgs.gov

**John McRaney**

Southern California Earthquake Center  
University of Southern California  
University Park  
Los Angeles, CA 90089-0742  
(213) 740-5842 (213) 740-0011  
mcraney@usc.edu

**Charles Meertens**

UNAVCO  
UCAR  
3340 Mitchell Lane PO Box 3000  
Boulder, CO 80301-2260  
(303) 497-8011 (303) 447-8028  
chuckm@unavco.ucar.edu

**Timothy Melbourne**

Dept Of Geological Sciences  
Central Washington University  
400 East Eighth Avenue  
Ellensburg, WA 98926-7418  
(509) 963-2799 (509) 963-2821  
tim@geology.cwu.edu

**Robert Mellors**

Dept of Geological Sciences  
San Diego State University  
5500 Campanile Drive MC-1020  
San Diego, CA 92182  
(858) 552-7828 (858) 552-4372  
rmellors@geology.sdsu.edu

**Hal Mendoza**

Stanford University  
5871 Evergreen Lane  
Mariposa, CA 95338  
(209) 966-4489  
halm@sti.net

**Kate Miller**

Dept Of Geological Sciences  
University of Texas, El Paso  
El Paso, TX 799668-0555  
(915) 747-5424 (915) 747-5073  
miller@geo.utep.edu

**M. Meghan Miller**

Department of Geological Sciences  
Central Washington University  
400 East Eighth Avenue  
Ellensburg, WA 98926-1418  
(509) 963-2825 (509) 963-2821  
meghan@geology.cwu.edu

**Brian Mitchell**

Dept of Atmospheric Sciences  
Saint Louis University  
6507 Laclede Avenue  
Saint Louis, MO 63103  
(314) 977-3123 (314) 977-3117  
mitchbj@eas.slu.edu

**Raffaella Montelli**

Department of Geosciences  
Princeton University  
Guyot Hall  
Princeton, NJ 08544  
(609) 258-5031 (609) 258-1671  
montelli@princeton.edu

**Walter Mooney**

Branch Of Seismology  
US Geological Survey  
345 Middlefield Road MS 977  
Menlo Park, CA 94025  
(650) 329-4764 (650) 329-5136  
mooney@usgs.gov

**Igor Morozov**

Dept of Geological Sciences  
University Of Saskatchewan  
114 Science Place  
Saskatoon, SK, S7N 2G1  
CANADA  
(306) 966-2761 (306) 966-8593  
igor.morozov@usask.ca

**Janice Murphy**

US Geological Survey  
345 Middlefield Road MS 977  
Menlo Park, CA 94025  
(650) 329-5451 (650) 329-5163  
murphy@usgs.gov

**Jessica Murray**

Geophysics Department  
Stanford University  
Mitchell Building 397 Panama Mall  
Stanford, CA 94305  
(650) 723-5485  
jrmurray@pangea.stanford.edu

**Mark Murray**

Seismological Laboratory  
University of California, Berkeley  
215 McCone Hall  
Berkeley, CA 94702-4760  
(510) 642-2601 (510) 643-5811  
mhmurray@seismo.berkeley.edu

**Doug Myren**

US Geological Survey  
345 Middlefield Road MS-977  
Menlo Park, CA 94025  
(650) 329-4858  
dmyren@usgs.gov

**John L. Nabelek**

College of Oceanic & Atmos Sciences  
Oregon State University  
104 Ocean Admin Building  
Corvallis, OR 97331-5503  
(541) 737-3504 (541) 737-2064  
nabelek@oce.orst.edu

**Ruth Neilan**

Jet Propulsion Laboratory/ NASA  
165 Central Bureau MS 238-540  
4800 Oak Grove Drive  
Pasadena, CA 91109  
(818) 354-8330 (818) 393-6686  
ruth.neilan@jpl.nasa.gov

**Meredith Nettles**

Dept of Earth & Planetary Sciences  
Harvard University  
20 Oxford Street  
Cambridge, MA 02138  
(617) 496-8364  
nettles@eps.harvard.edu

**Andrew Newman**

Dept of Earth & Environmental Sciences  
Los Alamos National Laboratory  
MS D462 IGPP  
Los Alamos, NM 87545  
(505) 665-3570  
anewman@lanl.gov

**Susan Newman**

Seismological Society of America  
201 Plaza Professional Building  
El Cerrito, CA 94530  
(510) 559-1782 (510) 525-7204  
snewman@seismosoc.org

**James Ni**

Department of Physics  
New Mexico State University  
Box 30001/Dept 3D  
Las Cruces, NM 88003-0001  
(505) 646-1920 (505) 646-1934  
jni@nmsu.edu

**Craig Nicholson**

Institute For Crustal Studies  
University of California, Santa Barbara  
1140 Girvetz Hall  
Santa Barbara, CA 93106-1100  
(805) 893-8384 (805) 893-8649  
craig@crustal.ucsb.edu

**Fenlin Niu**

Rice University  
6100 Main Street  
Houston, TX 77005  
(713) 348-4122 (713) 348-5214  
niu@rice.edu

**Guust Nolet**

Department Of Geosciences  
Princeton University  
110 Guyot Hall  
Princeton, NJ 08544  
(609) 258-4128 (609) 258-1274  
nolet@princeton.edu

**Andrew Nyblade**

Department of Geosciences  
Penn State University  
447 Deike Building  
University Park, PA 16802  
(814) 404-5884  
andy@essc.psu.edu

**Jack Odum**

Branch of Geology  
US Geological Survey  
Box 25046 MS 966  
Denver, CO 80225  
(303) 273-8645 (303) 273-8600  
odum@usgs.gov

**David Okaya**

Department Of Earth Sciences  
University of Southern California  
133 South Science Building  
Los Angeles, CA 90089-0740  
(213) 740-7452 (213) 740-0011  
okaya@usc.edu

**John Oldow**

Department of Geological Sciences  
University of Idaho  
University of Idaho Campus  
Moscow, ID 83844-3022  
(208) 885-7327  
oldow@uidaho.edu

**Lani Oncescu**

Geotech Instruments  
10755 Sanden Drive  
Dallas, TX 75238  
(214) 221-0000x7618 (214) 343-4400  
lani.oncescu@geoinstr.com

**John Orcutt**

Scripps Institution of Oceanography  
University of California, San Diego  
9500 Gilman Drive  
La Jolla, CA 92093-0225  
(858) 534-2836 (858) 822-3372  
jorcutt@ucsd.edu

**José Otero**

Scripps Institution of Oceanography  
University of California, San Diego  
10610 Porto Court  
San Diego, CA 92124  
(858) 534-0126 (858)  
jdotero@ucsd.edu

**Susan Owen**

Earth Sciences Department  
3651 Trousdale Parkway  
Los Angeles, CA 90089-  
(213) 740-6308 (213) 740-8801  
owen@terra.usc.edu

**John Owen**

UNVACO  
3340 Mitchell Lane  
Boulder, CO 80301  
(303) 497-8046 (303) 497-8028  
jowen@unavco.ucar.edu

**Thomas Owens**

Department of Geological Sciences  
University of South Carolina  
701 Sumter St. Rom EWSC 617  
Columbia, SC 29201  
(520) 621-8628 (520) 621-2672

**Arda Ozacar**

Department of Geosciences  
University of Arizona  
Gould-Simpson Bldg. 1040 E Fourth St  
Tucson, AZ 85721-0077  
(520) 621-3348 (520) 621-2672  
arda@email.arizona.edu

**Kristine Pankow**

Seismograph Stations  
University of Utah  
135 South 1460 East Room 705  
Salt Lake, UT 84112-0111  
(801) 585-6484 (801) 585-5585  
pankow@seis.utah.edu

**Jeffrey Park**

Dept of Geology & Geophysics  
Yale University  
PO Box 208109  
New Haven, CT 06520-8109  
(203) 432-3172 (203) 432-3134  
jeffrey.park@yale.edu

**Tim Parker**

PASSCAL Instrument Center  
New Mexico Tech  
100 East Road  
Socorro, NM 87801  
(505) 835-5075 (505) 835-5079  
tparker@passcal.nmt.edu

**Paul Passmore**

Refraction Technology, Inc.  
2626 Lombardy Lane Suite 105  
Dallas, TX 75220  
(214) 353-0609 (214) 353-9659  
p-passmore@reftek.com

**Michael Pasyanos**

Department Of Seismology  
Lawrence Livermore National Lab  
7000 East Avenue L-205  
Livermore, CA 94550  
(925) 423-6835 (925) 423-4077  
pasyanos1@llnl.gov

**Gary Pavlis**

Dept Of Geological Sciences  
Indiana University  
1001 East 10th Street  
Bloomington, IN 47405  
(858) 534-0126 (858) 534-6354  
pavlis@indiana.edu

**Terry Pavlis**

Dept of Geology & Geophysics  
University of New Orleans  
Lakefront  
New Orleans, LA 70148  
(504) 280-6797 (504) 280-7396  
tpavlis@uno.edu

**Zhigang Peng**

Earth Science Department  
University of Southern California  
3651 Trousdale Parkway  
Los Angeles, CA 90089-0740  
(213) 740-7174 (213) 740-8801  
zpeng@email.usc.edu

**Wayne Pennington**

Dept Of Geological Engineering  
Michigan Technological University  
1400 Townsend Drive  
Houghton, MI 49931  
(906) 487-3573 (906) 487-3371  
wayne@mtu.edu

**Christine Powell**

CERI  
The University of Memphis  
Campus Box 526590  
Memphis, TN 38152-6590  
(901) 678-8455 (901) 678-4734  
powell@ceri.memphis.edu

**Thomas Pratt**

US Geological Survey  
University of Washington  
School of Oceanography  
Seattle, WA 98195  
(206) 543-7358 (206) 543-6073  
tpratt@ocean.washington.edu

**William Prescott**

UNAVCO  
3360 Mitchell Lane Suite C  
Boulder, CO 80301-2245  
(720) 565-5973 (720) 565-5992  
prescott@unavco.org

**Rosemarie Price**

UNAVCO  
3360 Mitchell Lane Suite C  
Boulder, CO 80301-2245  
(720) 565-5973 (720) 565-5992  
rprice@unvaco.org

**Daniel Quinlan**

Boulder Real Time Technologies, Inc.  
2045 Broadway Suite 400  
Boulder, CO 80302  
(303) 449-3229 (720) 274-0096  
danq@brtt.com

**Sudhir Rajaure**

Department of Mines & Geology  
HMG of Nepal  
Lainchour, Kathmandu  
NEPAL  
+ 977.1.414.700 + 977.1.4412056  
srajaure@infoclub.com.np

**Robert Reilinger**

Dept of Earth, Atmospheric & Planetary Science  
Massachusetts Institute of Technology  
42 Carleton Street  
Cambridge, MA 02142-1324  
(617) 253-7860 (617) 253-6385  
reiling@erl.mit.edu

**Dominique Richard**

Department of Earth Sciences  
University of Southern California  
3651 Trousdale Parkway  
Los Angeles, CA 90089-0740  
(213) 821-2176  
drich@ucla.edu

**Arthur Rodgers**

Seismology Group/Earth Sci Division  
Lawrence Livermore National Laboratory  
L-205 8000 East Avenue  
Livermore, CA 94551  
(925) 423-5018 (925) 423-4077  
rodgers7@llnl.gov

**Steven Roecker**

Department of Geology  
Rensselaer Polytechnic Institute  
100 Eight Street  
Troy, NY 12180  
(518) 276-6773 (518) 276-6880  
roecks@rpi.edu

**Evelyn Roeloffs**

US Geological Survey  
1300 SE Cardinal Court  
Vancouver, WA 98683  
(360) 993-8937 (360) 993-8980  
evelynr@usgs.gov

**Frederique Rolandone**

Berkeley Seismological Lab  
University of California, Berkeley  
215 McCone Hall  
Berkeley, CA 94720-4760  
(510) 642-8374 (510) 643-5811  
fred@seismo.berkeley.edu

**Justin Rubinstein**

Geophysics Department  
Stanford University  
397 Panama Mall  
Stanford, CA 94305  
(650) 723-9316 (650) 725-7344  
justin@pangea.stanford.edu

**Oivind Ruud**

UNVACO  
3340 Mitchell Lane  
Boulder, CO 80301  
(303) 497-8030 (303) 497-8028  
ruud@unavco.ucar.edu

**Michael Rymer**

Western Earthquake Hazards  
US Geological Survey  
345 Middlefield Road  
Menlo Park, 94025  
(650) 329-5649 (650) 329-5163  
mrymer@usgs.gov

**Teresa Saavedra**

IRIS  
1200 New York Avenue NW  
Suite 800  
Washington, DC 20005  
(202) 682-2222 (202) 682-2444  
teresa@iris.edu

**Jason Saleeby**

Caltech  
GPS Division Mail Stop 100-23  
Pasadena, CA 91125  
(626) 395-6141 (626-683-0621  
jason@gps.caltech.edu

**Eric Sandvol**

Dept of Geological Sciences  
University of Missouri  
101 Geology Building  
Columbia, MO 65211  
(573) 884-9616 (573) 882-5458  
sandvole@missouri.edu

**Som Sapkota**

Department of Mines & Geology  
National Seismological Centre  
Lainchour, Kathmandu  
NEPAL  
+ 977.1.410141 + 977.1.412056  
som\_sapkota@hotmail.com

**David Schmidt**

Geophysics Department  
Stanford University  
Mitchell Earth Sciences Room  
360, 397 Panama Mall  
Stanford, CA 94305-2215  
(650) 723-9594 (650) 725-7344  
dasch@pangea.stanford.edu

**Susan Schwartz**

Earth Sciences Department  
University Of California, Santa Cruz  
1156 High Street  
Santa Cruz, CA 950064  
(408) 459-3133 (408) 459-3074  
sschwartz@es.ucsc.edu

**Dogan Seber**

Inst for the Study of the Continents  
Cornell University  
2122 Snee Hall  
Ithaca, NY 14853-1504  
(607) 255-1159 (607) 254-4780  
ds51@cornell.edu

**Paul Segall**

Department of Geophysics  
Stanford University  
Mitchell Bldg Panama Mall Room 397  
Stanford, CA 94305  
(650) 725-7241  
segall@stanford.edu

**Kaye Shedlock**

National Science Foundation  
4201 Wilson Boulevard Room 785 S  
Arlington, VA 22230  
(703) 292-4693 (703) 292-9025  
kshedloc@nsf.gov

**Anne Sheehan**

Dept Of Geological Sciences & CIRES  
University of Colorado, Boulder  
CB 399 Benson Earth Sciences Bldg  
Boulder, CO 80309  
(303) 492-4597 (303) 492-2606  
afs@cires.colorado.edu

**David Shelly**

Department of Geophysics  
Stanford University  
Mitchell Building  
Stanford, CA 94305-2215  
(650) 561-0091  
dshelly@pangea.stanford.edu

**Candy Shin**

IRIS  
1200 New York Avenue NW  
Suite 800  
Washington, DC 20005  
(202) 682-2222 (202) 682-2444  
candy@iris.edu

**Wayne Shiver**

UNAVCO  
3360 Mitchell Lane Suite C  
Boulder, CO 80301  
(720) 565-5982 (720) 565-5992  
shiver@unavco.org

**Paul Silver**

Department of Terrestrial Magnetism  
Carnegie Institution of Washington  
5241 Broad Branch Road NW  
Washington, DC 20015  
(202) 478-8834 (202) 478-8821  
silver@dtm.ciw.edu

**David W. Simpson**

IRIS  
1200 New York Avenue NW  
Suite 800  
Washington, DC 20005  
(202) 682-2222 (202) 682-2444  
david@iris.edu

**Robert Smalley**

CERI  
University of Memphis  
3876 Central Avenue  
Memphis, TN 38152  
(901) 678-4929 (901) 678-4734  
rsmalley@memphis.edu

**Ken Smith**

Seismology Department  
University of Nevada, Reno  
Seismological Laboratory MS 174  
Reno, NV 89557  
(775) 784-4218 (775) 784-1833  
ken@seismo.unr.edu

**Robert Smith**

Dept Of Geology & Geophysics  
University of Utah  
135 S 1460 East Room 702  
Salt Lake City, UT 84121  
(801) 581-7129 (801) 581-5585  
rbsmith@mines.utah.edu

**Scott Smithson**

Dept Of Geology & Geophysics  
University of Wyoming  
Box 3006  
Laramie, WY 82071  
(307) 766-5280 (307) 766-6679  
sbs@uwyo.edu

**Catherine Snelson**

Geosciences Department  
University of Nevada, Las Vegas  
4505 Maryland Parkway  
Las Vegas, NV 89154-4010  
(702) 895-2916 (702) 895-4064  
csnelson@unlv.edu

**J. Arthur Snoke**

Dept Of Geological Sciences  
Virginia Tech  
4044 Derring Hall (0420)  
Blacksburg, VA 24061  
(540) 231-6028 (540) 231-3386  
snoke@vt.edu

**David Snyder**

Polaris  
Geological Survey of Canada  
615 Booth Street  
Ottawa, Ontario K1A 0E9  
CANADA  
(613) 992-9240  
snyder@nrcan.gc.ca

**Seok Goo Song**

Geophysics Department  
Stanford University  
Mitchell Building  
Stanford, CA 94305  
(650) 723-9316  
seisgoo@pangea.stanford.edu

**Grigory Steblou**

Academy of Science  
Geophysical Service of Russian  
10 B Gruzinskaya  
Moscow 123995  
RUSSIA  
+ 7.902.6205009 + 7.095.3351954  
steblov@gps.gsras.ru

**Seth Stein**

Department of Geological Sciences  
Northwestern University  
Locy Hall  
Evanston, IL 60208  
(847) 491-5265 (847) 491-8060  
seth@earth.northwestern.edu

**Ralph Stephen**

Dept Of Geology & Geophysics  
Woods Hole Oceanographic Institution  
360 Woods Hole Road MS24  
Woods Hole, MA 02574-0567  
(508) 289-2583 (508) 457-2150  
rstephen@whoi.edu

**William Stephenson**

US Geological Survey, Denver  
Box 25046 MS 966  
Denver, CO 80225  
(303) 273-8573 (303) 277-8600  
wstephens@usgs.gov

**David Stowers**

Section335  
Jet Propulsion Laboratory  
4800 Oak Grove Drive  
Pasadena, CA 91109  
(818) 354-7055 (818) 393-4965  
dstower@jpl.nasa.gov

**Susan Strain**

IRIS  
1200 New York Avenue NW  
Suite 800  
Washington, DC 20005  
(202) 682-2222 (202) 682-2444  
susan@iris.edu

**John Taber**

IRIS  
1200 New York Avenue NW  
Suite 800  
Washington, DC 20005  
(202) 682-2222 (202) 682-2444  
taber@iris.edu

**Pradeep Talwani**

Department of Geological Sciences  
University of South Carolina  
701 Sumter St EWSC Bldg Room 517  
Columbia, SC 29208  
(803) 777-6449 (803) 777-6610  
talwani@geol.sc.edu

**Ying Tan**

California Institute of Technology  
Caltech 252-21  
Pasadena, CA 91125  
(626) 395-6932  
ytan@gps.caltech.edu

**Toshiro Tanimoto**

Department of Geological Sciences  
University of California, Santa Barbara  
Santa Barbara, CA 93106  
(805) 893-5073 (805) 893-2314  
toshiro@geol.ucsb.edu

**Mary Templeton**

New Mexico Tech  
PASSCAL Instrument Center  
100 East Road  
Socorro, NM 87801  
(505) 835-5073 (505) 835-5079  
maryt@passcal.nmt.edu

**Wayne Thatcher**

Branch Of Seismology  
US Geological Survey  
345 Middlefield Road MS-977  
Menlo Park, CA 94025  
(650) 329-4810 (650) 329-5163  
thatcher@usgs.gov

**Michael Thorne**

Department of Geological Sciences  
Arizona State University  
Box 871410  
Tempe, AZ 85287-1404  
(480) 965-7680 (480) 965-8102  
mthorne@asu.edu

**Anahita Tikku**

Ocean Research Institute  
University of Tokyo  
1-15-1 Minamidai, Nakano-Ku  
Tokyo 164-8639  
JAPAN  
+ 81.3.5351.6442 + 81.3.5351.6438  
ani@ori.u-tokyo.ac.jp

**Hrvoje Tkalčić**

Dept of Energy & Environ. Earth Science  
Lawrence Livermore National Laboratory  
PO box 808 L-206  
Livermore, CA 94550  
(925) 422-7332 (925) 422-3118  
tkalcic1@llnl.gov

**Tatiana Toteva**

School of Earth & Atmospheric Sciences  
Georgia Institute of Technology  
311 Ferst Drive  
Atlanta, GA 30332  
(404) 894-4407  
ttoteva@eas.gatech.edu

**Anne Trehu**

College of Oceanic & Atmospheric Sciences  
Oregon State University  
Ocean Admin Building 104  
Corvallis, OR 97331  
(541) 737-2655 (541) 737-2064  
trehu@coas.oregonstate.edu

**Greg van der Vink**

IRIS  
1200 New York Avenue NW  
Suite 800  
Washington, DC 20005  
(202) 682-2222 (202) 682-2444  
greg@iris.edu

**Robert D van der Hilst**

Dept of Earth Atmos & Planetary Sciences  
Massachusetts Institute of Technology  
77 Massachusetts Ave Room 54514  
Cambridge, MA 02139-4307  
(617) 253-6977 (617) 253-9697  
hilst@mit.edu

**Frank Vernon**

Scripps Inst Of Ocean/IGPP0225  
University Of California, San Diego  
9500 Gilman Drive  
La Jolla, CA 92093-0225  
(858) 534-5537 +1 (858) 534-6354  
flvernon@ucsd.edu

**John Vidale**

Dept Of Earth & Space Sciences  
University Of California, Los Angeles  
595 Charles Young Drive East  
Los Angeles, CA 90095-1567  
(310) 206-3935 (310) 825-2779  
vidale@ucla.edu

**Christa von Hillebrandt-Andrade**

Puerto Rico Seismic Network  
University of Puerto Rico, Mayagüez  
PO BOX 9017  
Mayaguez, PR 00681-9017  
(787) 833-8433 (787) 265-5452  
christa@midas.uprm.edu

**Lisa Wald**

Denver Federal Center  
US geological Survey  
MS 966 PO Box 25046  
Denver, CO 80225  
(303) 273-8543 (303) 273-8600  
lisa@usgs.gov

**William Walter**

Geophysics & Global Security  
Lawrence Livermore National Laboratory  
PO Box 808 IGPP L-205  
Livermore, CA 94551  
(925) 423-8777 (925) 423-4077  
bwalter@llnl.gov

**Linda Warren**

Scripps Institution of Oceanography  
University of California, San Diego  
9500 Gilman Drive, 0225  
La Jolla, CA 92093-0225  
(858) 534-8119 (858) 534-5322  
lwarren@ucsd.edu

**Frank Webb**

Jet Propulsion Laboratory  
California Institute Of Technology  
4800 Oak Grove Drive MS 238-600  
Pasadena, CA 91109  
(818) 354-4670 (818) 393-4965  
fhw@jpl.nasa.gov

**Spahr Webb**

Lamont-Doherty Earth Observatory  
Columbia University  
61 Route 9W  
Palisades, NY 10964  
(845) 365-8439 (845) 365-8150  
scw@ldeo.columbia.edu

**Bruce Weertman**

IRIS  
1408 NE 45th Street Suite 201  
Seattle, WA 98105  
(206) 547-0393 (206) 547-1093  
bruce@iris.washington.edu

**Robert Wesson**

Central Geologic Hazards Team  
US Geological Survey  
Box 25046  
Denver, CO 80225  
(303) 273-8524  
rwesson@usgs.gov

**Michael West**

Department of Physics  
New Mexico State University  
MCS 3D  
Las Cruces, NM 88003  
(505) 646-4446  
west@nmsu.edu

**Jim Whitcomb**

Division of Earth Sciences  
National Science Foundation  
4201 Wilson Boulevard Room 785  
Arlington, VA 22230  
(703) 292-4749 (703) 292-9025  
jwhitcomb@nsf.gov

**Clark Wilson**

Department of Geological Sciences  
University of Texas, Austin  
Austin, TX 78712  
(512) 471-5008 (512) 471-9425  
crwilson@mail.utexas.edu

**David Wiltschko**

Dept of Geology & Geophysics  
Texas A&M University  
MS 3115  
College Station, TX 77843-3115  
(979) 845-9680 (979) 845-6162  
d.wiltschko@tamu.edu

**Francis Wu**

Department of Geological Sciences  
SUNNY, Binghamton  
Vestal Parkway E  
Binghamton, NY 13850  
(607) 777-2512 (607) 777-2288  
francis@binghamton.edu

**Zhaohui Yang**

Department of Geology  
University of Illinois, Urbana-Champaign  
1301 W Stoughton St NHB 245  
Urbana, IL 61801  
(217) 244-6048  
zyang1@uiuc.edu

**George Zandt**

Department of Geosciences  
University of Arizona  
Tucson, AZ 85721  
(520) 621-2273 (520) 621-2672  
zandt@geo.arizona.edu

**Colin Zelt**

Department of Earth Sciences  
Rice University  
6100 Main Street MS-126  
Houston, TX 77005-1892  
(713) 348-4757 (713) 348-5214  
czelt@rice.edu

**Rongmao Zhou**

Department of Geological Sciences  
Southern Methodist University  
PO Box 750395  
Dallas, TX 75275-0395  
(214) 768-2747 (214) 768-2701  
zhou@passion.isem.smu.edu

**Lupei Zhu**

Department of Earth Sciences  
Saint Louis University  
3507 Laclede Avenue  
Saint Louis, MO 63103  
(314) 977-3118 (314) 977-3117  
lupei@eas.slu.edu

**Mark Zoback**

Department Of Geophysics  
Stanford University  
Mitchell Bldg Panama Mall Room 397  
Stanford, CA 94305-2215  
(650) 725-9295 (650) 725-7344  
zoback@pangea.stanford.edu





# IRIS Poster Sessions

## Software, Instrumentation, Infrastructure & Networks

1. The New Data Handling Infrastructure at the IRIS DMC : Possible Uses in USArray
2. Automated Analysis of Seismic Data Quality at the DMC
3. Development of a New Broadband Optical Seismometer
4. IU GSN Site Noise
5. Coordinates from the National CORS Network
6. The Combined Motion Model, Time Series, and Analysis Tools from the Southern California Integrated GPS Network (SCIGN) Analysis Committee
7. Access to GPS Data through the GPS Seamless Archive Centers (GSAC) and the Role of GSAC in PBO
8. Mini-PBO - A Prototype Plate Boundary Observatory (PBO) Cluster in the San Francisco Bay Area
9. Expected Performance of the Proposed PBO Network
10. ANSS Detection Threshold
11. Source of Seismic Noise from Directional Information: Implications Ranging from Network Design to Ocean Wave Height
12. IRIS Station Information System Application.
13. PERISCOPE: An Offshore Component of EarthScope for Southern California
14. Utah Regional Seismic Network -- Exploring Potential EarthScope-ANSS Synergy
15. Overview of National Seismological Network, Nepal
16. Network Installation in The Yanqing-Huailai Basin, China And Preliminary Study of Natural and Man-induced Events

## Geodesy & Plate Deformation

17. Understanding the Driving Forces of Western North America Deformation Using Geodesy, Seismology, and Geology
18. Results from Long-Base Strain Measurements in Los Angeles, California and Yucca Mountain, Nevada
19. Broadband Observations of Plate Boundary Deformation in the San Francisco Bay Area
20. Seafloor Geodetic Measurements on the Juan de Fuca Plate: A Progress Report
21. Using GPS to Determine the Kinematics of the Adriatic Region (Central Mediterranean) and Assess the Seismic Potential in the Eastern Alps (Italy).
22. Evolving 3-D Strain Field of the Active Eastern Sunda Arc-Continent Collision, Indonesia.
23. The Resolving Power of the Current State of GPS Information in North America: Implications for EarthScope Planning
24. Critically Stressed Intraplate Crust: Everywhere or Here and There?
25. Applications of Joint Analysis of Broadband Seismology and Tilt
26. Baseline and Error Distribution Results from the Southern California Integrated GPS Network (SCIGN) Analysis Committee
27. Addressing Seasonal Noise when Modeling Transient Deformation Processes
28. Post-Earthquake Deformation from INSAR and Strainmeters Correlated to Pore-pressure Transients
29. North Eurasia GPS Deformation Array (NEDA)
30. Ground Deformation Studies on Large Silicic Volcanic Systems: An Eruption Forecasting Tool Earthscope Can Greatly Improve

31. Newly Detected Deformation in Yellowstone's Upper Geyser Basin
32. Monitoring Deformation of the Long Valley Caldera with EDM and GPS
33. Vertical and Horizontal Velocity Results from GPS in Relation to Mapped Structures, Southern Taiwan
34. Episodic Tremor and Slip (ETS) on the Cascadia Subduction Zone: The Chatter of Silent Slip
35. Geodetic Evidence of Slow Faulting During the 2001 Mw=8.4 Peru Earthquake Sequence

## **Earthquakes, Seismicity & Fault Structure**

36. Southern California Regional Earthquake Probability Estimated from Continuous GPS Data
37. 2-D Numerical Modeling of New Madrid and Charleston Seismic Zones - Implications for Seismogenesis in Stable Continental Regions
38. Can Earthscope Help Demystify the Rupture Physics of Large Earthquakes?
39. Measuring Fault Slip - Why and How?
40. Seismology with a Dense Seismic Network
41. The 2000 Mw 6.8 Ulegorsk Earthquake and Regional Plate Boundary Deformation of Sakhalin from Geodetic Data
42. Comparison of Seismology and InSAR-based Measurements for Moderate Size Earthquakes in Southern California
43. High Seismicity Rate in Bhutan Based on Results from a Local Earthquake Seismic Network
44. Spatial and Temporal Distributions of Shear Wave Anisotropy and Analysis of Repeating Earthquakes in the Karadere-Duzce Branch of the North Anatolian Fault
45. The Evolution of the Seismic-aseismic Transition during the Earthquake Cycle: Constraints from the Time-dependent Depth Distributions of Aftershocks
46. Temporal and Spatial Variations in the Limits of the Seismogenic Zone, Costa Rica
47. Characteristic Earthquakes as Possible Artifacts: Application to New Madrid Validation of a Schematic Model for Stable Continental Region Earthquakes
48. Modeling Source Parameters and Locating Regional Earthquakes with Broadband Waveform Data
49. Anomalous Fault Zone Weakness from Geodetic and Seismic Measures: A Case Study between the Landers and Hector Mine Ruptures
50. Earthquake Apparent Stress Scaling
51. Systematic Determination of Earthquake Fault Planes from a Directivity Analysis of Long-period Spectra
52. Relocation of Hypocenters and Local Earthquake Tomography in Taiwan

## **Strong Ground Motion**

53. The Las Vegas Valley Seismic Response Project
54. Characterizing the Las Vegas Basin for Strong Ground Motions: Past, Present, and Future Active Source Experiments
55. Analysis of Broadband Teleseismic Data in Las Vegas Valley
56. The Seismic Response of the Seattle Sedimentary Basin, Washington State, to Teleseisms Recorded on the Seattle SHIPS Array
57. Lingering Strong-motion Induced Damage to the Earth's Crust
58. Resolving Structural Details of Earthquake Rupture That Give Rise to Damaging Ground Motion and Extending This Capability to Small-magnitude Events Using PBO Borehole Instrumentation

## **San Andreas Fault & SAFOD**

59. Physical Properties and Controls on Shear Wave Velocity Anisotropy in the Crust Adjacent to the San Andreas Fault in Parkfield, CA. as Calibrated by the SAFOD Pilot Hole
60. Stress-Induced Borehole Failure in the SAFOD Pilot Hole: Implications for the Strength of the San Andreas Fault at Parkfield
61. Low-Velocity Core Structure of the San Andreas Fault at Parkfield from Fault-Zone Guided Waves
62. Geophysical Setting of the San Andreas Fault Observatory at Depth (SAFOD) at Parkfield, California
63. Refined Fault Zone Structure and Earthquake Locations at Parkfield, CA
64. Physical Properties and Controls on Shear Wave Velocity Anisotropy in the Crust Adjacent to the San Andreas Fault in Parkfield, CA. as Salibrated by the SAFOD Pilot Hole
65. The San Andreas Fault Observatory at Depth (SAFOD): Testing Fundamental Theories of earthquake Mechanics
66. First Results of Physics-based, Integrative Models of the San Andreas Fault System near the Big Bend Including Fluids, Tectonics, and Post-seismic Relaxation.
67. Reinterpreting Stress Orientations Near the San Andreas Fault

## **Core- CMB**

68. A Search for Lateral Variations in the Structure of at the Top of the Inner Core
69. New Evidence for Seismic Scatterers Within Earth's Inner Core
70. Exploring the Possibility of an Inner Core Transition Zone
71. Fine-Scale Structure of the Core-Mantle Boundary from FARM and PASSCAL Data

## **Shallow Imaging**

72. High Resolution Waveform Tomography at a Groundwater Contamination Site: Combined Surface Reflection and VSP Data
73. High-resolution Seismic Surveying at a Groundwater Contamination site: Results from 3-D Traveltime Tomography
74. Potential for Geothermal Exploration Using EarthScope Seismic and GPS Data
75. Sonic Stimulation of Hydrocarbon Production: Calibration of Borehole Tools
76. Using Borehole Fluid Pressure and Strain Data to Study the Hydrologic and Mechanical Properties of the Nojima Fault, Japan
77. The Embayment Seismic Excitation Experiment - An Active Source Broadband Experiment
78. Earthscope (USArray) Targets in Southern California: Mid-Crustal Decollements Beneath the Transverse Ranges
79. The Northern Walker Lane Seismic Refraction Experiment
80. Definition of the Silver Creek Fault and Evergreen Basin from Active- Source Seismic Reflection Imaging, San Jose, California

## **Crust and Mantle Structure**

81. Broadband Seismic Noise Analysis of the Himalayan Nepal Tibet Seismic Experiment
82. Mapping Lithospheric Strength Heterogeneities at Regional Scales Using P-Wave Tomography

83. Imaging the South Central Andean Lithosphere Using Passive Broadband Seismology: Chile-Argentina Geophysics Experiment
84. Preliminary Results on Crust and Upper Mantle Structure Beneath the East African Rift System in Ethiopia, Kenya and Tanzania from PASSCAL Experiments
85. Lower Mantle Superplume Structure Beneath Africa
86. Joint Inversion of Receiver Functions, Surface-wave Dispersion and S-wave Travel-times in East Africa
87. Using Surface Waves to Constrain the Crust and Upper Mantle S-wave Velocity Structure of the Southern African Craton
88. The Mantle Flow Field Surrounding Southern Africa: Constraints from Shear Wave Splitting Measurements and Mantle Flow Calculations
89. New Images of Q in the Upper Mantle: Constraints from Surface Waves
90. Crustal Q and Mantle Velocity Distributions beneath Eurasia and their Relationship to Subduction/Orogenic

### **Processes of the Tethysides Belt**

91. Depth-domain Processing of Teleseismic Receiver Functions and Generalized Three-dimensional Imaging
92. Tomographic Imaging of  $V_p/V_s$  along the LARSE II Profile in Southern California
93. Surface-wave Constraints on the Radially Anisotropic S-velocity Structure of the North American Upper Mantle
94. Physical Property of the Chemical Heterogeneities in the Mid-mantle: a Strong and Slightly Dipping Seismic Reflector beneath the Mariana Subduction Zone
95. Finite Frequency Global P Wave Tomography
96. Seismic Imaging of the Down-going Indian Lithosphere Beneath Central Tibet
97. Using a High-resolution Surface Wave Model to Image Lithospheric Structure of Western Eurasia and North Africa
98. Regional  $L_g$  Attenuation for the Continental United States
99. Crust and Upper Mantle Shear-wave structure of the Colorado Plateau, Rio Grande Rift and Great Plains
100. Integrated Seismological Studies of Crust/Upper Mantle Structure and Anisotropy in Western Anatolia

### **Denali Earthquake & Other Strike Slip Faults**

101. Real Time Seismology with the Global Positioning System: Observations of the Denali Earthquake with the Orange County Real Time Network
102. Ongoing Efforts at Studying Postseismic Deformation Following the 2002 Denali Fault Earthquake
103. Broadband Seismograms Reveal Widespread Triggering by the M7.9 Denali Earthquake
104. Coseismic Displacements from the 2002 Mw6.7 Nenana Mountain Earthquake and Mw7.9 Denali Fault Earthquake, Measured with GPS
105. Source Process of the 2002 Denali Fault Earthquake Compared to Other Large Strike-slip Events
106. Using 1Hz GPS Data to Measure Permanent and Seismic Deformations Caused by the Denali Fault Earthquake
107. Geodetic Constraints on the Earthquake Deformation Cycle along the Western North Anatolian Fault: Implications for Earthquake Mechanics on Continental Strike-slip Faults

## **Tectonics and Subduction**

108. Xenolith Constraints on Seismic Velocities in the Upper Mantle beneath Southern Africa
109. Delamination of the Sierra Nevada: Seismological Observations and Tectonic Implications
110. Drip Drag?
111. Crustal Production and Loss in Continental Magmatic Arcs: Evidence from the Sierra Nevada
112. The Yavapai-Mazatzal Boundary: A Long-lived Assembly Structure in the Lithosphere of Southwestern North America
113. Are Deep Earthquakes beneath the High Himalaya in the Crust or in the Mantle?
114. Mantle Earthquakes beneath the Himalayan-Tibetan Collision Zone and Rheology of the Continental Lithosphere
115. An Overview of Northern Cordilleran Tectonics in the Context of the Late Miocene to Recent Oblique-collision of the Yakutat Microplate
116. Geophysical Evidence for Widespread Serpentinized Forearc Upper Mantle along the Cascadia and Alaskan Margins: A Juicy Target for the U.S. Array?
117. Possible Forearc Sliver at the Northern Half of the Lesser Antilles Arc
118. Complex Anisotropic Structure of the Mantle Wedge beneath Kamchatka Volcanoes
119. Downgoing Slab Seismicity in Japan Examined Through High Precision Earthquake Hypocenters
120. The Ultimate Goal: a Unified Seismic Model of Magma Transport Mechanics
121. Mapping the Mantle Lithosphere for Diamond Potential
122. Rifting Issues in the Gulf of California

## **E&O**

125. Making Earthquakes Relevant to Students
126. A Real-Time Seismic Network for K-12 Science Education in Nevada



## THE NEW DATA HANDLING INFRASTRUCTURE AT THE IRIS DMC: POSSIBLE USES IN USARRAY

*Tim Ahern and Chris Laughbon*

*IRIS DMC 1408 NE 45th Street Suite 201 Seattle, WA 98105*

The IRIS Data Management System has been supporting the development of the FISSURES framework for handling scientific data for several years. The Data Handling Interface (DHI) is a subset of the FISSURES framework that focuses on methods to transfer information from data centers to client applications over the Internet. Based upon CORBA, the DHI is robust and promises to provide a strong platform from which new methods of waveform and metadata information can be distributed.

This poster will highlight the current data center services that are operating at the IRIS DMC. These include access to event information from NEIC and ISC catalogs, network information with details about networks, stations, and channels, and also a strong suite of waveform services. At the present time, the DMC's four repositories (Archive, BUD, FARM and SPYDER®) are all available through the DHI waveform services.

BUD is the IRIS DMS real time system. It currently ingests data from more than 700 stations around the world every day. It is designed to accept data from a variety of seismic data handling systems and presently can directly accept data from

1. Antelope,
2. Earthworm wave servers,
3. LISS servers, and
4. SEEDlink.

BUD converts the data into a common data handling system and eases access to data for end users. Since BUD is a real time system, the BUD DHI DataCenter does also provide data to end users in real time.

The Data Management System has sponsored the development of several DHI client applications, most of which are available at <http://www.iris.washington.edu/DHI/clients.html>

All of these applications are written in Java and have been tested on OS X, Windows XP, Linux and Solaris operating systems.

1. JEvalResp was written by ISTI and connects to the DMC network service to access and evaluate channel response information
2. JPlotResp was written by ISTI and is similar to JEvalResp except that it also displays the responses graphically or produces local text files.
3. VASE is a client that allows a user to specify individual channels from all networks, stations, and channels in the BUD, FARM or SPYDER® repositories and transfer the selected data to the client application. It allows the seismograms to be viewed, converted to SAC or saved as miniSEED files on the local workstation. It is capable of accessing data in real time or data that can be a few hours to several years old.
4. GEE is the Global Earthquake Explorer and was developed by the University of South Carolina for the IRIS E&O program.
5. SOD is the Standing Order for Data and was also USC developed. It allows a user to specify types of earthquakes of interest to them and when one occurs to automatically transfer the data from appropriate stations to the client application. Currently configured through an XML file, plans for next year include the introduction of a GUI.

Additional interfaces are being developed for directly connecting to MATLAB and to function as a data request tool similar to WEED.

The DHI system, and specifically the BUD Waveform DataCenter and VASE portions of it, are being considered as the method by which to distribute both event products (SPYDER® and FARM) and continuous waveforms in USArray. While all of the traditional DMS request mechanisms will allow access to USArray data, the DHI is envisioned as the primary method for distributing data in real time from the DMC. The BUD/VASE system has been designed in such a way that any VASE system can act as both a client that receives data from a DHI Waveform DataCenter and can become a server to which other DHI VASE clients can connect. This capability allows data distribution to be managed in a fan-out system that insures that everyone that wishes to receive large amounts of USArray data will be able to do so.

This poster will summarize the developments currently underway at the DMC that make use of the Data Handling Interface and the BUD real time system.

# **SOUTHERN CALIFORNIA REGIONAL EARTHQUAKE PROBABILITY ESTIMATED FROM CONTINUOUS GPS DATA**

*Greg Anderson*

*US Geological Survey, Pasadena [ganderson@usgs.gov](mailto:ganderson@usgs.gov)*

Current seismic hazard estimates are primarily based on seismic and geologic data, but geodetic measurements from large, dense arrays such as the Southern California Integrated GPS Network (SCIGN) can also be used to estimate earthquake probabilities and seismic hazard. Geodetically-derived earthquake probability estimates are particularly important in regions with poorly-constrained fault slip rates. In addition, they are useful because such estimates come with well-determined error bounds. Long-term planning is underway to incorporate geodetic data in the next generation of United States national seismic hazard maps, and techniques for doing so need further development.

I present a new method for estimating the expected rates of earthquakes using strain rates derived from geodetic station velocities. I use geodetic station velocities from SCIGN and strain modeling methods by Yaru Hsu and Mark Simons [Y.\ Hsu and M.\ Simons, pers.\ comm.] to estimate the horizontal strain rate tensors at each point on a regular grid spanning southern California. Combining those tensors with spatially-variable seismogenic thickness estimated from regional seismicity, using the methods of WGCEP [1995], Savage and Simpson [1997], and Ward [1998], I compute the equivalent seismic moment rate release density. By integrating the moment rate release density over an area surrounding a fault of interest, I estimate the rate at which moment would need to be released seismically along the fault in order to match the observed strain rates. I then convert this required moment release rate to the expected rate of earthquakes of a given magnitude using a Gutenberg-Richter relationship, and from that, estimate earthquake probability. I will present results of a study applying this method to data from the SCIGN array to estimate earthquake rates in southern California, but my technique is generally applicable to any region with a sufficiently dense geodetic array and well-located seismicity.

Savage, J.C. and R.W. Simpson, Surface strain accumulation and the seismic moment tensor, *Bull. Seismol. Soc. Am.*, 87, 1345--1353, 1997.

Ward, S. N., On the consistency of earthquake moment rates, geological fault data, and space geodetic strain: the United States, *Geophys. J. Int.*, 134, 172--186, 1998.

Working Group on California Earthquake Probabilities, Seismic hazards in southern California: Probable earthquakes, 1994 to 2024, *Bull. Seismol. Soc. Am.*, 85, 379--439, 1995.

# HIGH-RESOLUTION SEISMIC SURVEYING AT A GROUNDWATER CONTAMINATION SITE: RESULTS FROM 3-D TRAVELTIME TOMOGRAPHY

*A. Azaria, C. Zelt, A. Levander*

*Center for Computational Geophysics, Department of Earth Science,  
MS-126, Rice University, Houston, TX, 77005-1892, USA, czelt@rice.edu*

As part of an ongoing environmental characterization project at Hill Air Force Base near Ogden, Utah, a 3-D seismic survey led by a team from Rice University was performed over a contaminated aquifer in 2000. This site contains significant amounts of dense non-aqueous phase liquids (DNAPLs) in a shallow aquifer less than ~15 m deep. The aquifer is bounded below by a clay aquiclude, in which a paleochannel acts as a trap for the contaminants. The overburden consists of Quaternary sands, gravels and clays. Imaging the structure of the paleochannel at depths up to 15 m is the main target of the survey. The four week experiment included 3-D refraction, 3-D reflection, a combined surface/dual vertical seismic profile experiment, and checkshot surveys using wells up to 15m deep. For results from the reflection and VSP/surface data see presentations at this meeting by Dana et al. and Gao et al.

Here we present traveltimes tomography results from the 3-D refraction survey which consisted of 596 RefTek Texan recorders deployed uniformly in a stationary rectangular grid over an area of 95m by 36m. A shot from a .223 caliber rifle was fired 30cm from each receiver station, yielding a dataset with about 360,000 traces. The arrival times of the refracted waves were used in a 3-D tomographic inversion to image the seismic velocity structure of the study area. The iterative, nonlinear tomographic approach employs regularization to smooth the model perturbations with respect to a simple 1-D starting/reference model.

The resulting velocity model shows that the near-surface velocity increases by roughly a factor of 5 in the upper 15m, from about 300m/s to 1500m/s. Cross-sections through the model show a north-south trending low-velocity feature interpreted to be the channel structure. The low-velocity feature is best viewed via depth slices which define an anomaly that roughly outlines the geometry of the buried paleo-channel based on well data. A comparison between the 3-D velocity model and time slices through a stack of the 3-D reflection data also show close agreement. Checkerboard tests applied to the velocity model establishes a 7.5m lateral resolution throughout most of the depth range of interest. While the long wavelength features of the model reveal the paleo-channel, the velocity model is likely a broad and smooth characterization of the true velocity structure.

# ESTIMATING EARTHQUAKE HAZARDS IN THE SAN PEDRO SHELF REGION, SOUTHERN CALIFORNIA

*Shirley Baher, Gary Fuis*  
*U.S. Geological Survey*

Within the Inner Continental Borderlands, one of the most prominent features of the San Pedro Shelf region is the Palos Verdes Fault system. This system is generally shown to extend about 100 km from Lausen Knoll in the south across the San Pedro Shelf, along the northeastern base of the onshore Palos Verdes Hills, and into Santa Monica Bay. Although no large earthquakes have occurred along this fault in historic time, vertical slip-rate estimates (0.02-0.7 mm/yr.) and fault length considerations indicate that this fault could produce an earthquake as large as M7. Furthermore, since horizontal slip rates have not been determined, they are estimated to be greater than vertical, which adds to the potential hazard for the region. The Whittier Narrows (1987, M5.9) and Northridge (1994, M6.7) earthquakes provide estimates of the regional seismic hazard and the economic dislocation that can result from earthquakes with similar magnitude along onshore faults. Along with the Palos Verdes fault, this region also has the potential for hazard from the Thums-Huntington Beach and Cabrillo faults that will be included in this study.

To estimate the earthquake and tsunami hazards posed by offshore faults, we examine the offshore component of the Los Angeles Region Seismic Experiment (LARSE) line 1 (October, 1994) and multichannel seismics obtained during 1998 through 2000. The data were collected with goal of mapping in detail the crustal structure of the Inner continental Borderlands and their transition to mainland California. Using these two data sets an initial velocity and structural model is developed and tested using forward modeling of the observed P-arrival times. Our initial estimates of slip rates are determined from modeled fault offset and constrained by nearby borehole data.

# **USING GPS TO DETERMINE THE KINEMATICS OF THE ADRIATIC REGION (CENTRAL MEDITERRANEAN) AND ASSESS THE SEISMIC POTENTIAL IN THE EASTERN ALPS (ITALY).**

*Maurizio Battaglia, Roland Bürgmann, Mark H. Murray  
UC Berkeley Seismological Laboratory, Berkeley, CA USA*

*David Zuliani, Alberto Michelini  
Centro Ricerche Sismologiche, OGS, Udine, ITALY*

The Adriatic region is part of the zone of distributed deformation between the African and Eurasian plate. Seismic activity in the region is concentrated in a belt that runs through the Italian peninsula and the Balkans, roughly corresponding to the Apennines, Alps and Dynarides mountain chains. Clusters of intense seismic activity mark the southern and central Apennines, the eastern Alps, and the Albanian and Croatian coastal regions. The GPS-measured site motions in the Adriatic region are highly variable with velocities decreasing from south (~ 5 mm/yr) to north (~ 2 mm/yr). Considerable uncertainty surrounds the present kinematics of the Adriatic area, seen alternatively as an independent microplate within the Africa-Eurasia plate boundary or as a promontory of North Africa.

We use the secular pattern of surface velocities recorded by GPS measurements to investigate the active deformation of the Adriatic area. We employ publicly available GPS observations made at 23 stations of the European Reference Permanent Network (EUREF) and the Italian Space Agency (ASI) continuous GPS networks to estimate deformation in the Adriatic region. To improve the realization of a stable reference frame for the velocity solution, additional sites from the International GPS Service (IGS) and EUREF networks are included through the publicly available global regional loosely constrained solutions performed by the Scripps Orbit and Permanent Array Center (SOPAC). All together, our analysis includes more than 40 sites with at least two years of continuous GPS data available. We use a three-dimensional block-modeling approach to quantitatively test the different hypothesis proposed to explain the kinematics of the Adriatic region. This approach assumes backslip on shallow rectangular dislocations in an elastic half space to provide a reasonable approximation to observed deformation patterns. Preliminary results indicate that the Adriatic region motion is independent from the African plate motion as defined by the REVEL model for Nubia, questioning the possibility of the Adriatic region being a promontory of North Africa.

The population density and the vulnerability of the many historical towns situated in the eastern Alps (Friuli region, Italy) make the assessment of the potential of major earthquakes in this area critical. The use of GPS to monitor crustal deformation is part of the geophysical research undertaken to better understand the seismic hazard of this vulnerable area. The eastern Alps have experienced a number of destructive earthquakes, the most recent being the 1928 event (earthquake intensity  $I_0 = IX$ ) and the 1976 event ( $ML=6.4$ ,  $I_0 = X$ ). A network of continuously operating GPS receivers, the Friuli Regional Deformation network (FReDNet), is now monitoring the regional distribution of crustal deformation, providing data for earthquake hazard assessment. The FReDNet geodetic network is operated by the Centro Ricerche Sismologiche (CRS) of the Istituto Nazionale di Oceanografia e di Geofisica Sperimentale (OGS). Currently, four permanent GPS stations are operating and three more will be installed by the end of 2003. Most of the GPS sites are co-located with existing stations of the OGS monitoring seismic network. Network installation and data analysis began in the summer of 2002, and results and data are now available at <http://www.crs.inogs.it/frednet>.

# **THE MANTLE FLOW FIELD SURROUNDING SOUTHERN AFRICA: CONSTRAINTS FROM SHEAR WAVE SPLITTING MEASUREMENTS AND MANTLE FLOW CALCULATIONS**

*Mark D. Behn*

*Department of Terrestrial Magnetism, Carnegie Institution of Washington, 5241 Broad Branch Road, NW, Washington, DC, [behn@dtm.ciw.edu](mailto:behn@dtm.ciw.edu).*

*Clinton P. Conrad*

*Department of Geological Sciences, University of Michigan, Ann Arbor, MI, [cpconrad@umich.edu](mailto:cpconrad@umich.edu)*

*Paul G. Silver, Department of Terrestrial Magnetism, Carnegie Institution of Washington, 5241 Broad Branch Road, NW, Washington, DC, [silver@dtm.ciw.edu](mailto:silver@dtm.ciw.edu).*

*William Holt*

*State University of New York, Stony Brook, NY, [wholt@horizon.ess.sunysb.edu](mailto:wholt@horizon.ess.sunysb.edu)*

Dynamic topography generated by large-scale mantle upwelling beneath southern Africa has been proposed as a mechanism for the regional uplift associated with the African superswell. Such a large-scale upwelling should exert significant driving forces on the surrounding plates and affect the regional horizontal mantle flow field. To test this model we compare seismic anisotropy inferred from shear wave splitting measurements with instantaneous flow calculations that incorporate mantle density structure derived from seismic tomography, which exhibits a well-known low-velocity anomaly in the lower mantle beneath southern Africa. We calculate splitting parameters for 10 ocean island stations from the IRIS and GEOSCOPE networks surrounding southern Africa. Splitting measurements from ocean-island stations are ideal for interpreting anisotropy induced by asthenospheric flow due to the lack of a thick overlying lithosphere. In addition, these stations have good regional coverage, lying on the each of the 4 major plates in the south Atlantic and Indian Oceans. Splitting parameters are calculated at each station from a suite of earthquake events using the stacking method of Wolfe and Silver [1998]. We use the observed fast polarization directions to test the following hypotheses regarding the mantle deformation field. First, we test for a possible lithospheric contribution by comparing to the fossil spreading directions, and find that they are a poor fit to the data. We then consider several asthenospheric models with varying assumptions about the velocity at the base of the asthenosphere: that it is 1) stationary in a hotspot reference frame, 2) stationary in a no-net rotation reference frame, 3) determined by a mantle flow field predicted by instantaneous flow calculations where the flow is the result of imposed plate velocities or 4) density-driven mantle flow as inferred by mantle seismic tomography. We find that the best-fitting flow fields are those produced by instantaneous flow calculations that include density heterogeneity. Moreover, we obtain an estimate for the magnitude of the subasthenospheric flow velocity. This result suggests that we are able to directly observe the effects of large-scale upwelling on the upper mantle flow field beneath the south Atlantic and Indian Oceans.

# MAPPING LITHOSPHERIC STRENGTH HETEROGENEITIES AT REGIONAL SCALES USING P-WAVE TOMOGRAPHY

*Glenn P. Biasi*

Maps of upper mantle velocity variations using tomographic methods has become a standard product of regional seismic arrays. Tomographic maps may be interpreted in terms of lithospheric strength variations when two observations are combined. The first observation is that qualities that increase seismic velocity also increase strength. Temperature scaling is the most obvious example. While the scaling of temperature variation to velocity may be debated, the sign of it is not. Even at 50 degrees per percent  $dV_p$ , a one percent anomaly would correspond to as much as an order of magnitude increase in strength at modest strain rates. Depending on the numerical value of the derivative, even smaller velocity variations could be important for mantle lithospheric strength. Relative degrees of depletion is another example where higher velocities may reflect a greater distance from the solidus, and thus are likely to be stronger. The second observation is that while tomographic maps usually remove knowledge of absolute velocity, relative velocity variations still correspond to relative strength variations, and thus should have some influence over lithospheric dynamics. Thus strength variations are "floating" and the absolute strength is typically not known.

The ability of shallow velocity variations to predict strength variations can be tested by comparison to the locations of active faults. Results of this comparison in California and western Nevada are quite good. For example, the eastern California Shear Zone complex that included the 1992 Landers earthquake occurs just at the east end of the Transverse Range upper mantle anomaly. Faulting in the southeastern Sierra Nevada Mountains does not coincide with the pre-existing Kern Canyon fault, but rather occurs further to the east, at the edge of the upper mantle velocity body there. This is the effective western boundary of the Basin and Range at this latitude. The general lack of earthquakes in the Sierran Foothills corresponds with a long, narrow high velocity anomaly in the shallowest mantle.

There are apparent exceptions, such as where the continuous Transverse Ranges anomaly is cut by the San Andreas fault. In this case it may be that separate San Gabriel and San Bernardino Mountain elements happen to align, or the San Andreas may reflect a kinematic necessity in excess of the resisting strength. In other cases there is no mantle anomaly. In such places the crustal portion of the lithospheric strength dominates the total, and the crust does whatever is kinematically expedient. In general tomographic P-wave velocity variations do a good job of predicting fault locations in California and western Nevada, as a review of the complete map will show.

## POTENTIAL FOR GEOTHERMAL EXPLORATION USING EARTHSCOPE SEISMIC AND GPS DATA

*Geoff Blewitt (1), John Louie (1), Mark Coolbaugh (1), Don Sawatzky (1), Bill Holt (2), Jim Davis (3), and Rick Bennett (3), and Weston Thelen (1); (1) University of Nevada, Reno, NV; (2) State University of New York, Stony Brook, NY; (3) Smithsonian Astrophysical Observatory, Cambridge, MA.*

The Great Basin Center for Geothermal Energy (GBCGE) is an applied research program of peer-reviewed geothermal research projects with the goal of increasing production and utilization of geothermal energy in the Great Basin. As an example of how EarthScope might be applied to societal problems of economic significance, we note that two current geothermal exploration projects which commenced in March 2002 at GBCGE involve technologies adopted by EarthScope:

- (1) A project entitled "Targeting potential geothermal resources in the Great Basin from regional relationships between geodetic strain and geological structures" (Blewitt, P.I.) uses GPS measurements to test the hypothesis that geothermal plumbing systems might in some regions be controlled by fault planes acting as conduits that are continuously being stressed apart by tectonic activity.
- (2) A project entitled "Assembly of a crustal seismic velocity database for the western Great Basin" (Louie, P.I.) is developing a three-dimensional reference model of seismic velocity for the western Great Basin region of Nevada and eastern California to assist in the exploration for hidden geothermal resources, for which a realistic crustal and upper-mantle model is essential to understand the deep sources of geothermal heat.

Both these projects are already showing promising results. Existing geothermal power production and well temperatures correlates strongly with (1) depth to Moho, (2) the magnitude of regional strain rates, and (3) spatial change in the regional trend of Quaternary fault strike. In particular, extensive regional shear strain normal to regional tendency of fault strike in a region of low depth to Moho is an excellent predictor of currently power producing sites. For example, several power producing plants can be found along the Humboldt structural zone (an almost linear structural feature traced by Highway 80 between Reno and Battle Mountain), where there is (1) an apparent regional-scale discontinuity in both the fault-strike trend and in GPS-inferred strain orientations, and (2) anomalously high crustal heat flux, which can be explained by the seismic results showing low depth to Moho. Another more obvious example is the Walker Lane, where power producing plants (e.g., Fish Valley) can be found to be associated with step-overs in the strike-slip system. Such geothermal hot spots show up clearly in the orientation of the regional shear strain tensor with respect to fault orientation.

We anticipate that increased spatial resolution in the GPS and seismic data should improve our understanding of the precise location of existing power plants, and should therefore improve our ability to target new potential resources. The GPS and seismic data from EarthScope are clearly well suited to enhance the scientific return on these projects, and therefore its potential role in such economically beneficial applications should be further exploited, and should be emphasized to the taxpaying public.

# REAL TIME SEISMOLOGY WITH THE GLOBAL POSITIONING SYSTEM: OBSERVATIONS OF THE DENALI EARTHQUAKE WITH THE ORANGE COUNTY REAL TIME NETWORK

*Yehuda Bock, Linette Prawirodirdjo, Timothy Melbourne*

Instantaneous positioning of low-rate (30 s) Global Positioning System (GPS) data in southern California previously detected seismic waves associated with the Mw 7.1 1999 Hector Mine earthquake, including large-amplitude, long-period resonances in the Los Angeles basin left undetected by conventional seismic instruments. In response, an effort has been in progress since 2000 to upgrade sites in the Southern California Integrated GPS Network (SCIGN) sites to high-rate (1 Hz) low-latency ("real-time") (1-2 s) data collection and analysis. The first realization of this effort is the 10-station Orange County Real Time Network (OCRTN). We report on the successful detection by OCRTN of seismic waves generated by the Mw 7.9 November 3, 2002 Denali earthquake in Alaska, with horizontal amplitudes up to 30 mm and total duration of about 700 seconds. The instantaneous 1 Hz GPS horizontal displacements agree within 2-3 mm rms with nearby integrated TriNet and ANZA broadband data indicating that GPS can provide direct measurements of long-period ground motions from radiated seismic waves without the deconvolution, and clipping problems often associated with seismic measurements of large earthquakes. Thus GPS, besides measuring permanent surface deformation, can complement seismology in the study of dynamic earthquake processes at regional and global scales. Furthermore, precise high-rate, real-time GPS data have many other societal benefits, for example, intelligent transportation, public safety through airplane and harbor navigation and early earthquake notification; meteorology and short-term weather forecasting through atmospheric water vapor monitoring; infrastructure location through geographical information systems; and structural tracking through building, bridge, and dam monitoring. The synergism of real-time GPS and seismology should be taken into account in the design and implementation of Earthscope.

## **ACCESS TO GPS DATA THROUGH THE GPS SEAMLESS ARCHIVE CENTERS (GSAC) AND THE ROLE OF GSAC IN PBO**

*Fran Boler, UNAVCO Boulder Facility; Michael Scharber, Scripps Institution of Oceanography; Bob King, Massachusetts Institute of Technology; Chuck Meertens, UNAVCO Boulder Facility; Yehuda Bock, Scripps Institution of Oceanography*

The GPS Seamless Archive was created to help people find and access GPS-related data and to encourage their use and preservation for scientific investigations. It allows the user to view the holdings of all the participating data centers ("GSAC Wholesalers") through a single point of access ("GSAC Retailer"). Data kept on-line may then be downloaded through the Retailer; off-line data may be requested from the Wholesaler. Any group can become a Wholesaler by making available in an anonymous ftp directory and in a standard format a listing of its holdings of GPS observations (raw and/or RINEX), monument descriptions, solutions (SINEX), and orbital information (RINEX navigation or sp3). Any group can become a GSAC "Retailer" by providing a web or ftp interface between users and the lists provided by all Wholesalers. GSAC listings maintain a record of the original data provider as well as Wholesaler, thus providing both credit for their efforts and a clear path for corrections.

The GSAC currently comprises six Wholesalers (CDDIS, NCEDC, PANGA, SCEC, SOPAC, UNAVCO) which together hold the complete IGS data set, a nearly complete set of continuous and survey-mode data for the western US, and a substantial number of continuous and survey-mode data for the world's active tectonic zones. The current data holdings record count is over four million.

Interest in participating has been expressed by a substantial number of global, regional, and national data centers (BKG, GSD/NRCan, IGN, NGS, National Mapping/Australia) as well as several groups being funded to develop regional or national archives of continuous and/or survey-mode data (ANU, CWU, ENS, Nottingham, PGC).

SOPAC and UNAVCO currently host Retailers, which can be accessed for search and data download through a command line client or a web client. Search modes include spatial bounding box, spatial proximity, by monument metadata such as 4-character id, and/or time window. In addition, a map interface can be used for a visual search.

All PBO data and derived products will be held at two primary archives (UNAVCO and SOPAC), and will be cataloged, searchable, and downloadable via the GSAC. As part of PBO data management, the GSAC will be used for monitoring the timeliness of availability of PBO data and products.

## IU GSN SITE NOISE

*Harold Bolton Bob Hutt*

There have been a number of studies over the years that have attempted to evaluate Earth noise characteristics at the site of seismic installations. At the USGS Albuquerque Seismological Laboratory (ASL) this issue has recently been elevated for two different reasons.

The IRIS GSN SC has recently inquired as to site noise levels to aid in determining whether alternate instrumentation may be appropriate at some sites. The ASL Data Collection Center (DCC) has also been interested in acquiring and cataloging the long-term noise signatures at the different station sites for the purpose in aiding automatic QC procedures.

As an initial look into both of these processes we have generated a summary of the IU GSN site noise for the year 2002. An initial selection was made of 12 different days distributed over 2002. Each chosen day had no QED event of over 5.0Mb. We also made reasonable effort to insure that the day preceding the chosen day did not contain any large teleseismic events.

We have generated for each station a low-noise spectral estimate from each day by using 1 hour of BH (20 sps) data that has been windowed into 50% overlapping sequences. A median for each day is then constructed from the quietest 10% of each of these PSD estimates. A low noise median is then calculated for each station by calculating a median from the low noise estimates of each available day.

The resulting station signatures can be used, with appropriate care, to highlight stations that may require a revamping of the instrumentation used at the site.

# **PHYSICAL PROPERTIES AND CONTROLS ON SHEAR WAVE VELOCITY ANISOTROPY IN THE CRUST ADJACENT TO THE SAN ANDREAS FAULT IN PARKFIELD, CA. AS CALIBRATED BY THE SAFOD PILOT HOLE**

*Naomi L. Boness and Mark D. Zoback*

In June/July 2002 the SAFOD Pilot Hole was drilled 1.8 km southeast of the surface trace of the San Andreas Fault near Parkfield, CA. A comprehensive suite of geophysical logs was collected within the Pilot Hole from a depth of 700 m down to 2200 m in the highly fractured Salinian granite. In this paper we characterize the petrophysical properties of the granite such as velocity, density and resistivity as well as shear wave velocity anisotropy using data from a dipole sonic shear velocity tool. The numerous macroscopic fractures in the crust have no preferred orientation. However, the direction of maximum horizontal compression is very consistent with the fast polarization direction of the shear waves. The most likely cause of the seismic anisotropy appears to be the preferential closure of fractures in a highly fractured crust in response to the anisotropic stress state. Additional support for this interpretation is that intervals without borehole breakouts are found to correlate with regions of both increased velocity anisotropy and low seismic velocities indicating the presence of anomalously low stress magnitudes.

# **GEOPHYSICAL EVIDENCE FOR WIDESPREAD SERPENTINIZED FOREARC UPPER MANTLE ALONG THE CASCADIA AND ALASKAN MARGINS: A JUICY TARGET FOR THE U.S. ARRAY?**

*Thomas M. Brocher, Richard J. Blakely, and Ray E. Wells (U.S. Geological Survey, 345 Middlefield Rd., MS 977, Menlo Park, CA 94205; 650-329-4737, brocher@usgs.gov)*

Petrologic models suggest that metamorphism of downgoing slabs in subduction zones releases water that hydrates and serpentinitizes overlying forearc mantle. To test these models, we use the results of controlled-source seismic surveys, earthquake tomography, and potential field data to map hydrated upper mantle along the Cascadia and southern Alaskan margins. We find anomalously low velocities in the upper mantle and/or weak wide-angle Moho reflections in a narrow region along the margin, compatible with recent teleseismic studies and interpreted as a serpentinitized mantle wedge.

Further evidence for a serpentinitized forearc upper mantle wedge is provided by gravity and magnetic anomalies. Serpentinite is low in density and typically very magnetic, and thermal models suggest that upper mantle above the subducting Juan de Fuca plate is cooler than the Curie temperature. These physical properties are consistent with the curious juxtaposition of high-amplitude magnetic anomalies and low-amplitude gravity anomalies observed over the Oregon forearc. Forward modeling indicates that the subducting oceanic slab cannot account for these observations whereas the serpentinitite upper mantle wedge can. Thus, gravity and magnetic anomalies may allow us to map the wedge beneath Cascadia and at other subduction zones. A comparison of tomography and aeromagnetic data, thermal models, and earthquakes in southern Alaska suggests that magnetic mantle may be a common occurrence in forearc settings.

The existence of hydrated forearc upper-mantle wedges would have several profound geological and geophysical implications. First, they would be causally related to dehydration of the downgoing slab, a process that contributes to intraslab earthquakes. Second, in Cascadia (a warm subduction zone), the seaward limit of the forearc mantle wedge would form the downdip limit of both the transition zone of the Cascadia megathrust where long term slip rates may be accommodated by a combination of thrusting during megathrust earthquakes occurring on average every 600 years and by "rupture" of slow slip events on the megathrust occurring on average every 14 months. Third, in southern Alaska and at other cool subduction zones, the seaward edge of the hydrated mantle wedge would form the downdip limit of the locked zone of the megathrust and, consequently, the landward limit of megathrust earthquakes.

Interestingly, the geophysical anomaly characteristics of the serpentinitized upper mantle are absent south of the Blanco fracture zone, suggesting that either (1) the hotter Gorda slab releases water farther seaward of the forearc upper mantle than does the cooler Juan de Fuca slab or (2) the upper mantle wedge temperature is higher than the Curie temperature, rendering magnetite in the wedge unstable and nonmagnetic. In any case, progressive dehydration of the hydrated mantle wedge and upward flux of water through the continental crust south of the Mendocino triple junction may enhance the thermal effects of a slab gap during the evolution of the California margin by lowering the crustal melting point. This anomalous upper mantle wedge thus provides a tempting target for future U.S. Array and other Earthscope studies in the Pacific Northwest.

## **SEAFLOOR GEODETIC MEASUREMENTS ON THE JUAN DE FUCA PLATE: A PROGRESS REPORT**

*C. D. Chadwell, F. N. Spiess, J. A. Hildebrand and H. Dragert*

We report the status of measuring seafloor plate motion using a combination of precise kinematic GPS positioning of a shipboard hydrophone and acoustic ranging to seafloor transponders. This GPS-Acoustic approach has been applied at three different sites on the Juan de Fuca plate, at 150 km offshore Vancouver Island and at 150 km and 500 km offshore Newport, Oregon. The latter site being 25 km east of the south Cleft segment of the Juan de Fuca Ridge. At each site motions of a few cm/yr have been observed. We will report these results and discuss their implications.

## **STRUCTURE NEAR THE SAFOD PILOT HOLE: IMAGING RESULTS FROM VERTICAL SEISMIC ARRAY**

*J. Andres Chavarria, Eylon Shalev, Peter Malin*

In July 2003 we installed a 32 level array of 15 Hz, 3-component seismometers in the San Andreas Fault Observatory at Depth Pilot Hole. The Pilot Hole sits on the southwestern side of the Parkfield segment of the San Andreas Fault Zone. The array levels are spaced 40 m apart and cover the depth interval of 856 to 2096 m. Both surface explosion and earthquake data have been recorded with the array using sampling rates of 1 or 2 KHz. Because of their location below the complex structure and strong attenuation of the near surface, the microearthquake recordings contain seismic energy up to very high frequencies, for some events as high as 600 Hz.

Travel time curves from these data and secondary phases contain evidence for the scattering of P and S waves within the fault zone. Further, the fault zone P and S wave velocity structures appear to vary in significantly different fashions.

We have implemented a Kirchhoff migration scheme in order to analyze the possible origin of the secondary phases seen in the data. Migration analysis of converted waves has enabled us to get a direct glimpse into the complexity of the San Andreas Fault structure in the area of the SAFOD proposed drilling site. Secondary arrivals in the seismic records appear to correspond to a number of scatterers in the borehole area. These scatterers are interpreted to be associated to the complex fault structure that surrounds the study area and that includes the San Andreas Fault itself. These structures are important since future drilling of the SAFOD project will have to go through them.

# **A SEARCH FOR LATERAL VARIATIONS IN THE STRUCTURE OF AT THE TOP OF THE INNER CORE**

*Vernon F. Cormier and Anastasia Stroujkova Department of Geology and Geophysics  
University of Connecticut Storrs, CT 06269-2045*

Broadband PKIKP + PKIIKP+...+ PKiKP waveforms in the distance range 120 to 140 deg. are inverted for velocity and parameters for both viscoelastic and scattering models of attenuation in the inner core. Reference waveforms used in the inversion, which include a network averaged mantle attenuation operator, are constructed from source-time functions determined from P waves observed in the 30 to 90 deg. range. To determine whether a simple hemispherical variation of inner core properties can be robustly detected with existing data, tests of spatial aliasing are made using waveforms synthesized along observed paths in spatially complex inner core structures. Among these structures is a model in which attenuation in the upper 300 km of the inner core is assumed to be correlated with the pressure field of fluid flow in the outer core predicted at the core-mantle boundary from the geomagnetic field.

## **NEW IMAGES OF Q IN THE UPPER MANTLE: CONSTRAINTS FROM SURFACE WAVES**

*Colleen Dalton and Goran Ekstrom, Department of Earth and Planetary Sciences, Harvard University, Cambridge, MA 02138.*

Studies of the Earth's anelastic structure can provide important constraints on mantle dynamics that are complementary to those obtained from elastic velocity modeling. In particular, warm features and the presence of melt may be highlighted in images of attenuation. However, determining seismic wave attenuation, which is measured by the decay of wave amplitudes, is a difficult problem. Seismic wave amplitudes are sensitive not only to the Earth's anelastic structure but also to uncertainty in the earthquake source moment and to focusing effects from lateral heterogeneities. We present new global measurements of Q in the upper mantle in the period range 150-300 seconds. Even- and odd-degree Q structure is examined with several techniques that make use of improved amplitude measurements of Rayleigh and Love waves (Ekstrom et al., 1997). We initially calculate Q by constructing a datum that uses the amplitudes of four consecutive wave trains (i.e., R1, R2, R3, R4) to remove the extraneous effects on the amplitude. The results are inverted for maps of even-degree attenuation structure. We also obtain new globally-averaged values of Q from this procedure and compare them to existing models. Next, the amplitudes of the minor-arc and major-arc wave trains are inverted for maps of even- and odd-degree Q structure. We examine how the results are affected by the inclusion of a "focusing" term that approximates the effect on the amplitudes due to focusing by elastic structure. The resulting maps are compared to existing maps of Rayleigh and Love wave Q values from earlier studies. The significance of these results in terms of variations in Q structure with depth is also considered.

## **THE ULTIMATE GOAL: A UNIFIED SEISMIC MODEL OF MAGMA TRANSPORT MECHANICS**

*Phillip Dawson and Bernard Chouet Volcano Hazards Team US Geological Survey  
dawson@usgs.gov, chouet@usgs.gov*

By developing a comprehensive theory of the seismic sources of volcanic activity, a quantitative interpretation of the elastic wavefields associated with magmatic and/or hydrothermal transport in volcanoes can be made. The seismic methods developed toward meeting this theory provide unique tools that enable the understanding of the dynamics of active magmatic systems, the determination of in situ mechanical properties of the systems, and enable the mapping of the extent and evolution of magmatic sources. To provide adequate real-time hazards analyses of volcanic activity a unified seismic model that describes magma transport mechanics and the associated structural parameters of active magmatic systems should be the ultimate goal. Our efforts toward this goal have been targeted toward understanding the nature and dynamics of seismic sources associated with magmatic injection and magmatic transport. These efforts include: (1) deriving high-resolution three-dimensional P- and S-wave velocity models to understand the structure of volcanic systems; (2) conducting moment-tensor inversions of broadband waveform data to characterize the location, geometry, and orientation of conduit systems and to quantify mass transport processes in volcanic edifices; (3) quantifying the source properties of volcano-tectonic (VT) and long-period (LP) earthquakes associated with magma migration and eruptions; (4) investigating the composition of tremor wavefields, tracking tremor sources in space and time, and elucidating the fine-scale surficial velocity structure of volcanoes using small-aperture seismic antennas; (5) performing numerical investigations of seismic waves and magma dynamics associated with volcanic eruptions; (6) probing the nature of fluid compositions beneath volcanoes by evaluating the complex frequencies of LP earthquakes; (7) conducting laboratory experiments to investigate the properties of foam flows; and (8) performing numerical simulations of conduit flows of multi-phase fluids.

As Earthscope marches on, we believe that significant emphasis should be applied toward the quantitative understanding of volcanic processes, thereby improving our ability to predict the onset of volcanic activity during crisis situations. A prerequisite for the quantification of these processes is the ability to extend the frequency range of recorded seismicity, spanning the gap between traditional static measurements and short-period seismometry. To this end, the use of dense arrays of broadband seismometers targeting specific volcanic and hydrothermal systems is the next logical step toward our goal.

# **BROADBAND SEISMIC NOISE ANALYSIS OF THE HIMALAYAN NEPAL TIBET SEISMIC EXPERIMENT**

*Thomas de la Torre, Anne Sheehan, and Fred Blume*

A background noise analysis is conducted as part of the Himalayan Nepal Tibet Seismic Experiment (HIMNT), a Passcal broadband seismic deployment involving 28 seismometers deployed in eastern Nepal and southern Tibet from Fall 2001- Fall 2002. The noise study was performed in order to assess experimental vault construction design, determine noise variations with time of day and season, to determine site characteristics and response, and to identify sites of seismometer placement for future experiments. Power Spectral Density (PSD) estimates of background noise are calculated for each component of the fifteen Streckeisen STS2 broadband seismometers deployed in Nepal, and then compared to the High Noise Model (HNM) and Low Noise Model (LNM) of Peterson (1993). All waveforms from designated day and night local time windows for twenty-five to twenty-seven day time periods are included in the calculation without parsing out events. Noise levels are found to be considerably higher for the first month of the experiment (October 2001) relative to later times (March 2002), particularly in the low frequencies. The time period needed for the site to stabilize is investigated. Preliminary estimates from the January time period show moderate noise levels with all stations falling within the HNM and LNM bounds, except for the southern Nepal (Terai) stations, which exceed the HNM at frequencies greater than 1 Hz. Vaults in the high water table area of southern Nepal were installed in specially constructed above ground vaults. The noise characteristics of two different site designs for the Terai relative to each other and to the other stations of the array is discussed.

# **EPISODIC TREMOR AND SLIP (ETS) ON THE CASCADIA SUBDUCTION ZONE: THE CHATTER OF SILENT SLIP**

*Herb Dragert and Garry Rogers*

The Cascadia subduction zone is a region that has repeatedly ruptured in great thrust earthquakes of moment magnitude ( $M_w$ ) greater than 8. Recently, the occurrence of discrete slip events on the deeper part of the northern Cascadia subduction zone interface has been recognized by observing transient surface deformation on a network of continuously recording Global Positioning System (GPS) sites. For the plate interface underlying southern Vancouver Is., these slip events have occurred down-dip from the currently locked, seismogenic portion of the subduction zone, and appear to repeat at 13 to 16 month intervals. These past slips were not accompanied by earthquakes and were thought to be seismically “silent”. However, using records from the regional digital seismic network, unique non-earthquake signals have now been identified to accompany the occurrence of slip. These pulsating, tremor-like seismic signals appear similar to those reported in the fore-arc region of Japan, but the signals observed in Cascadia correlate temporally and spatially with the six deep slip events observed over the past seven years. At other times, this tremor activity is minor or non-existent. These tremors have a lower frequency content than nearby earthquakes, and they appear uncorrelated with the deep or shallow earthquake patterns in the region. They have been observed only near the subduction zone interface and specifically in the same region as the deep slip events. These observations establish that Cascadia transient slip has a characteristic seismic signature, and we refer to this associated tremor and slip phenomenon as Episodic Tremor and Slip (ETS).

## **CRUSTAL PRODUCTION AND LOSS IN CONTINENTAL MAGMATIC ARCS; EVIDENCE FROM THE SIERRA NEVADA**

*Mihai N. Ducea University of Arizona, Dept. of Geosciences, Tucson, AZ 85721  
ducea@geo.arizona.edu Jason Saleeby Caltech, Geological and Planetary Sciences,  
Pasadena, CA 91125 jason@gps.caltech.edu*

Garnet pyroxenites are the most common deep-lithospheric xenolith assemblages found in Miocene volcanic rocks that erupted through the central part of the Sierra Nevada batholith. Elemental concentrations and isotope ratios are used to argue that the Sierra Nevada granitoids and the pyroxenite xenoliths are, respectively, the melts and residues/cumulates resulting from partial melting/fractional crystallization at depths exceeding 35-40 km. The estimated major element chemistry of the protolith resembles a basaltic andesite. Effectively, at more than about 40 km depth, batholith residua are eclogite facies rocks. Isotope ratios measured on pyroxenites document unambiguously the involvement of Precambrian lithosphere and at least 20-30% (mass) of crustal components. The mass of the residual assemblage was significant, 1 to 2 times the mass of the granitic batholith. Dense garnet pyroxenites are prone to foundering in the underlying mantle. An average removal rate of 25-40 km<sup>3</sup>/km m.y is estimated for this type Cordilleran arc, although root loss could have taken place at least in part after the cessation of arc magmatism. This rate is matched by the average sub-crustal magmatic addition of the arc (~23-30 km<sup>3</sup>/km m.y), suggesting that the net crustal growth was close to zero. It is also suggested that in order to develop a convectively removable root, an arc must have a granitoid melt thickness of at least 20-25 km. Residues of thinner arcs should be mostly in the granulite facies; they are not gravitationally unstable with respect to the underlying mantle.

# **SOURCE OF SEISMIC NOISE FROM DIRECTIONAL INFORMATION: IMPLICATIONS RANGING FROM NETWORK DESIGN TO OCEAN WAVE HEIGHT**

*Paul S Earle, Vera Schulte-Pelkum, Dan E McNamara, and Frank Vernon*

The Earth is never quiet. Broadband seismographs dotting the globe continuously record vibrations generated by passing cars, blowing trees, and stormy oceans. Knowing the source of this non-earthquake background noise at a given site can aid network design and provide insights into the physical phenomena responsible for the noise. Determining the source of seismic noise generally relies on amplitude measurements. Here we investigate the additional information provided by directional data. We focus on ocean-generated microseisms, the dominant feature in the noise spectrum. Time-lapse movies of ocean swells and concurrent microseism polarizations and array beam azimuths reveal a direct causal relationship between swells arriving at different North American coastal areas and the observed microseism propagation direction. We find dominant source areas for microseismic noise observed in southern California as distant as Newfoundland and British Columbia, and show that microseism amplitudes strongly depend on the direction of the approaching swell.

# GEODETIC CONSTRAINTS ON THE EARTHQUAKE DEFORMATION CYCLE ALONG THE WESTERN NORTH ANATOLIAN FAULT: IMPLICATIONS FOR EARTHQUAKE MECHANICS ON CONTINENTAL STRIKE-SLIP FAULTS

*S. Ergintav(1), S. McClusky(2), E. Hearn(3), R. Cakmak(1), O. Lenk(4), E. Evren(5), H. Ozener(6) and R. Reilinger(2) (1) TUBITAK, Marmara Research Center, Earth and Marine Sciences Research Institute, Gebze 41470, Turkey, (2) Department of Earth, Atmospheric, and Planetary Sciences, Massachusetts Institute of Technology, Cambridge, MA, USA (reilinge@erl.mit.edu), (3) Department of Earth and Ocean Sciences, The University of British Columbia, Vancouver, V6T 1Z4, Canada, (4) General Command of Mapping, Cebeci, Ankara, Turkey, (5) Istanbul Technical Univ., Eurasia Earth Science Institute, Ayazaga, Istanbul, Turkey, (6) Kandilli Observatory and Earthquake Research Institute, Bogazici Univ., Istanbul, Turkey*

The 1999 Izmit (M=7.5) and Duzce (M=7.1) earthquake sequence on the western North Anatolian fault is providing quantitative information to constrain the mechanics of strike-slip faulting, the physical nature of the earthquake deformation cycle, and the rheology of the lower crust/upper mantle in NW Turkey. We present geodetic estimates of pre-seismic, co-seismic (Izmit), early post-seismic (first 3 months), and late post-seismic (after 3 years) motions around the Marmara Sea/Izmit earthquake area. We interpret the observed deformation in terms of aseismic fault slip at depth (pre-seismic) that loads the seismogenic fault (i.e., above about 20 km), catastrophic failure within the seismogenic zone (coseismic), and accelerated aseismic fault slip following the earthquake concentrated below fault patches with high coseismic slip and on shallower patches that experienced reduced coseismic slip (including the hypocentral area). In addition, we show that the early phase of postseismic afterslip is a plausible mechanism that helped trigger the Duzce earthquake that occurred approximately 3 months after the Izmit earthquake. We document significant differences between the pattern and rate of strain accumulation observed before and after (3 years) the 1999 earthquake sequence (i.e., late in the earthquake cycle vs. early in the earthquake cycle). In particular, we interpret rapid strain accumulation rates observed early in the earthquake deformation cycle in terms of continuing deep afterslip and/or relaxation in the lower crust and upper mantle in response to stresses induced by sudden coseismic slip within the seismogenic layer. We are actively investigating, and expect to report on the implications of these data for fault mechanics, and crustal, and upper mantle rheology. Given the similar character of the North Anatolian and San Andreas faults, these results will be useful for designing the PBO network and interpreting observations along the San Andreas fault system.

# **FIRST RESULTS OF PHYSICS-BASED, INTEGRATIVE MODELS OF THE SAN ANDREAS FAULT SYSTEM NEAR THE BIG BEND INCLUDING FLUIDS, TECTONICS, AND POST-SEISMIC RELAXATION.**

*Delphine D. Fitzenz (1), Fred Pollitz (1), and Stephen A. Miller (2) (1) U.S. Geological Survey, Menlo Park (2) Geophysics Institute, ETH Zurich (CH)*

We present a set of time-forward physics-based, regional models of a fluid-saturated San Andreas Fault system near the Big Bend. The aim is to develop an interplay between modeling and observational data such as seismic imaging, seismicity, and geodetic data to establish the large-scale boundary conditions, choose the model geometry, and validate model hypotheses. Targeting measurable properties in or around fault zones, (e.g. pore pressures, seismicity patterns, stress orientation, surface strain, triggering, etc.), allows inferences on the stress state of the system and on the extent and persistence of stress perturbations related to local seismicity. In a first model, faults are viscoelastic bodies subjected to ductile compaction and shear creep, embedded in an elastic half-space. The two 200 km-long specified faults are on the plate boundary and are oriented 20 degrees with respect to each other. Tectonic loading is modeled as a combination of shear drag parallel to the Northern segment and an East-West compression approximated by a vertical dislocation surface, with rates constrained by GPS measurements. Results show that over-pressured compartments on model faults through ductile compaction develop in response to the tectonic loading, specifically where high normal stress acts on long straight fault segments. We show that a transpressional tectonic regime develops South-West of the model Big Bend as a result of the loading boundary conditions. Large earthquakes initiating on one fault occasionally trigger events on the other fault (coseismic interaction). Stress transfer from fault slip are shown to induce significant perturbations in the local stress tensor (stress rotations). The changes in tectonic regimes indicate that the dynamic generation of new faults will have to be implemented for simulations of the long-term behavior. In a second simulation, the model was coupled to a visco-elastic lower crust and post-seismic relaxation was introduced as a time-dependent perturbation in the background plate motion. Results show large changes in the stressing rates for the two faults as well as a change in the Gutenberg-Richter statistics compared to the case without post-seismic effects. This approach can be used to develop tectonic models to mechanistically assess the seismic hazard of regional systems.

# UNDERSTANDING THE DRIVING FORCES OF WESTERN NORTH AMERICA DEFORMATION USING GEODESY, SEISMOLOGY, AND GEOLOGY

*Lucy M. Flesch (Carnegie Institution of Washington, Department of Terrestrial Magnetism) , William E. Holt, Lianxing Wen, Elliot Klein (Department of Geosciences, SUNY - Stony Brook), A. John Haines (Bullard Laboratories, University of Cambridge), and Bingming Shen-Tu (Air Worldwide)*

To fully understand the deformation occurring along the western North American plate boundary zone it is necessary to quantify the forces responsible for such deformation. We take an integrated approach to investigate the combined effect of basal tractions, lithospheric gravitational potential energy (GPE), and Pacific-North American relative plate motion on western North America deformation. The first step involves solving for the velocity gradient tensor field using ~1200 GPS observations, 226 fault slip segments, and ridge spreading rates. We then use a finite element approach to separately quantify the vertically averaged (over 100-km) deviatoric stress field associated with GPE variations and basal tractions. GPE estimates are determined using the ETOPO5 data set, the EGM96 geoid model, and the CRUST2.0 seismic crustal thickness model. We determine the basal traction inputs from an isoviscous three-dimensional large-scale mantle convection model with mantle density variations determined using tomographic data. In an iterative inversion, we then solve for a stress field boundary condition associated with the accommodation of Pacific-North America relative plate motion. In this inversion for a stress field boundary condition we seek a best fit of the model deviatoric stress field, defined by the sum of the boundary condition solution, the basal traction solution, and the GPE contribution, to stress field indicators. We assume that the relation between deviatoric stress directions and strain rate directions is isotropic, and thus the directions and style of principal axes of kinematically defined strain rates are the appropriate stress field indicators. In a second iterative inversion we not only solve for a best-fit stress field boundary condition but also a single scaling factor for the stress field associated with basal tractions to place an upper bound on the level of basal tractions acting within western North America. Results to date suggest that there must be a significant decoupling between deeper mantle circulation and the lithosphere in western North America. The deeper mantle circulation beneath the lithosphere in western North America appears to be dominated by an E-NE directed flow associated with the deeper negative buoyancy of the Farallon slab, present in the tomographic data. A strong coupling of this flow to the overlying lithosphere results in a poor fit to extension directions along the eastern margin of the Great Basin. There is a trade-off between the magnitude of the stresses associated with basal tractions, and the stress field boundary condition. Using basal scaling factors of 0.1-0.4 produces total deviatoric stress fields that fit the stress field indicators and produce similar sum of square values. The overall relative role of driving mechanisms are similar to that obtained by Flesch et al. [2000] with Pacific-North America plate interaction contributing about 50% of the driving forces responsible for Great Basin deformation, GPE differences about 30 - 50%, and basal tractions less than 20%. Once a best-fit total deviatoric stress field solution is determined we infer the absolute magnitudes of the vertically averaged effective viscosities of the lithosphere by dividing the magnitudes of our deviatoric stresses by the magnitudes of the strain rates, inferred from geodesy and geology. Using this effective viscosity distribution, body force distribution used to estimate GPE variations, and a velocity boundary condition determined in the kinematic solution, we solve for dynamic stress and strain rate fields, as well as a dynamic velocity field that can be directly compared to GPS measurements. The modeling technique we present can provide information that can aid in strategic placement of GPS for EarthScope planning. Results to date indicate many regions where the dynamics are poorly resolved due to poor resolution of surface strain rates inferred from GPS observations. Improved tomography and crustal thickness models, as well as more accurate three dimensional circulation models, are also likely to lead to significantly improved resolution of dynamic models.

# RESOLVING STRUCTURAL DETAILS OF EARTHQUAKE RUPTURE THAT GIVE RISE TO DAMAGING GROUND MOTION AND EXTENDING THIS CAPABILITY TO SMALL-MAGNITUDE EVENTS USING PBO BOREHOLE INSTRUMENTATION

*J. B. Fletcher and A. McGarr US Geological Survey Menlo Park, CA 94025*

Slip models of major earthquakes have revealed considerable complexity in the distribution of fault displacement, with localized asperities of high slip separated by broader regions of much lower average slip. Slip models, which entail the division of an earthquake fault zone into many subfaults, result from inverting seismic and geodetic data to estimate the time-dependent slip within each subfault as it increases from zero to its final value. It has recently been shown that, in addition to the distribution of time-dependent slip over an earthquake fault zone, the slip-model information, including the rupture velocity, can be used to estimate the seismic energy radiation and the apparent stress for each subfault, as well as static stress drop and stiffness (McGarr and Fletcher, 2002). With the capability to produce maps of energy radiation and apparent stress over the fault plane, as well as slip or seismic moment, we can address a number of fundamental questions critical to our understanding of how earthquakes work including what factors give rise to patches of especially intense energy radiation, the extent to which "characteristic earthquakes" are really similar, the influence of the geology of the seismogenic crust on the earthquake source, and the nature of earthquake scaling.

Maps of the distribution of seismic energy radiation in space and time, for instance, has revealed, that its distribution is heterogeneous marked by peaks apparently associated with asperities rather than a smooth rupture front. Of more interest, the time-dependent power radiated from an earthquake fault zone is not well correlated with seismic moment rate; the peaks in power tend to precede the major moment releases.

In addition to the seismic energy radiated from each subfault, we are also able to estimate the nearby quasi-static strain energy release that results in the seismic slip. In this way, it is possible to determine distributions of static stress drop and fault stiffness, both of which show substantial variability. At the hypocenter of the 1995 Kobe, Japan, M6.9 earthquake, for instance, a slip of about 1.65 m was associated with a stress drop of 6.4 MPa, yielding a stiffness of about 3.9 MPa/m. Smaller values are found in the near-surface layer. Together with results from previous studies, which indicated how apparent stress is related to the shear stress causing fault slip, knowledge of the static stress drop allows us to estimate the yield stress for each subfault, which can be compared to independent estimates of crustal strength based on other types of information, including borehole in situ stress measurements. At the hypocenter of the Kobe earthquake, the yield stress appears to be about 12 MPa.

For purposes of investigating these various issues, however, the current set of slip models has the limitation that nearly all of them are for major earthquakes. This is largely because of band-limited seismic data that are not capable of resolving the slip distributions of smaller earthquakes in detail. Clearly, progress in understanding the earthquake source would be accelerated considerably if we could develop slip models for much smaller, and more frequent, earthquakes (see Fletcher and Spudich, 1998 for one attempt). For example, slip-model studies of smaller magnitude earthquakes would enhance the possibility of investigating the issue of the extent to which characteristic, or repeating, earthquakes are the same structurally.

The PBO component of Earthscope provides an excellent opportunity to extend slip-model analysis to smaller magnitude earthquakes. In particular, we strongly recommend installing broad-band, wide-dynamic-range seismometers in the strainmeter boreholes planned for western North America, especially at intensely studied sites such as Parkfield, California. These arrays of borehole tensor strainmeters and seismic recorders would provide for small magnitude earthquakes the information necessary to develop slip models at levels of relative detail comparable to what can currently be resolved for major earthquakes using strong ground motion, teleseismic, and geodetic data.

Fletcher, J.B. and P. Spudich (1998). Rupture characteristics of the three M~4.7 (1992-1994) Parkfield earthquakes, *Jour. Geophys. Res.*, 103, 835-854.

McGarr, A. and J.B. Fletcher (2002). Mapping apparent stress and energy radiation over fault zones of major earthquakes, *Bull. Seism. Soc. Amer.*, 92, 1633-1647.

## NEW EVIDENCE FOR SEISMIC SCATTERERS WITHIN EARTH'S INNER CORE

*Jill M. Franks and Keith D. Koper Dept. of Earth and Atmospheric Sciences Saint Louis University St. Louis, MO 63103, USA*

It is well known that Earth's inner core is a region of high seismic attenuation, however it is less clear if the dominant mechanism is scattering or anelasticity. The recent discovery of seismic energy backscattered from within the inner core (ICS) strongly suggests the existence of small-scale heterogeneities in the outer portion of the inner core. Possible explanations for the heterogeneities include variations in composition, such as pods of partial melt, or variations in orientation or strength of seismic anisotropy.

We have recently begun a search for observations of ICS using data from the small aperture array stations of the International Monitoring System. These stations generally have poorer slowness resolution than LASA (the now defunct array at which the original ICS observations were made), but are small enough that high frequency energy remains coherent across the array and can be substantially enhanced through beamforming. We selected seismic event data from the Harvard CMT database beginning on 1/1/1995 and ending on 2/20/2000. Our search criteria required events to occur at distances between 50-90 degrees, along with a depth of 50-800km, and a favorable focal mechanism by means of a radiation pattern coefficient greater than 0.7.

Out of the 275 event/receiver combinations we were able to obtain data for, 35 were positive for ICS, 75 were negative for ICS, and 165 were inconclusive.

The criteria for designating an observation as positive were (1) a significant increase in high frequency energy at the theoretical PKiKP arrival time on beams formed with the theoretical PKiKP slowness and (2) an observed slowness for this energy that was substantially lower than that observed for P/PcP energy on the same record. We intend to experiment with different event search criteria in an attempt to expand our dataset as well as utilize our current observations of ICS in order to seek an understanding of the type and size of heterogeneities in the inner core.

## **ONGOING EFFORTS AT STUDYING POSTSEISMIC DEFORMATION FOLLOWING THE 2002 DENALI FAULT EARTHQUAKE**

*Jeffrey T. Freymueller Roland Burgmann Eric Calais Andy Freed Sigrun Hreinsdottir Chris Larsen*

The 2002 Denali Fault earthquake was the largest continental strike-slip earthquake in the North America since the 1857 Fort Tejon earthquake on the San Andreas fault. The existence of numerous GPS sites surveyed before the earthquake, and a rapid post-earthquake response, makes this an ideal opportunity to study postseismic deformation following a large event, and to learn about the rheological properties of the crust and upper mantle, and a mature fault zone at depth. In addition to surveying numerous survey-mode GPS points, we established (with critical support from UNAVCO engineers) ten continuous GPS sites and four quasi-continuous sites within two weeks of the earthquake.

The measurements to date reveal rapid postseismic deformation, with temporal variations ranging from days to months. This poster will present a summary of the most interesting results to date.

## **EARTHSCOPE (USARRAY) TARGETS IN SOUTHERN CALIFORNIA: MID-CRUSTAL DECOLLEMENTS BENEATH THE TRANSVERSE RANGES**

*Fuis, G.S., V.E. Langenheim, K.A. Howard, S. Baher, R.D. Catchings, J.M. Murphy, and M.J. Rymer (U.S. Geological Survey, Menlo Park, CA 94025; 650-329-4758; fuis@usgs.gov), D.A. Okaya and T.L. Henyey (University of Southern Calif., Los Angeles, CA 90089; 213-740-7452; okaya@usc.edu), R.W. Clayton and E. Hauksson (Calif. Institute of Technology, Pasadena, CA 91125; 626-395-6909; clay@gps.caltech.edu), P.M. Davis (University of Calif. Los Angeles, Los Angeles, CA 90024), and C. Nicholson and M.E. Oskin (University of Calif., Santa Barbara 93106; craig@crustal.ucsb.edu)*

The Transverse Ranges of southern California, straddling a stretch of the San Andreas fault that is oblique to plate motion vectors, promise to be a productive region in which to investigate the linkage of strike-slip and compressional tectonics using flexible arrays under the USArray component of Earthscope. The central Transverse Ranges have been investigated recently by two active- and passive-source seismic-imaging surveys approximately 70 km apart (Los Angeles Region Seismic Experiment--LARSE I and LARSE II). These surveys imaged mid-crustal reflective zones, interpreted as decollements, that originate at the San Andreas fault, extend southward beneath the Transverse Ranges and sedimentary basins of the Los Angeles region, and connect or appear to connect upward to compressional faults, including the exposed Sierra Madre and San Gabriel faults and the thrust faults that ruptured in the 1971 San Fernando and 1987 Whittier Narrows earthquakes. In the Transverse Ranges north of the Whittier Narrows epicenter, the reflective zone contains anomalously bright reflections and is subhorizontal (LARSE I); in the Transverse Ranges north of the San Fernando epicenter, the reflective zone contains clear but not anomalous reflections and dips moderately northward (LARSE II). These interpreted decollements may be continuous with one another. To test this possibility, we propose to image the region between the two LARSE surveys, through the vicinity of downtown Los Angeles, where such a decollement may be connected upward to postulated blind thrust faults beneath the Elysian Park anticline. We propose a seismic-imaging survey that begins at the coast, approximately follows the Los Angeles River northward, crosses the Elysian Park anticline, passes through the triple junction of the Hollywood, Verdugo, and Raymond faults, and passes over the Transverse Ranges to the Mojave Desert.

In addition to this proposed transect, there are at least two other proposed transects, both east and west of the Los Angeles region, where mid-crustal decollements are likely to be imaged. In the eastern Transverse Ranges, exposed thrust faults along both north and south flanks of the San Bernardino Mountains dip beneath the mountains toward the complex San Andreas fault zone. A seismic-imaging transect through this region may determine if there is a mid-crustal decollement that roots at the San Andreas fault and connects upward to the exposed thrusts. A decollement may even link the San Andreas with the eastern California shear zone on the northeast and with the San Jacinto/Elsinore system on the southwest. A western transect, across the western Transverse Ranges, would address whether one could image a mid-crustal slip surface above which the upper crust is interpreted to have rotated by more than 90 degrees clockwise beginning in the early Miocene (~19 Ma).

## **2-D NUMERICAL MODELING OF NEW MADRID AND CHARLESTON SEISMIC ZONES – IMPLICATIONS FOR SEISMOGENESIS IN STABLE CONTINENTAL REGIONS**

*Abhijit Gangopadhyay and Pradeep Talwani*

Simplified two-dimensional numerical modeling using a Distinct Element Method was performed for New Madrid and Charleston seismic zones. In each case the model geometry was developed with appropriately oriented blocks and suitable elastic properties and were subjected to an appropriately oriented horizontal stress field.

In the case of New Madrid Seismic Zone the model results show higher concentrations of shear stresses and shear strain near the fault intersections inside the Reelfoot rift particularly the intersections of the Blytheville Fault Zone and the Reelfoot fault, Blytheville Fault Zone and Missouri batholith, and Reelfoot fault and New Madrid fault (North). The sense of rotation as predicted by the model for the New Madrid fault (North) is also in agreement with its observed offset from independent geologic studies. Absence of comparative shear stress and hence shear strain build-up along the Reelfoot rift boundary faults also corroborated well with the observations that there is almost no slip along the rift boundary faults.

In the Charleston seismic zone seismicity occurs within the South Georgia rift basin. The results of modeling indicated an anomalous stress build-up in the vicinity of the intersections of the Woodstock and Ashley River faults, and it was located on the northeast periphery of a buried pluton. The location of this stress build-up was consistent with the locations of observed seismicity and enhanced strain rate accumulation derived from GPS.

The observed location of seismicity for both cases matches the locations of modeled stress build up suggesting that local stress concentrators play an integral role in the genesis of Stable Continental Region earthquakes.

## HIGH RESOLUTION WAVEFORM TOMOGRAPHY AT A GROUNDWATER CONTAMINATION SITE: COMBINED SURFACE REFLECTION AND VSP DATA

*Fuchun Gao (1), Alan Levander (1), Gerhard Pratt (2), Colin Zelt (1) and Sangwon Ham (1) (1) Center for Computational Geophysics, Rice University, Houston, TX, 77005 (2) Department of Geological Science, Queensj~ University in Kinston, Ontario, Canada alan@rice.edu/Fax: 1-713-348-5214*

This study first applies a form of waveform tomography (Pratt et al., 1998) to datasets from a vertical seismic profile (VSP) and a surface dataset from Hill Air Force Base (HAFB), Utah. The data were acquired in 2000 along with 3D surface reflection and 3D surface tomography datasets (see companion posters by Dana et al., and Azaria et al.). A good match (69.6% reduction in spectral misfit) was obtained between the observed and synthetic seismograms. The inversion model shows velocities from ~300m/s at the surface to 1600m/s at 15.0m depth, an extremely high vertical gradient of ~80.0 m/s/m. Laterally velocities at a given depth vary by as much as 79.4 % from the mean. Geologically, the model is interpreted as a thin layer of desert hardpan overlying a heterogeneous layer of dry unconsolidated gravel, grading into increasingly saturated gravels and clay to 16.0m depth. A resolution analysis made with a synthetic dataset compared the relative performance of travel time tomography and waveform tomography and estimated the smallest scale feature recovered with each. Features as small as ~1.5m scale are reconstructed with waveform tomography, whereas travelttime tomography on the same dataset identifies features only as large as ~7.0m. This agrees well with the rules of thumb that the resolution in waveform inversion scales with wavelength and the resolution in travel time tomography scales with Fresnel zone. The waveform tomography velocity model is interpreted petrophysically by forward modeling the 1D velocity profile averaged from the waveform tomography model using the Hertz-Mindlin theory and Gassmanj~s equation.

The transmitted waves recorded at depths in the VSP data constrain deep structures better than the surface data. However, surface data with large offsets could provide good depth-constraining seismic phases such as refraction/reflection waves which are not contaminated by ground roll. This study applies waveform tomography to two 36.0-meter-long surface profiles almost perpendicular to the surface spread of the VSP experiment. The 2D profiles are part of the 3D surface reflection dataset from the HAFB seismic experiment. Travel time tomography applied to the profiles provides initial velocity models for the waveform tomography. Seismic velocity increases from ~300.0m/s at the surface to ~1500.0m/s at 16.0m depth. The cross-sectional geometry of the paleo-channel, the structural trap containing most of the DNAPLs, can be identified in the final velocity models. The combination of velocity models from waveform tomography applied to the VSP and surface reflection datasets provides a 3D perspective on velocity structure imaged with relatively high resolution.

# IMAGING THE SOUTH CENTRAL ANDEAN LITHOSPHERE USING PASSIVE BROADBAND SEISMOLOGY: CHILE-ARGENTINA GEOPHYSICS EXPERIMENT

*Hersh Gilbert, Susan Beck, George Zandt, Patricia Alvarado, Megan Anderson, Robert Fromm, Lara Wagner, and Tom Owens<sup>1</sup> University of Arizona <sup>1</sup>University of South Carolina*

The surface tectonics and volcanism of central Chile and Argentina where the subducting Nazca plate flattens differs from surrounding regions to the north and south where the slab dips more steeply. However, the factors contributing to the near horizontal subduction of the Nazca plate near 100 km depth, and the interaction between that plate and the overriding lithosphere remain poorly constrained. The recent Chile-Argentina Geophysics Experiment (CHARGE) was deployed to gain a better understanding of why the Nazca plate subducts at a shallow angle, and the nature of the coupling between the flat subducting plate and the South American lithosphere.

The CHARGE PASSCAL array consisted of 22 broadband seismometers configured in two east-west transects at 30°S and 36°S. These instruments recorded continuously between November 2000 and May 2002. Data from teleseismic P and PP arrivals were used to calculate receiver functions, which isolate P-to-S converted arrivals to image crustal and upper mantle structure. By geographically stacking receiver functions into common conversion point bins, we observe that the crust is near 40 km thick below the Sierras Pampeanas to the east of the Andes. Estimating crustal thickness within the Andes has proven to be more difficult, as we have not been able to confidently isolate arrivals from the base of the crust on receiver functions. This difficulty may result from scattering of the teleseismic wavefield due to the non-planar structure of the Andean crust, or the presence of a gradient zone between the crust and mantle such that a simple sharp converted arrival would not be produced.

Below the Moho, the receiver functions display evidence for the flat subducting Nazca plate near 100 km depth below the northern line (30°S) as well as the slab dipping more steeply below the southern line (36°S). At greater depths, we observe a strong laterally continuous arrival from the 410-km discontinuity, but a much less coherent arrival from the 660-km discontinuity, which fluctuates in amplitude and pulse shape. The thickness of the transition zone (region between the 410- and 660-km discontinuities) increases to the east, consistent with cooler temperatures associated with the presence of a slab towards the east.

Utilizing local seismicity has helped identify the flat slab, and state of stress in the crust and flat slab. Relocating hypocenters illustrated a strong clustering of events in the flat slab region. Slab events appeared to cluster at a depth of around 100 km, and crustal events extend to a depth of 33 km. Moment tensor inversions of crustal earthquakes were used to determine focal mechanisms and better constrain earthquake depth estimates by finding the best fit between observed and synthetic waveforms. Earthquakes located in the Sierras Pampeanas and the southeastern flank of the Cordillera (~35°S) were found to be thrust events, with the depth of one Pampeanas event at 33 km, which is near the base of the crust, while the event near the Cordillera had a shallower depth near 3 km.

## **BROADBAND SEISMOGRAMS REVEAL WIDESPREAD TRIGGERING BY THE M7.9 DENALI EARTHQUAKE**

*Joan Gomberg, US Geological Survey & Paul Bodin, The University of Memphis*

Although it has been over a decade since the M7.4 Landers, California earthquake triggered widespread remote seismicity rate increases and surprised us all, questions regarding the underlying physical processes still abound. Answering these has been partly hampered by the apparent uniqueness of the Landers observations. However, the results of an analysis of broadband seismic data from a time period encompassing the 2002 M7.9 Denali, Alaska earthquake demonstrate that the Landers remotely triggered seismicity was not unique. High-pass filtered data recorded throughout western North America show a clear increase in the rate of small earthquake production during or immediately following the arrival of the Denali surface waves at numerous stations. The rate increases are not apparent in the catalogs compiled by the Advanced National Seismic System or the Canadian Geologic Survey (CGS), highlighting the value of having broadband data readily accessible from the IRIS and CGS online data servers. The sites with clear rate increases distribute along the azimuth of the rupture strike, which is the expected direction of maximum Love wave radiation and directivity. Although this suggests triggering may be related to the transient seismic deformations, the peak transverse-component amplitudes measured from broadband recordings of the Denali mainshock in the US (records in Canada all clipped) occur slightly west of this expected maximum. The distribution of sites of triggered seismicity correlates qualitatively with the combined distribution of Holocene and younger volcanoes and locations of geothermal activity, and also with active faulting and locally high background seismicity rates. However, these indicators of active tectonics do not provide reliable predictors of triggered activity, as triggering did not occur in many clearly active areas. Future analyses of the broadband data should better constrain the temporal evolution of the triggered activity, which is key in discriminating among possible causative physical mechanisms. Additionally, refined models of the Denali rupture, the radiated wavefield, and long-range aseismic deformation, will help us to assess and understand the deformations that may cause seismicity rate increases.

## REINTERPRETING STRESS ORIENTATIONS NEAR THE SAN ANDREAS FAULT

*Jeanne L. Hardebeck and Andrew J. Michael, US Geological Survey, MS 977, 345 Middlefield Rd, Menlo Park, CA 94025*

The strength of the San Andreas Fault (SAF) and the orientation of stress in its vicinity are currently the subject of much controversy. The SAFOD borehole should contribute significantly to our knowledge about the stress state around the SAF, and it is worthwhile putting this experiment into context by reviewing and re-evaluating some prior work. Two end-member models for the SAF have been proposed: the “strong fault” model (in which the SAF strength is equivalent to laboratory samples) and the “relatively weak fault” model (in which the SAF is an order of magnitude weaker than the surrounding crust). These two models imply that the maximum compressive stress axis should be at “low angle” (~30 degrees) or at “high angle” (~80 degrees) to the fault strike, respectively. Several recent studies have attempted to test these models by inverting the focal mechanisms of small earthquakes for stress orientation near the SAF. Some studies support one model while some support the other, so we have not yet reached a consensus as to which model is most consistent with the stress observations. Particularly disturbing are two studies in southern California (Hardebeck and Hauksson, 1999, 2001; and Townend and Zoback, 2001) that use the same focal mechanism data set but reach opposite conclusions as to whether the stress is at “high” or “low” angle to the SAF. Townend and Zoback (2001) proposed that the difference arises from the use of different schemes for spatially binning the seismicity for inversion. We test this idea by comparing the results of the two studies over the entire region, and find that the stress orientations are actually very similar, usually to within the uncertainty of the inversion results. The difference between the studies is not in the observed stress orientations, and must therefore lie in the interpretation. The stress orientations reported by both studies are often at “middle” angles (~40-60 degrees) to the SAF, not consistent with either the “high angle” or the “low angle” model, which understandably has confused the interpretation of these results. We perform inversions using a new high-quality focal mechanism data set for southern California, and stack the data from different fault segments so that noise and other signals not related to the SAF will tend to cancel out. We again observe “middle” angles near the SAF. Some “middle” angles are also observed in central and northern California (Provost and Houston, 2001, 2003), where stresses near the SAF are typically 40-60 degrees to the fault. Farther away from the fault, the stress orientations range from ~30 degrees in the north to ~80 degrees in the central creeping section, covering the whole range from “low” to “high” angles. In light of these observations, it appears that neither the “strong fault” nor the “relatively weak fault” model satisfactorily describes the SAF along its entire length, and most of the fault is not consistent with either model. The first conclusion that we reach is that the relative frictional strength of the SAF may vary considerably along strike, which means that while the SAFOD borehole may help us better understand one part of the SAF, the observations made there may not apply to the entire SAF. Our second conclusion is that alternatives to the “strong” and “relatively weak” models are needed, which can explain the “middle” angles observed along much of the fault.

## **CAN EARTHSCOPE HELP DEMYSTIFY THE RUPTURE PHYSICS OF LARGE EARTHQUAKES?**

*Ruth A. Harris (U.S. Geological Survey)*

We presently have a general (order of magnitude) idea of what to expect in terms of ground motion from large earthquakes, but we still lack the ability to make accurate forecasts of size, location, or timing. We still don't understand many of the key underpinnings of large earthquakes, that is, how they work. It is unlikely that progress will be made on these basic problems without collection of high-quality near-field data such as stress, strain, acceleration, fluid pressure, and material properties. Earthscope comes into play in this exercise by providing data about earthquake behavior at the SAFOD site. Ingredients that we think to be important for earthquake physics include frictional behavior, material properties of the rocks immediately surrounding the faults, fault geometry, and stress conditions. SAFOD will provide us with direct information about fault geometry and material properties, about stress state, and about nucleation and propagation behavior of small earthquakes. If we are very fortunate, SAFOD will also record a large earthquake in action. It is this latter opportunity that will most likely advance our understanding of large earthquake rupture physics. In the meantime, spontaneous rupture modelers have been able to use computer simulations to reproduce significant features of a number of large earthquakes using very simple assumptions about materials, stress, friction, and fault geometry. These efforts include simulations of the 1999 Izmit, Turkey, and 2002 Denali, Alaska earthquakes. Two key questions we are now faced with are, where we can go from here, and how will Earthscope advance our understanding of these societally significant events?

# **EVOLVING 3-D STRAIN FIELD OF THE ACTIVE EASTERN SUNDA ARC-CONTINENT COLLISION, INDONESIA.**

*Harris, R. Nugroho, N. and Merritts, D.*

The transition from subduction of oceanic lithosphere to arc-continent collision in the eastern Sunda arc of Indonesia is associated with a variety of tectonic processes that result from the redistribution of deformation along preexisting and newly forming geologic structures. Distribution of strain away from the trench and into the backarc region causes the Sunda Arc to accrete to the underthrust Australian continental margin and form new plate boundary segments.

The oblique convergence in the eastern Sunda arc region provides a rare chance to examine the subduction-collision transition at different stages of development along the arc, thus allowing us to address a series of fundamental tectonic questions about how strain is distributed at different scales of space and time along an evolving orogen. More specifically to an arc-trench system, where (and how) is plate convergence from the trench transferred to the back arc during progressive arc-continent collision and subduction polarity reversal? Are there discrete lateral-slip faults that link zones of opposing convergence? If so, how does this connective system propagate with the collision? What proportion of the rate of convergence (7-8 cm/yr.) is distributed along known faults versus more diffuse structures of the accretionary zone? Is there evidence of block rotation? How do patterns of strain measured at different temporal scales compare?

To address these questions we have conducted surveys of the GPS velocity field and associated uplift pattern revealed by deformed coral terrace deposits throughout the region. These measurements cover a wide range of temporal and spatial scales.

Well-preserved flights of uplifted coral terraces provide regional marker horizons capable of recording deformation patterns over time scales of 10-1000 ka. This is the temporal range least represented in previous studies of this and other actively plate boundary zones. By determining the age of the most prominent uplifted coral terraces through the use of U/Th and <sup>14</sup>C age analyses, we reconstruct the uplift history of island coastlines for comparison with the GPS velocity field. The most active plate boundary segments are near coastlines with multiple uplifted coral terraces. Warping and faulting of these terraces throughout the region provide a delicate measure of the detailed deformation pattern through time associated with various segments of the evolving plate boundary zone.

Geodetic measurements of the horizontal velocity field were conducted in 2001 of stations occupied by Genrich et al. (1996) in the early 90's. The GPS and coral terrace studies were conducted simultaneously on several islands throughout the plate boundary transition zone in collaboration with Indonesian Universities and the Indonesian Geodetic Survey (Bakosurtanal).

The results of the investigation demonstrate the importance of transcurrent fault systems in linking different parts of the orogenic wedge, and distributing strain from the trench to the back arc. These structures exploit existing weaknesses and with time, step in the direction of collision propagation. Each step transfers large, discrete and fault-bounded blocks of the Sunda arc-trench system to the Australian continental margin.

The eastern Sunda arc terminates at the transcurrent fault off the west coast of Timor. This sinistral structure links the opposing dips of the Sunda and Wetar convergent plate boundaries systems, and accommodates most of the motion between the SE Asian and Australian plates.

## LOWER MANTLE SUPERPLUME STRUCTURE BENEATH AFRICA

*Don V. Helmberger and Sidao Ni*

Beneath southern Africa is a large structure about 1200 kilometers across and extending obliquely 1500 kilometers upward from the core-mantle boundary with a shear velocity reduction of about 3%. SKS travel times observed on the South African Array display jumps of about 6 sec when ray paths cross these nearly vertical boundaries. Back projecting these delays onto the core-mantle boundary allows a clear image of the horizontal extent of this structure starting at mid-Africa (15°S, 5°E) where it strikes roughly northwest to beyond the tip of South Africa (45°S, 55°E). Here it bends sharply towards the Indian Ocean, producing a volume greater than 10 billion km<sup>3</sup>. Waveform sections of S, ScS, SKS, and SKKS are modeled along two corridors, one along strike and one at right angles to establish its uniformity. We show that the boundaries appear sharp, with a width less than 50 km, in that both SKS and Sdiff are multi-pathed along some profiles. If this structure is stabilized by a localized viscosity condition or a dense-core as suggested by some joint inversions, gravity, and free-oscillations, it may be isolated from mantle stirring and therefore very old with, perhaps, unique chemistry.

## **THE COMBINED MOTION MODEL, TIME SERIES, AND ANALYSIS TOOLS FROM THE SOUTHERN CALIFORNIA INTEGRATED GPS NETWORK (SCIGN) ANALYSIS COMMITTEE**

*Thomas Herring, MIT, Nancy King, USGS, John Langbein, USGS, Michael Heflin, JPL, Kenneth Hurst, JPL, Sharon Kedar, JPL, and Linette Prawirodirjo, SIO*

The analysis results from the three SCIGN analysis groups, the Jet Propulsion Laboratory (JPL), the Scripps Institution of Oceanography (SIO), and the United States Geological Survey (USGS) are combined into a single analysis and set of products. The USGS analysis, carried out with a 47-day lag and includes data from sites that are not downloaded in near-real time, is not yet included in the current combination but will be shortly. The current status of the combined analysis is given at [http://bowie.mit.edu/~tah/SCIGN\\_MIT/](http://bowie.mit.edu/~tah/SCIGN_MIT/). The Matlab based tools to interactively view the velocity fields and time series from the combined analysis, the combination committee analysis of STACOV files from JPL and H-files from SIO, and the analyses performed by the individual centers are available on the web at <http://bowie.mit.edu/~tah/GGMatlab/>. The analysis of the combined results uses the GLOBK program and is performed iteratively and in multiple stages. The time evolution of a site position is modeled with secular velocities, discontinuities at the times of earthquakes, antenna and other equipment changes (in many cases), and postseismic motions. The GPS site name is changed with each discontinuity. From an initial analysis of the time series behaviors, a set of (currently) 349 site names which show little non-secular motion are chosen and their positions and velocities are determined with the GLOBK Kalman filter by rigorously combining the solutions and full covariance matrices from the daily analyses. (Because of the site renaming, the 349 site names correspond to 208 distinct locations). After rotation into a common frame, the RMS difference of the horizontal velocities from the JPL and SIO analysis is 0.6 mm/yr (see web site for more details and other comparisons). The positions and velocities from this analysis are used as the reference frame for time series analysis of all sites (i.e., each day of data is separately analyzed from either the JPL or SIO analyses or from the combinations of the daily results from the two analysis centers). The RMS difference of the horizontal velocity estimates for the 373 site names (272 distinct sites) in times series analysis is 0.5 mm/yr. In all analyses, process noise models are used to account for the non-white nature of the noise in the time series. The median horizontal velocity sigma from the times series analysis with site dependent process noise is 0.5 mm/yr. The median vertical velocity sigma is 1.6 mm/yr. The corresponding values from analysis using sites that show little non-secular motion are 0.3 mm/yr for horizontal and 0.6 mm/yr vertical velocities. The analysis of the combined SCIGN products is continuing with refinements to the stochastic modes and the addition of new data. The web site referenced above is updated on a regular basis.

# STRESS-INDUCED BOREHOLE FAILURE IN THE SAFOD PILOT HOLE: IMPLICATIONS FOR THE STRENGTH OF THE SAN ANDREAS FAULT AT PARKFIELD

*Stephen Hickman (U. S. Geological Survey, Menlo Park CA) and Mark Zoback (Stanford University, Stanford CA)*

The San Andreas Fault Observatory at Depth (SAFOD) is a comprehensive project to drill, core and instrument an inclined borehole across the San Andreas Fault Zone to a depth of 4 km. A 2.2-km-deep vertical pilot hole was drilled in the summer of 2002 at the same surface location planned for SAFOD. This site is 1.8 km southwest of the San Andreas Fault near Parkfield, CA, on a segment of the fault that moves through a combination of aseismic creep and repeating microearthquakes. One of the primary goals of the pilot hole was to better define the thermomechanical setting of the San Andreas Fault Zone at Parkfield prior to drilling of the main SAFOD hole.

Ultrasonic borehole televiewer and formation microimager logs acquired in the SAFOD pilot hole reveal extensive stress-induced borehole breakouts and drilling-induced tensile fractures at depths from 0.8 to 2.2 km. Analysis of the orientations of these features indicates that the direction of the maximum horizontal compressive stress, SHmax, is approximately 35° clockwise from the strike of the San Andreas Fault to a depth of ~1.5 km. However, a clockwise stress rotation is observed with increasing depth such that the SHmax direction is approximately 70° to the strike of the fault at 2.0 to 2.2 km. This lowermost stress orientation is in good agreement with SHmax directions seen at much greater distances (>10-20 km) from the San Andreas Fault in central California. Although the absolute magnitudes of the horizontal principal stresses will not be known precisely until hydraulic fracturing tests are conducted in the pilot hole next year, simultaneous observations of drilling-induced tensile fractures and borehole breakouts in the pilot hole indicate a transitional strike-slip to reverse faulting stress regime with high horizontal differential stress. Thus, the crust ~2 km southwest of the San Andreas Fault at this location is supporting high levels of shear stress predicted by Byerlee's law. However, the rotation of SHmax toward fault-normal compression near the bottom of the pilot hole indicates that shear stress resolved onto planes parallel to the San Andreas Fault at depth is very low. Although the causes for this stress rotation are not known, if the stress state observed in the bottom of pilot hole is representative of stresses acting on the San Andreas Fault at greater depth, then our results are consistent with regional (i.e., far-field) stress field indicators and a model in which the San Andreas is an anomalously weak fault embedded in an otherwise strong crust. The comprehensive stress measurement program planned for the main SAFOD hole will determine whether this rotation toward fault-normal compression persists with increasing depth and the manner in which stress orientations and magnitudes vary as we approach and then cross the fault zone.

## THE RESOLVING POWER OF THE CURRENT STATE OF GPS INFORMATION IN NORTH AMERICA: IMPLICATIONS FOR EARTHSCOPE PLANNING

*W. E. Holt, Department of Geosciences, SUNY at Stony Brook, R. Bennett, Harvard Smithsonian Center, G. Blewitt, University of Nevada, Reno, J. Davis, Harvard Smithsonian Center, L. M. Flesch, Dept. of Terrestrial Magnetism, Carnegie Institute of Washington, A. J. Haines, Bullard Labs, Cambridge University, C. Kreemer, Laboratoire de Geologie, Ecole Normale Supérieure, B. Shen-Tu, Air Worldwide*

We combine both permanent and campaign GPS data from mostly published work to infer a kinematic solution within western North America plate boundary zone. We interpolate GPS velocity vectors to infer the horizontal velocity gradient tensor field, which is important for both seismic hazards analysis and for constraints on the dynamics. The interpolation algorithm uses continuous bi-cubic splines on the surface of a sphere. The GPS vectors are matched by the model velocity field, in a specified reference frame, in a weighted least-squares inversion. The reference frames of each geodetic study are determined in the inversion procedure. That is, we seek angular velocities, one for each study, that rotate the vectors into one self-consistent frame of reference. The algorithm involves no a priori bias as to the location of fault zones or blocks. The a posteriori variance-covariance matrix of the model strain rates and rotation rates can be evaluated to determine where block behavior is statistically significant, where deformation rates are significant, as well as the significance of the style of inferred strain rates. These model results can be compared with active fault slip observations. The quantitative assessment of the strain rates and rotation rates can be compared with predictions from competing kinematic and dynamic models. Discrimination between such competing models takes into account the a posteriori uncertainties in the kinematic parameters. In cases where discrimination between competing models is not possible, due to large errors in the kinematic solution, then it is possible to investigate where an increased GPS coverage or accuracy is potentially critical in resolving differences between competing models.

## CRITICALLY STRESSED INTRAPLATE CRUST: EVERYWHERE OR HERE AND THERE?

*Susan E. Hough (U.S. Geological Survey, Pasadena, California; hough@usgs.gov), Leonardo Seeber, and John G. Armbruster (Lamont-Doherty Earth Observatory, Palisades, New York)*

Remotely triggered earthquakes appear to occur relatively commonly following large ( $M_w > 7$ ) mainshocks in stable continental regions (SCRs). Such events are important for several reasons: 1) they can give rise to locally high ground motions that can be mistaken for mainshock shaking, and thereby inflate isoseismal contours, 2) they can be potentially damaging events in their own right, and 3) they prove that remotely triggered earthquakes occur in diverse tectonic and mechanical settings. We present examples from several large SCR earthquakes including the 1811-1812 New Madrid sequence and the 1886 Charleston, South Carolina earthquake. We explore the possibility that in low strain-rate regions, remotely triggered earthquakes reflect a prevalence of faults that are close to failure rather than the presence of weak faults or geothermal/hydrothermal fluids. We further illustrate how, in a low strain-rate environment, permanent, non-elastic deformation might account for this prevalence, playing a larger role in stress accumulation than in high strain-rate regions. Using a simple model incorporating both elastic and anelastic strain release, we show that, for realistic parameter values, faults in intraplate crust might remain close to their failure stress for a longer part of the earthquake cycle than faults in high strain-rate regions. Our results furthermore reveal that remotely triggered earthquakes occur preferentially in regions of recent and/or future seismic activity, which suggests that faults tend to be at a critical stress state only here and there, not everywhere. It is not surprising that triggered earthquakes would serve as beacons that identify regions that are approaching a critical stress state. Their occurrence in regions that have experienced large earthquakes in the recent past (a few hundred years) provides evidence that, once developed, a critically stressed region of intraplate crust will persist or hundreds if not thousands of years and give rise to prolonged episodes of seismic unrest.

## **COSEISMIC DISPLACEMENTS FROM THE 2002 MW6.7 NENANA MOUNTAIN EARTHQUAKE AND MW7.9 DENALI FAULT EARTHQUAKE, MEASURED WITH GPS**

*Sigrun Hreinsdottir, Jeffrey T. Freymueller, Hilary J. Fletcher, Christopher F. Larsen, and Roland Burgmann*

On 3 November 2002 an Mw7.9 earthquake occurred in central Alaska, rupturing portions of the Susitna Glacier, Denali, and Totschunda faults. The earthquake was preceded on 23 October by an Mw6.7 right-lateral strike-slip earthquake on the Denali fault, with its epicenter only about 22 km west of the Mw7.9 epicenter. Following the Mw6.7 earthquake GPS measurements were repeated at 13 existing stations on the Parks Hwy (N-S profile west of epicenter) and on the Denali Hwy (E-W profile south of epicenter) in order to estimate coseismic slip at these stations from the earthquake. All but one had predetermined velocities based on measurements spanning 1997 to 2000/2. The GPS measurements do not reveal a simple right lateral deformation pattern for the earthquake, suggesting either that the earthquake was more complex than seismic data indicate, or that we have more than one source of deformation in the timeperiod between the pre and post earthquake GPS surveys. Several of these stations were still running when the Mw7.9 occurred. Including these GPS stations, 38 existing points in the interior and south central Alaska were measured within two weeks of the Mw7.9 earthquake. In addition 12 permanent GPS sites were operating within 500 km of the epicenter at the time of the earthquake. In general the coseismic GPS data show a right lateral deformation field. North of the fault sites have eastward displacements and sites to the south have westward displacements. GPS sites closest to the epicenter show the effect of thrust motion on the Susitna Glacier fault. Inversion of the displacements indicates that the event was dominated by a complex, right-lateral strike-slip rupture along the Denali fault.

## MEASURING FAULT SLIP - WHY AND HOW?

*Hudnut, K. W., G. Anderson, A. Aspiotes, A. Borsa, T. Heaton, N. King, J.-B. Minster, R. Moffitt, K. Stark*

To improve our understanding of earthquake physics, we must make observations of parameters that determine friction on the fault surface during rupture. Observables may include, for example, 3D point trajectories to fully record near-field dynamic phenomena such as slip pulses, as well as details of slip variation along strike. We have devised and tested new methods for observing these quantities in nature. First, we observed the details of topography along the 1999 Hector Mine surface rupture. This allowed us to estimate slip variation along strike with higher spatial resolution than has ever before been possible. The results are, however, complex due to ground surface irregularity and pre-existing topographic features. Evidently, slip variations along strike are greater than previously recognized, implying extreme slip heterogeneity. We will evaluate by dynamic modelling whether or not this could provide the source for high-frequency seismically radiated energy. Second, we have developed the concept for, and built a working prototype of, a GPS Fault Slip Sensor spanning the San Andreas fault. In addition to augmenting seismic early warning systems, such instrumentation could also provide unique records of near-field ground motions. Inertial sensors such as seismic instruments are not able to differ between a tilt and an acceleration, whereas GPS measurements can differentiate these, and can be made with respect to an absolute frame of reference. Other practical limitations exist, however, in both kinds of instrumentation and we will describe how they may best be integrated into a system that will achieve both the scientific observational objectives and support earthquake early warning.

# XENOLITH CONSTRAINTS ON SEISMIC VELOCITIES IN THE UPPER MANTLE BENEATH SOUTHERN AFRICA

*D. E. James(1), F.R. Boyd(1), D. Schutt(1,3), D. R. Bell(2), R. W. Carlson(1) (1) Carnegie Institution of Washington, 5241 Broad Branch Rd., N.W., Washington, D.C. 20015; (2) Arizona State University, Tempe, AZ 85287; (3)now at University of Wyoming, Laramie, WY 82071*

We impose geologic constraints on seismic 3-D images of the upper mantle beneath southern Africa by calculating seismic velocities and rock densities from approximately 100 geothermobarometrically calibrated mantle xenoliths from the Archean Kaapvaal craton and adjacent Proterozoic mobile belts. Velocity and density estimates are based on the elastic and thermal moduli of constituent minerals under equilibrium P-T conditions at the mantle source. The largest sources of error in the velocity estimates derive both from inaccurate thermobarometry and, to a lesser extent, from uncertainties in the elastic constants of the constituent minerals. Results are consistent with tomographic evidence that cratonic mantle is higher in velocity by 0.5-1.5% and lower in density by about 1% relative to off-craton samples at comparable depths. Seismic velocity variations between cratonic and non-cratonic xenoliths are controlled dominantly by differences in calculated temperatures, with compositional effects secondary. Different temperature profiles between cratonic and non-cratonic regions have a relatively minor influence on density, where composition remains the dominant control. Accordingly, the more fertile high-T lherzolite occupy the high end of the density-depth diagram and the highly depleted harzburgite the low end.

Low-T cratonic xenoliths exhibit a positive velocity-depth curve, rising from about 8.1 km/s at uppermost mantle depths to about 8.25 km/s at 180-km depth. S-wave velocities decrease slightly over the same depth interval, from about 4.7 km/s in the uppermost mantle to 4.65 km/s at 180-km depth. P and S wave velocities for high-T lherzolites are scattered, ranging from highs close to those of the low-T nodules to lows of 8.05 km/s and 4.47 km/s at depths in excess of 200 km. These low velocities, while not asthenospheric, are inconsistent with seismic tomographic images that indicate high velocity root material extending to depths of at least 250 km. We suggest that the high-T xenoliths may therefore have originated in halos around kimberlite embayments into the tectospheric root, consistent with the ancient Re-Os model ages of most high-T peridotites.

Seismic velocities and densities for cratonic xenoliths differ significantly from those predicted for both pyrolite (fertile) and eclogite mantle materials. A model pyrolite mantle under cratonic P-T conditions exhibits velocities about 1% lower for P and about 1.5% lower for S, a consequence of a more fertile composition and different modal composition. Pyrolite mantle is also about 2% more dense at 150-km depth than low-T garnet lherzolite. Calculations for a hypothetical "cratonic" eclogite (50:50 garnet/omphacite) with an assumed cratonic geotherm produce extremely high P and S velocities (8.68 km/s and 4.84 km/s, respectively, at 150 km depth) as well as high density (~3.54 gm/cc). The very high velocity of eclogite should render it seismically conspicuous in the cratonic mantle if present as large volume blocks or slabs. The seismic velocity data we have compiled in this paper from both xenoliths and generic petrologic models of the upper mantle deviate markedly from commonly used standard earth models.

## **MINI-PBO - A PROTOTYPE PLATE BOUNDARY OBSERVATORY (PBO) CLUSTER IN THE SAN FRANCISCO BAY AREA**

*M. Johnston\**, *M. Murray\*\**, *P. Silver\*\*\**, *B. Romanowicz\*\**, *D. Myren\**, *R. Mueller\**, *A. Bassett\*\**,  
*A.*

Mini-PBO is a PBO-style integrated instrumentation program for GPS, borehole tensor strain, borehole seismic velocity, pore pressure, borehole tilt and heat flow monitoring in the San Francisco Bay Area and Parkfield. It is a joint USGS, UCB, CIW, and UCSD project aimed at high-precision multi-parameter monitoring of plate boundary deformation and seismicity in these regions. This project is funded by the NSF/MRI program and the USGS with matching funds from the participating institutions and SCIGN. One major component of this project concerns the installation five borehole sites along the Hayward and San Andreas faults in the San Francisco Bay Area each with a continuous GPS, tensor strainmeter, 3-component seismometer, downhole pore pressure monitor and a 2-component tiltmeter. Each borehole site in the San Francisco Bay area has been drilled and equipped with down-hole strainmeters, seismometers, pore pressure and tilt sensors. Uphole electronics, recording systems and satellite telemetry are all operational. Some GPS units still need to be added. High sample rate data from GPS, borehole strainmeters, seismometers, pore pressure transducers and tiltmeters will soon be continuously telemetered over frame relay from all sites. All data are available to the community through the Northern California Earthquake Data Center. Results of geophysical interest obtained so far from the borehole data include: [a] earth tidal strain and tilt, [b] atmospheric and ocean tidal loading, [c] broad-band strain and seismic velocity seismograms from local and teleseismic earthquakes with just one local M4 earthquake close enough to allow measurement of the co-seismic strain offset, [d] interrelated dynamic strain, seismic velocity and pore pressure, recorded during the November 3, 2002 M7.9 Denali earthquake, that show how local pore pressure and strain, driven by this earthquake, may play a role in earthquake triggering and [e] determination of new constraints on the depth of creep episodes observed on the northern and southern Hayward fault.

# DELAMINATION OF THE SIERRA NEVADA: SEISMOLOGICAL OBSERVATIONS AND TECTONIC IMPLICATIONS

*Craig H. Jones, G. Lang Farmer, Peter Molnar, (all Dept. of Geological Sciences and CIRES, University of Colorado, Boulder, CO) and Jeffrey R. Unruh (William Lettis and Associates, Walnut Creek, CA)*

Pliocene (~3.5 Ma) removal of dense eclogitic material under the Sierra Nevada has been proposed on the basis of xenolith and volcanic rock petrology and geochemistry as well as seismological and magnetotelluric observations. The 1997 Sierran Paradox Continental Dynamics project included a PASSCAL experiment, with a deployment of 24 broadband seismometers across the region thought to have delaminated. SKS splits from this deployment show a consistent ENE fast direction, with large splits (to ~2s) mainly under the high Sierra and extending under areas underlain by eclogite at 10 Ma. Such large splits strongly indicate the presence of peridotites today, supporting the delamination hypothesis.

A necessary consequence of replacing eclogite with peridotite is that Sierran elevations and lithospheric gravitational potential energy both increase. An increase in potential energy should increase extensional strain rates in the area. If these forces are insufficient to significantly alter Pacific-North America plate motion, then increased extensional strain rates in the vicinity of the Sierra must be accompanied by changes in the rate and style of deformation elsewhere. Changes in deformation in California and westernmost Nevada agree well with these predictions. Uplift along the Sierran crest of >~1 km is dated to 3-8 Ma and should be associated with an increase in gravitational potential energy in excess of  $1.2 \cdot 10^{12}$  N/m. Extensional deformation within ~50 km of the eastern side of the Sierra initiated by about 3 Ma, and shortening that produced the California Coast Ranges is estimated to have begun about 3-5 Ma. The Pliocene uplift, adjoining extension and initiation of contraction all along the length of the Sierra suggests that this delamination event extended the whole length of the range. The area uplifted lies between two large, upper-mantle, high-P-wave-velocity bodies under the south end of the San Joaquin Valley and the north end of the Sacramento Valley that plausibly represent the material removed from the base of the crust. These physically-based expectations from delamination explain phenomena closely related in space and time that otherwise require several diverse and often inconsistent explanations. Additionally, consequences of delamination might extend to shifting the distribution of transform slip from the San Andreas to the Eastern California Shear Zone, a prediction that awaits better defined slip histories on both faults. These events suggest that locally derived forces can influence deformation kinematics within plate boundary zones.

This delamination provides important tests for the mechanism of delamination and the rheology of the upper mantle. We use the apparent change in mantle structure beneath the Sierra Nevada since ~10 Ma, which suggests convective removal of eclogite-rich mantle lithosphere, and scaling laws developed for Rayleigh-Taylor instability to place constraints on the average viscosity coefficient of the mantle lithosphere. By treating the lithosphere as a non-Newtonian fluid obeying power-law creep with an exponent of  $n=3.5$ , we may compare the inferred values of viscosity coefficient with those obtained from laboratory experiments on olivine and eclogite. The values that we obtain overlap those predicted by laboratory-based flow laws for the range of geotherms implied by heat flux measurements within the Sierra Nevada and by metamorphic geothermometry and geobarometry of xenoliths in volcanic rock erupted in the Sierra Nevada at ~10 Ma. Thus, this comparison offers support for laboratory-derived flow laws, and specifically for the high stress limits suggested by Evans and Goetze (1979). Conversely, this agreement shows that the high strength of cold mantle minerals does not prohibit its removal by convective instability.

# JOINT INVERSION OF RECEIVER FUNCTIONS, SURFACE-WAVE DISPERSION AND S-WAVE TRAVEL-TIMES IN EAST AFRICA.

*Jordi Julia, Charles J. Ammon, and Minoo Kosarian*

Seismic characterization of the Earth's crust and upper mantle is generally achieved by modelling physically independent data sets, separately. P- and S-wave travel-times from local events, surface-wave dispersion velocities from regional events, and teleseismic receiver functions are some well-known examples of such seismic observations. In general, the separate interpretations agree well at a broad scale, but differ in the details as a result of varying degrees of accuracy and resolution among the data. Geologic interpretation usually benefits from comparing independent results, although ideally one would seek an integrated model that provided the best compromise in fitting all the measurements. A joint inversion has the potential for providing such an integrated view. Moreover, the advent of Earthscope will provide a massive and routine collection of seismic data, and their mutually consistent interpretation would be highly desirable. Here, we illustrate the benefits of jointly inverting receiver functions, surface-wave dispersion and local S-wave travel-times to infer the S-wave velocity structure beneath seismic stations in the Tanzania craton. The craton is located adjacent to the East African Rift System, where the details of the plume tectonics framework have proven difficult to unravel. We expect the surface-wave and local S-wave travel times to provide vertical velocity averages within various depth ranges that will help resolve the intrinsic depth-velocity

trade-off in the receiver function modelling. The result will be S-wave velocity models that offer a better compromise to fitting the observations than any model obtained by inverting either of the independent data sets alone.

## **IRIS STATION INFORMATION SYSTEM APPLICATION.**

*Linus Kamb*

The IRIS DMC is developing an application to facilitate access to seismic station information such as site visit logs and notes, data problem and resolution reports, and station hardware inventory. With this information available, the user community will be able to query for known data problems or other station activity, or request a station's hardware configuration at a given time. An XML Schema-based format is used for the generated reports and query results.

This poster will present the IRIS Station Information System, highlighting the major features, including the data entry interface, querying tool, and XML Schema. An accompanying demonstration will show the user interface and current state of the application.

Network operators will be able to use the application to enter and manage station information as well as restrict access to potentially sensitive information. Field engineers can use the data-entry component to record notes and site visit actions. The Data Collection Centers may then provide web-based access to the user community for data problem reporting and querying as well as to the engineering logs and hardware inventory.

Logs and reports will be uploaded and synchronized with the DMC which will also support the reporting and querying interface for the user community. If a particular DCC does not wish to support the user community access interface, that responsibility can be handled entirely by the DMC. The synchronization messages between a DCC and the DMC will also be formatted in XML.

A goal of this effort is to enable simple, on- and off-line access by the user community, network operators, and field engineers to pertinent information about a station's operation and data. Field engineers will be able to browse data problem reports or past log entries in the field. Scientists may want to know if there any reported problems or hardware changes during the time period of their requested data. A future goal is to automatically include this information with every requested data set.

The Station Information System is being developed as a stand-alone application, but it is also planned to be available as a component of the next generation Portable Data Collection Center application.

## SEISMOLOGY WITH A DENSE SEISMIC NETWORK

*Hiroo Kanamori Seismological Laboratory, California Institute of Technology, Pasadena, CA 91125*

This paper presents two projects carried out using a dense seismic network, Hi-net, which has more than 550 wide-dynamic range instruments (100 m down-hole) distributed throughout the Japanese islands.

In one project, we (Kanamori and Ishida, 2002 SSJ abstract) explored the possibility of detecting dynamic triggering using Hi-net seismograms of the June 28, 2002, China-Russia border deep-focus earthquake ( $M_w=7.3$ ). (Hereafter, this event is called a driving event.) The seismograms were high-pass filtered at 7 Hz, and the seismograms 1 hour before and 1 hour after the driving event were compared to examine the evidence for dynamic triggering. In most areas, no difference was observed, suggesting that the crust is not close enough to failure to be activated with the stress perturbation (approximately 0.05 bar) caused by the driving event. At several stations in the northwestern part of Shikoku, however, the seismograms after the event exhibit a significant swarm-like activity, which is probably the low-frequency tremor activity near the plate interface. In some places where the background activity had been high (e.g., near Wakayama), the activity seems to have increased slightly after the driving event. It is premature to relate this observation directly to the regional seismic potential in the future. Nevertheless, the observation that the crust in different regions responds differently to a modest stress perturbation caused by the driving event suggests that systematic monitoring of dynamic triggering with a dense wide-dynamic range network such as Hi-net is useful for long-term monitoring of regional seismic potential.

In another project, we examined the waveforms of deep-focus (about 580 km) earthquakes near Japan recorded with Hi-net, as well as F-net. The waveforms are pulse like, and exhibit systematic spatial variations of pulse width and amplitude which can be related to the geometry of the subducting Pacific plate beneath Japan. To the first order, the pulse broadening seems to be caused by diffracted energy when the propagation paths are parallel to the deep seismic zone. The advantage of having spatially un-aliased coverage is that we can identify several systematic patterns which are not readily explainable with a simple plate geometry. Possible plate structures which may affect the waveforms include low-velocity channels parallel to the plate as well as geometrical complexities. This suggests that with detailed 3-D modeling, these patterns will provide important details of structures of the subduction zone.

## APPLICATIONS OF JOINT ANALYSIS OF BROADBAND SEISMOLOGY AND TILT

*Sharon Kedar - Jet Propulsion Laboratory, California Institute of Technology Bernard Chouet - United States Geological Survey Takao Ohminato - Earthquake Research Institute, Tokyo, Japan Phillip Dawson - United States Geological Survey*

In February 1996 a four-hour-long inflation and eruption episode was recorded at Kilauea, Hawaii, by an array of broadband seismographs operated by the U.S. Geological Survey in and around Kilauea caldera.

Joint analysis of tilt and broadband seismic records unraveled in unprecedented detail the progression of magma transport during the eruption episode. The spectrum of signals range from local high-frequency earthquakes and volcanic tremor through harmonic oscillations with period of 20 s and periodic 1-2 minute sawtooth-shaped jolts. Superimposed on these signals is a day-long tilt detected by both the tiltmeters and broadband horizontal acceleration.

The inflation is shown to be caused by an injection of magma into the summit reservoir at a depth of about 1 km. Four phases of fluid transfer are observed through the inflationary event, each of which is characterized by a distinct broadband seismic signature:

(1) Evacuation of gas through a ~1 km deep sill acting as a buffer for gas slugs that build up within the summit dike plexus; (2) An hour long episode of magma flow to the east rift that generated the 20-s oscillations within the conduit system; (3) A blockage of the conduit system triggered by a magnitude 2.6 earthquake several kilometers downstream, that in turn caused magma to back up toward the caldera and increased the inflation rate by a factor of three; the resulting pressure buildup inside the caldera strained the southern edge of the caldera, triggering a sequence of shallow earthquakes; (4) A resumption of the original inflation rate as the magma found its way past the blockage down to the East Rift.

This example demonstrates the geophysical constraints that can be inferred from active deformation measured at frequencies below those typically detected on short-period instruments and at resolution below that of continuous GPS. Earthscope is likely to benefit from a routine analysis of seismic and deformation data at the periods presented in this study.

## **BASELINE AND ERROR DISTRIBUTION RESULTS FROM THE SOUTHERN CALIFORNIA INTEGRATED GPS NETWORK (SCIGN) ANALYSIS COMMITTEE**

*N.E. King, John Langbein, Michael Heflin, Thomas Herring, Kenneth Hurst, Sharon Kedar, and Linette Prawirodirjo*

The 250-station Southern California Integrated GPS Network (SCIGN) has two independent precise processing centers. The Jet Propulsion Laboratory (JPL) uses GIPSY-OASIS software and the Scripps Institution of Oceanography (SIO) uses GAMIT/GLOBK/GLORG. Comparison of absolute positions requires adjustment in a common reference frame (see abstract by Herring et al.). Relative positions, however, are more precise than absolute position, less dependent on reference frame, and more relevant to crustal deformation. After deletion of 10 stations with very large SIO-JPL vertical differences, comparison of more than 20000 JPL and SIO relative positions (baseline vectors) from 1996 to 2002 shows good agreement. The mean difference is 0.1 mm in length and the horizontal components, and 0.2 mm in the vertical. This is equivalent to proportional errors of a few parts in 10<sup>10</sup> in the horizontal and a few parts in 10<sup>9</sup> in the vertical. The mean rms difference is 1.8 to 2.3 mm in length and the horizontal, and 6.6 mm in the vertical. The dependence of SIO-JPL vertical baseline difference on elevation difference is  $2.5 \times 10^{-7}$ , probably due to atmospheric effects. Preliminary analysis of the error distribution shows that the noise spectrum is more complex than flicker noise plus white noise. Random walk noise is detectable in more than half the time series, and ranges between 0.5 and 2 mm/yr<sup>0.5</sup> for the horizontal.

## THE 2000 MW 6.8 UGLEGORSK EARTHQUAKE AND REGIONAL PLATE BOUNDARY DEFORMATION OF SAKHALIN FROM GEODETIC DATA

*M.G. Kogan (1), R. Burgmann (2), N.F. Vasilenko (3), C.H. Scholz (1), R.W. King (4), G.M. Steblov (5); (1) Lamont-Doherty Earth Observatory, Palisades, NY; (2) Department of Earth and Planetary Science, University of California, Berkeley, CA; (3) Institute of Marine Geology and Geophysics, Yuzhno-Sakhalinsk, Sakhalin, Russia; (4) Department of Earth, Atmospheric, and Planetary Sciences, MIT, Cambridge, MA; (5) Geophysical Service, Russ. Acad. Sci., Obninsk, Russia.*

Significant, >1m, vertical displacements  $dH$  of 20 GPS stations caused by the August 4, 2000 Uglegorsk earthquake, were estimated by comparison of the preseismic spirit leveling with the postseismic GPS data. Corrections of the leveling for the geoid amount to 0.8 m and cannot be neglected. Estimated displacements of distant benchmarks are <0.1 m which we assume to be an upper limit in the uncertainty of  $dH$ .

The constrained inversion of  $dH$  provides strong evidence for a thrust-mechanism rupture on an east-dipping fault plane, in accordance with most well-determined seismic focal mechanisms for large earthquakes in Sakhalin. The kinematics of this event is consistent with the observed interseismic oblique-convergent velocity field across Sakhalin.

The Okhotsk microplate (OKH) scenario of Seno et al. [1996] places the EUR-OKH Euler pole at northern Sakhalin and predicts a clockwise rotation of the island relative to EUR with a consequent variation in horizontal velocity from 0 at the north to 5 mm/yr at the south. Nearly identical GPS velocities at stations OKHA, UGLE, and YSSK (northern, central, and southern Sakhalin respectively) disagree with the motion predicted by OKH. The disagreement is even more pronounced if the elastic effect of Pacific plate subduction is taken into account.

Interseismic GPS velocities in Sakhalin demonstrate that a large part (and maybe all) of the Eurasia - North America relative plate motion of 6-9 mm/yr can occur by distributed plate boundary deformation across Sakhalin and the Sea of Japan, since the velocities of GPS stations in the neighboring continental region relative to stable Eurasia are quite small, <2 mm/yr [Kogan et al., 2000; Wang et al., 2001].

## **MONITORING DEFORMATION OF THE LONG VALLEY CALDERA WITH EDM AND GPS**

*John Langbein, Elliot Endo, Stuart Wilkinson, and Jerry Svarc US Geological Survey, Menlo Park, CA., Vancouver, WA., and Mammoth Lakes, CA*

For the past 20 years, the deformation of the Long Valley Caldera has been monitored with a high-precision Electronic Distance Meter (EDM). The data have detected two periods of rapid inflation, and long periods of steady inflation. Since the last rapid inflation in 1997, the data has shown that the caldera has deflated at a low rate, of the order of 0.5 cm/yr. However, in 2002, the caldera started to re-inflate at a steady rate of 3-cm/yr. To improve our ability to monitor deformation in Long Valley, we have been installing continuous GPS stations in and around the caldera. Currently, 16 sites are continuously monitored. Of those, 6 sites are co-located with frequently measured EDM baselines. Comparison of line-length changes derived from positions obtained by the GPS with line-length changes measured by EDM show that both systems track very well. ([quake.wr.usgs.gov/research/deformation/twocolor/lv\\_2col\\_proxy.html](http://quake.wr.usgs.gov/research/deformation/twocolor/lv_2col_proxy.html)) In particular, over the past 3.5 years, the data from both systems overlay each other one-for-one. Both the deflation prior to mid-2002 and the re-inflation are clearly observed. Finally, modeling of both data sets for the source inflation suggest a depth of 9 km beneath the resurgent dome.

## **THE EMBAYMENT SEISMIC EXCITATION EXPERIMENT - AN ACTIVE SOURCE BROADBAND EXPERIMENT**

*Langston, C. A., Bodin, P., Withers, M., Powell, C. A., Horton, S., Center for Earthquake Research and Information, University of Memphis, 3876 Central Ave., Suite 1, Memphis, TN 38152-3050, clangstn@memphis.edu, MOONEY, W., U.S. Geological Survey, 345 Middlefield Rd., MS 977, Menlo Park, CA 94025-4764*

A 2600lb explosion was detonated near Marked Tree, AR, (October 28, 2002) and a 5000lb explosion near Mooring, TN, (October 29, 2002) within the New Madrid Seismic Zone and Cooperative New Madrid Seismic Network to excite fundamental and higher mode surface waves within the sediments of the Mississippi Embayment. The seismic network was augmented by 9 temporary broadband stations and two strong motion accelerograph arrays. The purpose of the experiment was to generate and record Rayleigh waves that propagate primarily within the unconsolidated sediments of the Mississippi embayment. Theoretical studies have shown that surface waves propagating within the sediments should be a sensitive probe of sediment anelasticity. The experimental hypothesis was that  $Q_s$  in the embayment sediments is much larger than a previous estimate of  $\sim 30$ . The immediate test of the experiment was to be observation of dispersed Rayleigh waves at distances greater than 15 km, relative to the sediment P wave. Surface waves from the larger explosion were observed out to a range of 130 km demonstrating that  $Q_s$  is much higher than expected. Recorded wave trains are composed of P wave and S wave modes that are trapped entirely within the sedimentary column and independently constrain  $Q_p$  and  $Q_s$  estimates. Use of explosion Rayleigh waves is a novel method for placing independent constraints on media anelasticity. The preliminary results suggest that sediment damping is much less than previously believed and that the unconsolidated sediments of the embayment will dramatically amplify seismic waves from local earthquakes. The array data provide important constraints on sediment P and S wave velocity structure and near-field strong motion recordings taken within 100 m of each shot show the development of the Rayleigh wave near the shot point

## **USING 1HZ GPS DATA TO MEASURE PERMANENT AND SEISMIC DEFORMATIONS CAUSED BY THE DENALI FAULT EARTHQUAKE**

*Kristine Larson, Paul Bodin, Joan Gomberg, Herb Dragert, and Andria Bilich*

The 3 November 2002 moment magnitude 7.9 Denali Fault earthquake generated large permanent surface displacements in Alaska and large amplitude surface waves throughout western North America. We find good agreement between strong ground motion records integrated to displacement and 1 Hz Global Positioning System (GPS) position estimates collected ~170 km from the earthquake epicenter. One Hz GPS receivers also detected seismic surface waves 750-3800 km from the epicenter, whereas these waves saturated many of the seismic instruments in the same region. High-frequency GPS increases the dynamic range and frequency bandwidth of ground motion observations providing a new tool for studying earthquake processes.

# USING SURFACE WAVES TO CONSTRAIN THE CRUST AND UPPER MANTLE S-WAVE VELOCITY STRUCTURE OF THE SOUTHERN AFRICAN CRATON

Angela Marie Larson and J. Arthur Snoke

Dept of Geological Sciences, Virginia Tech, Blacksburg, VA, 24061, USA, [alarson@vt.edu](mailto:alarson@vt.edu)

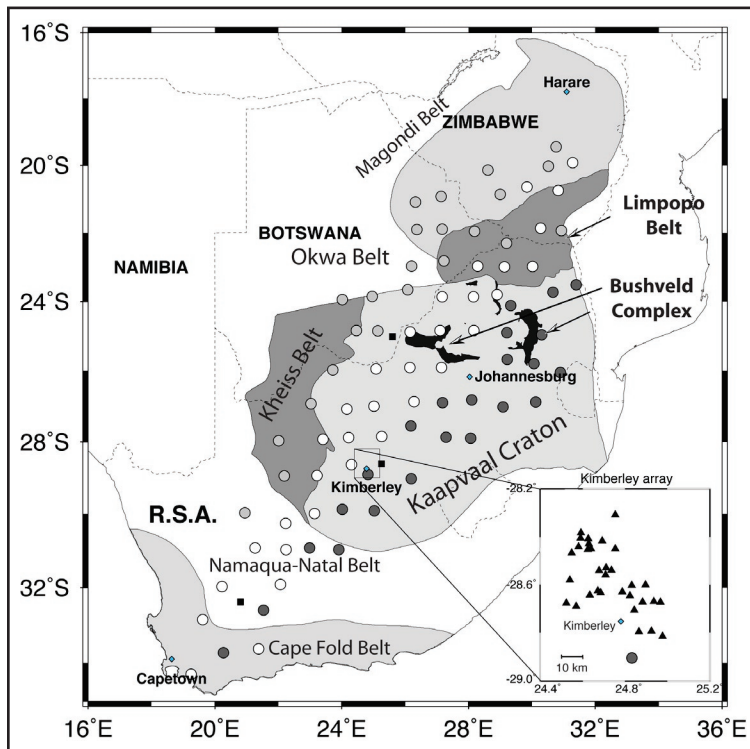
David E. James

Dept. of Terrestrial Magnetism, Carnegie Institute of Washington, Washington D.C., 20015, USA, [james@dtm.ciw.edu](mailto:james@dtm.ciw.edu)

Between April 1997 and July 1999, 55 broadband seismographs (REFTEK/STS2) were deployed in southern Africa (see figure below). Approximately half the stations were redeployed to new sites in April/May 1998 for a total of 81 stations occupied for at least a year. The instruments were sited on bedrock in Zimbabwe, Botswana, and the Republic of South Africa with an average spacing of 100 km.

Ph.D. theses by Gore and by Nguuri (completed, but not yet published) use surface waves from recorded events to constrain the S-wave velocity structures of the crust and uppermost mantle of the Kaapvaal and Zimbabwe cratons. These studies used least-squares inversion and assumed isotropic velocity structures.

The current research will extend these studies in order to improve the constraints on the depth of the Moho as well as on the velocity structure of the uppermost mantle. It will include events not considered previously, include anisotropy in the modeling, and replace the least-squares inversion with one using the Neighbourhood Algorithm (NA) developed by Malcolm Sambridge of the Australian National University. The NA is a direct-search algorithm for nonlinear inversion, which has the benefit of extracting specific data from an ensemble of models as well as determining the best-fit model. The NA was used in a smaller-scale study (compared to the current project) of the Brazilian Shield (Snoke and Sambridge, JGR, vol. 107, no. B5, 10.1029/2001JB000498, 2002).



Map showing the principal geologic provinces in southern Africa. The location of Southern Africa Seismic Experiment stations are shown as circles: white circles represent seismographs deployed for the full two years, while stations that were moved are shown first as light gray circles and then as dark gray circles. Black squares denote global digital seismic stations. Station locations of the Kimberley array are indicated by solid triangles in the map inset (from Niu and James, *Earth and Planetary Science Letters*, vol. 200, 121–130, 2002).

## COMPLEX ANISOTROPIC STRUCTURE OF THE MANTLE WEDGE BENEATH KAMCHATKA VOLCANOES

*Vadim Levin, Dept of Geological Sciences, Rutgers University Jeffrey Park, Dept of Geology and Geophysics, Yale University Evgenii Gordeev, and Dmitri Droznin, OMSD, Russian Academy of Sciences, Petropavlovsk-Kamchatsky*

Indicators of seismic anisotropy commonly employed in upper mantle studies include shear wave birefringence and mode-conversion between compressional and shear body waves. When combined together, these techniques offer complementary constraints on the location and intensity of anisotropic properties. The eastern coast of southern Kamchatka overlies a vigorous convergent margin where the Pacific plate descends at a rate of almost 80 mm/yr towards the northwest. We extracted seismic anisotropy indicators from two data sets sensitive to the anisotropic properties of the uppermost mantle. Firstly, we evaluated teleseismic receiver functions for a number of sites, and found ample evidence for anisotropically-influenced P-to-S conversion. Secondly, we measured splitting in S waves of earthquakes with sources within the downgoing slab. The first set of observations provides constraints on the depth ranges where strong changes in anisotropic properties take place. The local splitting data provides constraints on the cumulative strength of anisotropic properties along specific pathways through the mantle wedge and possibly parts of the slab. To explain the vertical stratification of anisotropy implied from receiver functions, and the strong lateral dependence of shear-wave splitting observations, we cannot rely on simple models of mantle wedge behaviour e.g., olivine-crystal alignment through subduction-driven corner flow.

Diverse mechanisms can contribute to the observed pattern of anisotropic properties, with volatiles likely being a key influence. For instance, we find evidence in favor of a slow-symmetry-axis anisotropy within the uppermost 10-20 km of the mantle wedge, implying either excessive hydration of the mantle or else a presence of systematically aligned volatile-filled cracks or lenses. Also, shear-wave splitting is weak beneath the Avachinsky-Koryaksky volcanic center, suggesting either vertical flow or the influence of volatiles and/or thermally-enhanced diffusion creep.

# EXPLORING THE POSSIBILITY OF AN INNER CORE TRANSITION ZONE

*Felipe Leyton, Keith Koper and Lupei Zhu*

Both body wave and normal mode data support the idea that the inner core has significant anisotropy with a symmetry axis nearly parallel with the Earth's axis of rotation. The strength and precise orientation of the anisotropy as a function of depth is poorly known as well as any possible lateral variations. Two recent suggestions for radial variations in anisotropy include a frontier between 200 and 300 km below the inner core boundary, which divides an upper isotropic part from a lower anisotropic part and another delimiting a change in the structure of the anisotropy at a radius of 300 km.

We are currently evaluating the possibility of seismic discontinuities within the inner core using a data set of precritical PKiKP waveforms assembled during a previous study. Specifically, we are stacking data from small aperture seismic arrays in order to increase the signal to noise ratio. Afterwards we define an empirical source time pulse (from the core reflection) and deconvolve this signal from the stacked trace to obtain the structure response below the inner core. Once each event is processed, a second stack is done to further enhance the signal coming from this discontinuity. We compare the results with theoretical computations done by means of generalized ray theory. Our initial results show a lack of a sharp transition in the upper few hundred kilometers of the inner core. We are performing resolution tests to determine our capability of finding these types of structures.

# LOW-VELOCITY CORE STRUCTURE OF THE SAN ANDREAS FAULT AT PARKFIELD FROM FAULT-ZONE GUIDED WAVES

*Yong-Gang Li, John E. Vidale and Elizabeth. S. Cochran*

Coordinated by the EarthScope/SAFOD, we conducted an extensive seismic experiment at the San Andreas fault (SAF), Parkfield to record fault-zone trapped waves generated by explosions and microearthquakes using dense linear seismic arrays of 52 PASSCAL 3-channel REFTEKs deployed across and along the fault zone. We detonated 3 explosions within and out of the fault zone. During the same time interval, the PASO experiment of UWM/RPI led by Thurber and Roecker also detonated 13 shots around the SAFOD drilling site. We observed prominent fault-zone trapped waves with large amplitudes and long duration with the dominant frequencies at 2-3 Hz for near-surface explosions and 4-5 Hz for microearthquakes. Spectral amplitudes of guided waves from the events located within the fault zone show a maximum peak at stations close to the main fault trace and a secondary amplitude peak at the north strand of SAF. Although those stations registered some trapped energy with larger amplitudes than the farther stations for events occurring away from the fault zone, the wavetrain after S-arrival was much shorter than that at the same station for events within the fault zone. However, seismograms recorded for both the stations and shots far away from the fault zone show brief-duration body waveforms. Fault-zone guided waves acquired in the current experiment are similar to those observed in previous studies at the SAF, Parkfield [Li et al., 1990; 1997]. Preliminary results from 3-D finite-difference simulations of seismograms show the existence of a well-developed, low-velocity waveguide along the SAF main trace. We derived group velocities of guided waves from multiple band-passed seismograms to constrain the waveform modeling. We obtained a good fit of synthetic guided waveforms and spectral amplitudes to observations for both explosion and earthquake data with a depth-dependent fault-zone structural model. The main fault has a zone ~150 m wide at surface, tapering to ~100 m at seismogenic depths, in which Q is 15-50 and S velocities are reduced by 30-40% from wall-rock velocities, with the greater velocity reduction at shallow depth and to southeast of the 1966 M6 epicenter. We tested different depths of the fault zone in modeling. Results show that the low-velocity waveguide extends to the depth of at least 4-5 km. We interpret that this distinct low-velocity zone is remanent of repeated damage due to recurrence of the large earthquakes on the principal slip plane. In contrast, a less developed and narrower low-velocity waveguide (with velocity reduction of 20% and width of 50 m) is evident on the north strand that experienced minor breaks at surface in the 1966 M6 event, most likely due to secondary slip during ruptures on the main fault.

## **MAKING EARTHQUAKES RELEVANT TO STUDENTS**

*Leland Timothy Long*

Seismology can be made relevant by recording earthquakes in the classroom. These events become person, and the excitement of seeing a large event while it is being recorded provides a learning moment. The classroom seismometer can be simple, homemade, or an advanced professional instrument. The theory of simple classroom seismometers is reviewed on the web site <http://GaESN.eas.gatech.edu>. Prices range from \$500 to \$3000 for systems that can record data in a digital format. A digital format is preferred for data exchange.

The public memory of a moderate or small earthquake is short. Even major earthquakes like Charleston, 1886, may not be familiar to large segments of the population. We are developing teaching exercises that incorporate historically significant earthquakes. We include not only the large damaging events, but also some of the small events that get lost with time. The objective is to remind students that earthquakes can occur anytime and anywhere. By also focusing on regionally significant events, students can appreciate the hazards associated with the rare large earthquakes in areas like the eastern United States.

## **POSSIBLE FOREARC SLIVER AT THE NORTHERN HALF OF THE LESSER ANTILLES ARC**

*Alberto M. Lopez Seth Stein*

Boundaries of the Caribbean Plate (CA) include two subduction zones at the western and eastern boundaries. Interestingly, there are two main points to note: 1) none of these have CA crust being subducted, and 2) both were excluded from global plate motion models due to their fitting problems. Several years have passed of research at plate boundaries, and we now know that misfits and discrepancies are now attributed to biased slip vectors at oblique subduction zones. Many researchers worked on the interactions between the CA, North America (NA), and the Cocos (CO) plates, yielding different results through different methods and data used. However, recently, the use of GPS have shed valuable information on the problem by comparing it to the standard procedures. DeMets (2000) have shown these results and have suggested the presence of a forearc sliver whose translation is parallel to the Middle America trench. Although the eastern Caribbean also suffered from misfits on global plate motions, and it is also an oblique plate scenario, plate motions are extremely slow compared to its western counterpart. However, slip vectors can be estimated and GPS measurements are currently taken. We propose the presence of a possible forearc sliver at the Lesser Antilles Arc.

## THE NORTHERN WALKER LANE SEISMIC REFRACTION EXPERIMENT

*Louie, J.N., S. B. Smith, W. Thelen, J. B. Scott, M. Clark, and S. Pullammanappallil 1 1  
Seismological Laboratory/174 and Dept. of Geological Sciences, Mackay School of Mines,  
University of Nevada, Reno NV 89557, USA Tel. +1-775-784-4219 Fax. +1-775-784-1833  
louie@seismo.unr.edu*

In May 2002 we collected a new crustal refraction profile from Battle Mountain, Nevada across western Nevada, the Reno area, Lake Tahoe, and the northern Sierra Nevada Mountains to Auburn, California. A 450-km-long transect of 199 PASSCAL "Texan" instruments recorded mine blasts and earthquakes. The use of large mine blasts and the ultra-portable Texan recorders kept the field costs of this profile to less than US\$10,000. The seismic sources at the eastern end were mining blasts at Barrick's GoldStrike pit. The GoldStrike mine produced several ripple-fired blasts using 10,000-40,000 kg of ANFO each, a daily occurrence. First arrivals from the larger GoldStrike blasts are obvious to distances exceeding 250 km in the raw records. We can pick first arrivals from a quarry blast west of the survey near Watsonville, Calif., located by the Northern California Seismic Network with a magnitude of 2.2, across the recording array to distances of 600 km. The Watsonville blast provides a western source, nearly reversing the GoldStrike blasts. A M2.4 earthquake near Bridgeport, Calif. produced pickable P-wave arrivals across at least half the transect, providing fan-shot data. Arrivals from M5 events in the Mariana and Kuril Islands also appear in the records. We find delays approaching four seconds over the northern Sierra Nevada in California and Nevada. These delays are evidence of a >45 km crustal root beneath the northern section of the Sierra, a feature not previously established. Advances in picked times of >2 s appear between the Carson Sink and Battle Mountain in north-central Nevada. Crust as thin as 19 km accompanies the higher heat flow and geothermal resources of that region.

## **RIFTING ISSUES IN THE GULF OF CALIFORNIA**

*Harold Magistrale Gary Pavlis Frank Vernon*

The Gulf of California presents an ideal opportunity to plumb the architecture of lithospheric rifting. It has identifiable conjugate margins; presents the gamut of processes accommodating extensional strain, from continental extension to seafloor spreading; has a reasonably well understood plate-tectonic kinematic framework; and is logistically accessible. The NSF Margins/RCL program has identified the Gulf as a focus area to study continental rapture.

Some outstanding questions are: How is strain partitioned in map view and with depth during lithosphere rupture? What is the scale of deformation of the lower crust? What is the relation between upper mantle processes and lithosphere rifting? Are low angle faults involved in rifting? Answering these requires constraining the relation between brittle upper crustal deformation, ductile lower crustal deformation, and processes of the upper mantle. The best tool to achieve these constraints is a dense array deployment of broadband instruments from the IRIS PASSCAL program to record teleseismic, regional, and local earthquakes. Analysis of data so collected using 3D converted wave imaging techniques can directly image Moho and upper mantle discontinuities. Seismic tomography can determine seismic velocities and structure of the crust and upper mantle. Shear wave-splitting analysis will provide a measure of the upper mantle tectonic fabric, which will constrain the interpretations of rifting mechanisms. Attenuation analysis will provide constraints on the shear and surface-wave anomalies previously mapped under the Gulf.

The potential of along-strike variations in rifting processes, or in the degree of rifting, provides an opportunity to integrate the existing fixed broadband arrays in southern California and movable Earthscope instruments. These elements can be combined into an array across the Salton trough along the international border, and the results compared to those obtained further south across the Gulf.

# THE YAVAPAI-MAZATZAL BOUNDARY: A LONG-LIVED ASSEMBLY STRUCTURE IN THE LITHOSPHERE OF SOUTHWESTERN NORTH AMERICA

*M.B. Magnani (1), A. Levander (1), K.C. Miller (2), K.E. Karlstrom (3) and Ken Dueker (4)*  
*(1) Department of Earth Science, Rice University, Houston, TX, USA, (2) Department of Geological Sciences, UTEP, El Paso, TX, USA, (3) Department of Earth and Planetary Sciences, University of New Mexico, Albuquerque, NM, USA, (4) Department of Geology and Geophysics, University of Wyoming, WY, USA. [beatrice@rice.edu](mailto:beatrice@rice.edu)*

The Proterozoic assembly of much of the continental lithosphere of the southwestern United States occurred between 1.8-1.6Ga, when a succession of island arcs collided with the Archean-age Wyoming province. During the assembly, which established northeast-striking boundaries and tectonic provinces, tectonic elements of different scale were incorporated in the Laurentia super-continent and the boundaries between these fragments persisted as steeply dipping structural and chemical boundaries, possibly reactivated during the subsequent magmatism or/and tectonic deformation. Geophysical, geological and geochemical data show that these northeast-striking boundaries influenced the tectonic history of the North American craton. In spite of this long-lived influence, some of the tectonic boundaries between crustal fragments are still elusive and their nature, origin and extension at depth are not well constrained. The Jemez Lineament, originally defined as an alignment of Tertiary-Quaternary volcanic centers, is a NE trending zone characterized by active uplift, low seismic velocity in the mantle, and repeated reactivation. It also parallels the inferred northeast-striking Paleoproterozoic boundary between the Yavapai Province (1.8-1.7Ga), to the north, and the Mazatzal Province (1.7-1.6Ga) to the south. Although the legacy of the Proterozoic grain has been invoked as a possible control on the location of the recent magmatism, a viable explanation has not been proposed yet.

A 170km long deep seismic reflection profile crossing the Jemez Lineament in north-central New Mexico was recorded as part of the Continental Dynamics of ROcky Mountain (CD-ROM) project. The profile images oppositely dipping zones of reflections that converge in the deep crust. We interpret this as a Paleoproterozoic bivergent orogen centered on the Jemez Lineament that formed during original Proterozoic crustal assembly by collision of Mazatzal island arcs with Yavapai proto-North American continent. The bivergent orogen is bound to the north by a ~5- km-wide south dipping zone of reflectivity that extends from 10-15 km depth to 30-35 km depth and dips at 25 degrees, and to the south by north dipping reflections extending through the middle and lower crust. We interpret the south dipping feature as part of a north vergent thrust system that developed within the southern edge of the Yavapai province during island arc-continent collision with the Mazatzal terranes at about 1.65-1.68 Ga and the north dipping reflectors as a crustal scale duplex that formed synchronously with the northern thrust system. The upper crust shows structures recording a succession of tectonic and magmatic events from the Paleoproterozoic to the Recent. Notable among these structures is a system of nappes that formed during development of the bivergent orogen. Elements of the nappe system are exposed in Rocky Mountain uplifts, and have been dated as having formed at 1.68 Ga, at depths of 10 km and at temperatures >500°C. We also see continuous bright reflections in the upper-mid crust that we associate with basaltic magmatism of 1.1Ga or Tertiary age. Weak Moho signal is detected at about 43-45km depth which coincides with the depth of the Moho detected by a ~1000km long refraction profile, recorded almost coincident to the reflection experiment.

The Jemez Lineament overlies the root of the bivergent Proterozoic orogen, and we suggest that this Paleoproterozoic zone of weakness has subsequently acted as a conduit for magmatism, and a locus of tectonism.

## **ANSS DETECTION THRESHOLD**

*D.E. McNamara and R.P. Buland*

We have computed minimum earthquake moment magnitude,  $M_w$ , detection thresholds, for a 1x1 degree grid across the US using the existing backbone stations of the Advanced National Seismic System (ANSS). For every grid point we compute the minimum  $M_w$  for which the P phase should be detectable by at least five ANSS stations. Detection is declared at a station when body wave power levels produced for a given  $M_w$  are above the frequency dependent 90th percentile noise level for the station. Noise levels were determined in a previous study from probability density functions of noise spectra computed for each ANSS backbone station (McNamara and Buland, 2003).

To determine event power levels, first earthquake moment,  $M_0$ , is computed as a function of apparent corner frequency using the source scaling formulas of Brune (1970, 1971). Apparent corner frequency is the frequency at which body wave spectral amplitudes are maximum (accounting for attenuation and short period filters applied during NEIC phase picking). The corresponding moment magnitude,  $M_w$  is computed after Kanamori (1977). Body wave amplitudes are then computed for each station depending on the distance and attenuation along each raypath. Amplitude is then converted to power (dB) and compared to station noise levels. The fifth lowest power, above station noise levels then corresponds to the minimum earthquake magnitude for that particular grid point. Our theoretical minimum  $M_w$  threshold compares favorably to  $m_b$  thresholds determined from USGS PDE catalogs. Results from this study are useful for characterizing the performance of existing ANSS broadband stations, for detecting operational problems, and should be relevant to the future siting of ANSS backbone stations. Results from this analysis could also be used to optimize the distribution of ANSS regional network stations.

# **GEOPHYSICAL SETTING OF THE SAN ANDREAS FAULT OBSERVATORY AT DEPTH (SAFOD) AT PARKFIELD, CALIFORNIA**

*Darcy K. McPhee*

We present compiled surveys of gravity, aeromagnetic and ground magnetic data in the Parkfield region of the San Andreas Fault (SAF), particularly focusing on the area around the San Andreas Fault Observatory at Depth (SAFOD). The gravity data, reduced to isostatic anomalies, comprise a compilation of three different data sets with a maximum of 1.6 km grid spacing for the scattered data and closely spaced (~40 m) stations along one SW-NE profile crossing the SAFOD pilot hole. Aeromagnetic data were flown at a nominal 300 m above the terrain along SW-NE flight lines perpendicular to the San Andreas Fault. Data were recorded at ~50 m spacing along flight lines approximately 800 m apart. Ground magnetic data recorded every 5 m along lines ~300 m apart cover a 3 x 5 km area surrounding the SAFOD pilot hole.

These potential field data, along with other geophysical and geological constraints, are used to characterize and develop more detailed geological models of the San Andreas fault zone at SAFOD. Regional gravity and magnetic data indicate two very distinct basement blocks separated by a steeply dipping SAF. The southwest side of the SAF is characterized by a local, highly magnetic linear feature sub-parallel to the SAF, interpreted to be due to Salinian block basement rocks. Magnetic highs on the NE side of the SAF are interpreted to result from a sliver of serpentinite in Franciscan basement rocks. Gravity highs observed SW of the SAF in Salinian block basement rocks are in sharp contrast to gravity lows observed just NE of the SAF, likely due to less dense basement rocks of the Franciscan Complex and serpentinite.

Gravity and magnetic data are used to compute a 2-D crustal model along a 5 km long southwest-northeast profile extending through the SAFOD pilot hole and along the high-resolution seismic refraction/reflection survey completed in 1998 (Catchings et al., 2002). Previous modeling showed that magnetic granitic basement rocks southwest of the SAF are divided by an inferred steep fault sub-parallel to the SAF. An order of magnitude change in newly acquired susceptibility measurements from the pilot hole, possibly indicative of the Buzzard Canyon fault, is used to constrain these previous models. A geological model incorporating these new data from the pilot hole is presented here. In addition, gravity data predicted from velocity models of the fault zone at SAFOD are compared with observed gravity and can help constrain tomographic modeling as well as refine our geological models.

Furthermore, we will use potential field geophysical data and surface geology to construct a 3-D digital model of the upper crust surrounding SAFOD that will act as a tool for directly comparing quantitative subsurface interpretations based on various methods including seismic refraction and reflection, seismicity, magnetotelluric, gravity, magnetic, and geologic techniques throughout the lifetime of the SAFOD project.

## **GEODETIC EVIDENCE OF SLOW FAULTING DURING THE 2001 MW=8.4 PERU EARTHQUAKE SEQUENCE**

*Timothy I. Melbourne Central Washington University 400 E. 8th Ave Ellensburg, WA 98926 USA  
Frank H. Webb Jet Propulsion Laboratory California Institute of Technology 4800 Oak Grove Dr Pasadena, CA 91109 USA*

Two-hour position estimates from a continuous GPS station located at Arequipa, Peru, document a wide range of deformation associated with the June 23rd 2001 Mw=8.4 earthquake. Coseismic displacements from the mainshock amount to nearly  $55 \pm 0.5$  cm of southwest extension and subsidence, despite Arequipa station lying nearly 200 km from the Nazca-South American trench. Several cm of coseismic offset is also observed during the largest events in the vigorous aftershock sequence. A strong preseismic signal beginning 16 hours prior to an Mw=7.6 aftershock appears on the north and east components as a slow displacement with an amplitude twice that of the subsequent coseismic. Analysis of four years of 18-hour rate measurements show this signal to be unprecedented and beyond four standard deviations from the mean rate. Directionally consistent with slow slip along the plate interface, the best fitting centroid suggests the preseismic deformation arises from creep near the aftershock rupture. This implies the Nazca-South American plate interface slipped slowly prior to seismogenic faulting. Arequipa also experienced rapid postseismic deformation that is marked by continued southwesterly extension and vertical rebound at rates that overwhelm interseismic deformation even two years after the event. The vertical uplift is consistent with postseismic slip located down-dip of the mainshock rupture, very similar in style to that observed following the 1995 Mw=8.0 Jalisco, Mexico earthquake. These observations suggest that spatially heterogeneous creep followed the mainshock, and that the Mw=7.6 earthquake grew out of slow slip along the plate interface. These data demonstrate the range in slip rates accommodated by subduction zone plate interfaces and emphasize the need for a broad range of instrumentation types needed to capture the full spectrum of deformation in tectonically active environments.

# COMPARISON OF SEISMOLOGY AND INSAR-BASED MEASUREMENTS FOR MODERATE SIZE EARTHQUAKES IN SOUTHERN CALIFORNIA

*Robert J. Mellors and Harold Magistrale*

Interferometric synthetic aperture radar (INSAR) is capable of resolving the deformation due to moderate size (less than Mw 6) earthquakes as well as large events. In an effort to determine realistic detection levels for InSAR and compare resolution of source parameters we compile a set of moderate size earthquakes in southern California that were observed with both InSAR and seismic data. We first calculate the expected surface deformation for all events larger than MI 4.0 and smaller than Mw 6 using location and focal mechanism parameters from published catalogs based on seismic data (both first-motion and waveform based). Fault ruptures were estimated using standard moment/magnitude relations and slip was scaled to length. An elastic half-space was used to calculate surface deformation. The results indicated that 32 events from Jan 1, 1992 to Jan 1, 2001 produced more than 10 mm of line-of-sight range change (assuming an ERS descending orbit). After eliminating events in areas of low correlation and events contaminated by deformation from large ruptures (such as the 1992 Landers, CA event or 1999 Hector Mine event), we compared the locations with available interferograms. So far, we have four candidate events (7/5/92 Pisgah, 12/4/92 Fawnskin, 3/18/97 Calico, and two co-located Hector Mine aftershocks on 10/21/99 and 10/22/99). Two of the events likely represent deformation from multiple and closely spaced earthquakes. One event (the 12/4/92 Fawnskin event) has been previously reported. We then used a grid search algorithm to determine the depth, moment, and focal mechanism by matching the observed surface deformation as observed on multiple independent interferograms of the same event (using both descending and ascending orbits where available and using both half-space and layered models). The epicentral location (as determined by seismic data) falls within the area of fault rupture for the events and consequently the InSAR data cannot improve the epicentral estimates (at least for Southern California). The InSAR data is useful in placing firm constraints on the depth estimates for shallow (< 5 km) events and for estimating the focal mechanism, although some trade-offs occur between depth, focal mechanism, and moment. Layered models fit the data better than a half-space. The depths and moments derived from InSAR were more consistent with the values from the catalogs based on waveform modeling rather than the depths from the catalog based on phase arrival times. In addition, it may be possible to determine the preferred rupture plane for some moderate size events using the InSAR data.

# CRUSTAL Q AND MANTLE VELOCITY DISTRIBUTIONS BENEATH EURASIA AND THEIR RELATIONSHIP TO SUBDUCTION/OROGENIC PROCESSES OF THE TETHYSIDES BELT

*Brian J. Mitchell and Alemayehu L. Jemberie*

Lg coda Q at 1 Hz exhibits large regional variations across Eurasia being highest in the stable cratons of northern Eurasia and in the cratonic part of India. Lowest values lie within the tectonically active Tethysides belt that stretches across southern Eurasia from Spain to eastern China. Substantial variations of Q occur within both the Tethysides belt (150-500) and regions outside it (250-1000). Variations of Lg coda Q generally correlate positively with Rayleigh-wave phase velocity variations at periods of 50 and 100 seconds. Low values of both Lg coda Q and velocity occur predominantly above mantle rock in which temperatures are higher than normal; the low values extend well beyond the northern limit of Tethysides slab material at a depth of 300 km. Similarities between mapped patterns of long-period Rayleigh-wave velocities and upper mantle temperatures suggest that high temperatures cause low velocities in the upper mantle. The high temperatures may generate fluids of hydration that travel upward to the crust and cause Lg coda Q to be low. An exception to the generally positive correlation between Lg coda Q and long-period Rayleigh-wave phase velocities occurs in the Arabian Peninsula where velocities increase from west to east while QC values decrease. Shorter-period (20-24 s) Rayleigh-wave phase-velocities, like Lg coda Q values, decrease from west to east. These observations suggest that relatively shallow mantle rock, where shear-wave velocities are high, strongly affect long-period Rayleigh wave velocities beneath western Saudi Arabia. 1-Hz Lg waves and 20 s Rayleigh waves in that region primarily sample cooler rock at shallower depths but QC values are still lower than expected for stable regions. This can be explained if fluids, released by high temperatures at depth, travel to the crust where they reduce values of both Q and velocity.

## **INTEGRATED SEISMOLOGICAL STUDIES OF CRUST/UPPER MANTLE STRUCTURE AND ANISOTROPY IN WESTERN ANATOLIA**

*Brian J. Mitchell and Lupei Zhu Department of Earth and Atmospheric Sciences, Saint Louis University Nihal Akyol Department of Geophysics, Dokuz Eylul University, Izmit, Turkey*

Western Turkey is one of the most seismically active continental regions in the world and much of it is undergoing extensive north-south extensional deformation. The extension has produced a large graben system that covers most of westernmost Turkey. The grabens trend in an east-west direction and are bounded on the north by the North Anatolian Fault. In a cooperative study, seismologists from Saint Louis University and Dokuz Eylul University in Izmir, Turkey, deployed 5 broadband and 24 short-period seismic stations in western Anatolia in November 2002. The high-frequency instruments were located along a NS 100 km long profile with 2 to 3~km station spacing in the central portion of the zone of extension. The remaining instruments were deployed as a regional array distributed throughout the region. We plan to use data from the high-frequency linear array to obtain a two-dimensional structural model of the grabens and underlying rock by using teleseismic receiver functions. We will use both the linear array and regional array recordings of local earthquakes to perform a combined inversion for precise event location and a tomographic velocity model of the region. We will use data from the broadband instruments to perform several studies. These include (1) using receiver functions to obtain a one-dimensional crust/upper mantle velocity model beneath each of the four stations in the temporary deployment, as well as for a permanent station just outside the zone of extension, (2) using receiver functions to obtain anisotropic models of the crust beneath each of the stations, (3) measuring shear-wave splitting for SKS and SKKS phases to obtain the azimuthal orientation of anisotropy in the upper mantle, (4) determining possible anomalous azimuthal variations in surface-wave velocity and polarization as a function of period to infer the possible existence of anisotropy and its orientation. We will use all instruments (2~Hz and broadband) to measure azimuthal variations in the velocity of Pn, and possibly other regional phases. We will also, as far as possible, measure shear-wave splitting and its azimuthal variation, using local and regional events.

# FINITE FREQUENCY GLOBAL P WAVE TOMOGRAPHY

*Raffaella Montelli, Guust Nolet, Guy Masters, F. Anthony Dahlen, Shu-Huei Hung*

The travel time of a finite frequency wave is sensitive to velocity structure off the geometrical ray within a volume known as the Fresnel zone.

We compute 3D travel time sensitivity efficiently by using the paraxial approximation in conjunction with ray theory and the Born approximation (Dahlen et al., 2000) to invert global travel times of long-period compressional waves.

Our data set consists of 67540 P and 20266 PP-P travel times measured by cross-correlation. The sensitivity of a broad-band P arrival time resembles a hollow-banana surrounding the unperturbed path with sensitivity being zero on the ray.

Typical widths of sensitivity kernels at the turning point are about 1000 km and 1300 km for a P wave at  $60^\circ$  and  $80^\circ$  epicentral distance, respectively.

The region of insensitivity around the geometrical ray is small near the source and the receiver but can extend to about 400 km near the turning point for a P wave at  $80^\circ$  epicentral distance.

Because of the minimax nature, surface reflected PP waves show a much more complicated shape of the sensitivity region, with the banana-doughnut shape replaced by a saddle-shaped region upon passage of a caustic.

Not surprisingly, the introduction of such complicated sensitivity has consequences for the final tomographic images.

We compare tomographic models inverted with the new method and with the more standard technique of ray theory for the same data fit (i.e. same  $\chi^2$ ) and each smoothed to resolve very similar length scales.

Depending on depth and size of the anomaly, amplitudes of the velocity perturbations in finite frequency images are on average 30%-60% higher than those obtained with ray theory. This demonstrates a major shortcoming of ray theory.

It is not possible to neglect wavefront healing effect, as ray theory does.

The images obtained by inverting long-period waves provide unambiguous evidence that a limited number of hot-spots are fed by plumes originating in the lower mantle.

To better constrain the P wave velocity structure in the Earth, we combine the long period data with ISC delays obtained at short period.

Inverting a combination of low and high frequency waves allows to properly constrain long wavelength heterogeneity with the kernels, while using the high-frequency data (e.g. ISC delays) to constrain smaller-scale structure.

We shall present the latest results of this inversion and discuss the improvements brought about by the various improvements in the theory.

## **DEPTH-DOMAIN PROCESSING OF TELESEISMIC RECEIVER FUNCTIONS AND GENERALIZED THREE-DIMENSIONAL IMAGING**

*Igor B. Morozov (Department of Geological Sciences, University of Saskatchewan, Saskatoon, SK S7N 5E2, Canada) Kenneth G. Dueker (Department of Geology and Geophysics, University of Wyoming, Laramie, WY 82071)*

Stacking, either by itself or as a part of depth migration, is usually used for noise suppression in teleseismic receiver function (RF) images. However, stacking is neither the only signal enhancement method available, nor is it the most efficient in the environment of source-generated noise typical for RF imaging. We generalize the methodology of pre-stack depth migration by including numerous signal-enhancement schemes known in reflection seismics. The method operates in full 3D geometry, incorporates most of the existing imaging techniques and suggests a generalized framework of RF depth imaging. We present four applications of this technique using the data from the teleseismic PASSCAL CD-ROM experiment: 1) building common-image gathers to assess depth focusing of RF images, 2-3) imaging using median and coherency filters for noise suppression, and 4) generalized 3D Common Conversion Point stacking. The results suggest that with the limited volumes and quality of the existing RF datasets, adaptive filters could be superior to record summation used in conventional depth migration.

## **TOMOGRAPHIC IMAGING OF VP/VS ALONG THE LARSE II PROFILE IN SOUTHERN CALIFORNIA**

*J.M. Murphy (1), G.S. Fuis (1), R. Catchings (1), M. Goldman (1), W. J. Lutter (2) (1) U.S. Geological Survey, Menlo Park, CA 94025 (murphy@usgs.gov, fuis@usgs.gov, catching@usgs.gov, goldman@usgs.gov) (2) University of Wisconsin, Madison, WI 53706 (wlutter@wisc.edu)*

In situ shear wave velocities were measured during the Los Angeles Region Seismic Experiment (LARSE). During Phase II of LARSE, wide-angle data were collected along a 150-km-long profile trending NNE from Santa Monica Bay to the southern Sierra Nevada. The profile was designed to image sedimentary basins and faults in the Transverse Ranges and the western Mojave Desert. It extended across the Santa Monica Mountains, San Fernando Valley, Santa Susana Mountains, Santa Clarita Valley, north-central Transverse Ranges, and western Mojave Desert (Antelope Valley), with a sparsely recorded extension through the Tehachapi Mountains and into the southern Sierra Nevada.

Shear (S) waves are observed from most shots along the profile, including shots in the three Cenozoic sedimentary basins (San Fernando, Santa Clarita, and Antelope Valleys) and shots in mountain ranges underlain by Cenozoic sedimentary rocks (Santa Monica and Santa Susana Mountains). S waves are generally strongest from shots in crystalline rocks of the central Transverse Ranges and Sierra Nevada. P-wave and S-wave arrivals were picked on the vertical component seismograms which had a nominal spacing of 100 meters. The picks were checked on the horizontal component seismograms, which had a spacing of ~ 600-700 meters and particle motion from selected 3-component sites were examined.

From south to north along the profile, S-wave velocities near the surface (200-300 meters) have the following values: 1200-1500 m/s in the Santa Monica Mts; 600-700 m/s (where observed) in the southern San Fernando Valley; 700-800 m/s in the northern San Fernando Valley; 800-900 m/s in the Santa Susana Mts; 900-1000 m/s in the Santa Clarita Valley; 1400-1800 m/s in outcrops of Pelona Schist in the Sierra Pelona; 1800-2000 m/s in the crystalline rocks north of the Sierra Pelona in the north-central Transverse Ranges; and 800-1200 m/s in the Antelope Valley. Shear wave velocities are observed in the northern San Fernando basin to depths of 1-2 kilometers and increase in velocity to ~2000 m/s between 1.5 and 2 km in depth. In the Santa Clarita basin, Shear wave velocity increases to 2000 m/s at ~1.5 kilometers. In the southern San Fernando basin, shear waves are only observed near the surface - ~200-400 meters. In the crystalline rocks of the Transverse Ranges and southern Mojave Desert, the  $V_p/V_s$  ratio is ~ 2.5 near the surface but drops below 2.0 at depths >1-2 km. In the sedimentary rocks of the Antelope Valley and Santa Clarita Valleys,  $V_p/V_s$  reaches as much as 3.0 near the surface. In the San Fernando Valley,  $V_p/V_s$  is consistently 3.0 or greater near the surface with highest, but most poorly constrained values (>3.5) in the southern San Fernando Valley. In the Santa Monica Mts,  $V_p/V_s$  is 2.4-2.7 near the surface.

## **BROADBAND OBSERVATIONS OF PLATE BOUNDARY DEFORMATION IN THE SAN FRANCISCO BAY AREA**

*Murray, M. H, Y. Bock, R. Bürgmann, M. J. S. Johnston, J. Langbein, A. Linde, B. Romanowicz, I. S. Sacks, D. T. Sandwell, P. G. Silver, W. Thatcher*

The Integrated Instrumentation Program for Broadband Observations of Plate Boundary Deformation (“mini-PBO”) is a joint project, partially funded by the EAR NSF/IF program with matching funds from the participating institutions and SCIGN, to develop an integrated pilot system of

instrumentation for the study of plate boundary deformation in central California. Under the project, 9 GPS stations were installed last year near Parkfield, a subset of sites of which will soon collect and process data in real-time, and a 5-m X-band SAR downlink facility has been supported in San Diego to collect and archive InSAR data for integration with other geodetic data. We report on the installation of 5 borehole stations with GPS, tensor strainmeter, and 3-component seismometer instrumentation along the Hayward and San Andreas faults in the San Francisco Bay Area. All 5 boreholes have been drilled and equipped with strainmeters and seismometers, and downhole pore pressure and tilt sensors, electronics, recording systems, and GPS systems have been or will soon be added. The GPS, strainmeter and seismometer data is telemetered over frame relay, while lower frequency data is telemetered using the GOES system. All data is available to the community through the NCEDC. The newly fabricated tensor

strainmeters are reliably measuring tidal strain, and local and teleseismic earthquake deformation, and the inferred strain provides constraints on the depth of creep observed on the northern Hayward fault. The GPS antennas are mounted at the top of the borehole casings in an experimental

approach to achieve stable compact monuments. While the time span has been too short to reliably assess long-term stability, the short-term repeatability in daily positions is similar to those obtained by more traditional monuments.

# ADDRESSING SEASONAL NOISE WHEN MODELING TRANSIENT DEFORMATION PROCESSES

*Jessica Murray and Paul Segall*

Frequently-recorded data from geodetic networks often show clear seasonal signals. In some cases this noise has fairly regular annual or semi-annual periods, but in others the pattern is less consistent. Moreover, it is often difficult to identify a causative physical process for the seasonal signal, or the complexity of the likely underlying process (or processes) makes including it in a model infeasible. The presence of seasonal noise becomes especially problematic when attempting to model the data for transient deformation sources. One approach is to “pre-clean” the data before conducting a deformation analysis, however doing so runs the risk of eliminating some component of the deformation signal that one ultimately hopes to model. Here we explore a means for imaging a transient deformation process in the presence of both random walk local motion and seasonal noise. Using a simple model for seasonal variation that consists of a sum of sines and cosines with time varying amplitude, we simultaneously estimate the fault slip history, random walk benchmark motion, and seasonal noise. This method has an advantage over seasonal state space methods in that the data need not be sampled evenly in time, and fewer repeats of the annual cycle are necessary to model the seasonal signal. We show results from simulations using synthetic data, which we conducted in order to better understand the contribution made by each component of the model, as well as results from modeling two-color EDM data collected at Parkfield, CA.

# **SURFACE-WAVE CONSTRAINTS ON THE RADIALY ANISOTROPIC S-VELOCITY STRUCTURE OF THE NORTH AMERICAN UPPER MANTLE**

*Meredith Nettles and Adam M. Dziewonski Department of Earth and Planetary Sciences, Harvard University*

The nature and depth extent of the relationship between the continental crust and the mantle that underlies it are of fundamental importance for our understanding of crust-mantle interactions. Seismic imaging provides the primary means by which heterogeneities in mantle structure can be detected, and it will be through quantitative comparisons of three-dimensional seismic velocity structure and other geophysical, geological, and geochemical data that a better understanding of the relationship between the crust, the lithosphere, and the convecting mantle will be achieved. With the large quantity and good quality of seismic data recorded globally and within North America, it is now becoming possible to resolve velocity heterogeneity within the mantle on a length scale short enough for such comparisons to be meaningful. We note that in order to be able to infer the thermal and chemical structure of the mantle from imaged velocity structure, it is important to account for the effects of seismic anisotropy, particularly as radial anisotropy is known to be strong in the top few hundred kilometers of the mantle.

In this study, we use Love and Rayleigh wave phase delays to determine both  $V_{sv}$  and  $V_{sh}$  velocity structure in the upper mantle under North America. Measurements of fundamental-mode dispersion are made for approximately 250,000 source-receiver pairs, where the receivers are stations of the Global Seismographic Network (GSN), the United States National Seismograph Network (USNSN), the Canadian National Seismograph Network (CNSN), and the temporary Missouri to Massachusetts (MOMA) stations, which were deployed as an IRIS PASSCAL project. The primary dataset consists of phase-delay measurements made at periods of 35-150 s using the method of Ekstrom et al. (1997); the longer-period (200-350 s) phase-velocity measurements of Nettles et al. (2000) are also included, to improve sensitivity to transition-zone structure. We invert these data for radially anisotropic, three-dimensional S-velocity structure from the base of the crust to a depth of 1000 km. The model we determine is global, but utilizes a finer parameterization within the North American continent, in an approach similar to that employed by Boschi (2002) for the Mediterranean region. This approach allows us to take into account the variations in seismic velocity outside of North America that are encountered by surface waves traveling through the continent, reducing artifacts within North America that would otherwise be produced by the mapping of global anomalies into the regional model. Our preliminary results show a distinct, fast, continental root under the Canadian shield, decreasing abruptly in thickness at the western limit of Appalachian deformation. Fast velocities extend to ~150 km depth under the western Atlantic, similar to the finding of Ekstrom and Dziewonski (1998) for the westernmost Pacific. The transition between significantly fast and slow velocities in western North America is found to be narrow, distributed over no more than a few hundred kilometers; this boundary appears to follow the western edge of the North American craton.

## **GROUND DEFORMATION STUDIES ON LARGE SILICIC VOLCANIC SYSTEMS: AN ERUPTION FORECASTING TOOL EARTHSCOPE CAN GREATLY IMPROVE**

*Andrew V. Newman Earth and Environmental Sciences Environmental Geology and Risk Assessment (EES9) MS D462 Los Alamos National Laboratory anewman@lanl.gov*

Volcanic eruptions are among the most widely feared and costly of natural disasters. Subduction zone silicic stratovolcanoes and calderas, such as Mt. St. Helens, Pinatubo and Etna, which experience catastrophic eruptions, tend to be located near large populations, thus causing tremendous potential hazard to human life. Fortunately, most volcanoes experience significant surface deformation in the days, months, or years prior to a large eruption as magmatic pressure or volume increases inside the volcano. Present state-of-the-art volcano forecasting consists of geodetic, seismological, geochemical and visual monitoring. Significant changes in one or more of these "vital signs" might generate an eruption forecast and prompt a costly and inconvenient evacuation. At this time, however, the use of individual signals for volcano forecasting is not precise and may lead to ambiguous and misleading eruption forecasts. Thus, it is necessary for us to better develop these tools for understanding volcanic systems. Earthscope, particularly PBO, US-Array's Bigfoot and In-SAR, should focus study on several of these active systems because, over the program's lifetime, there is good potential to capture an entire eruptive sequence with unprecedented detail. With more realistic modeling of data obtained here we should be able to better understand volcanic plumbing systems and develop more detailed and accurate eruption forecasts.

To improve the geodetic tools, I am developing more realistic numerical models exploring the effects of viscoelastic material and non-spherical sources on such silicic systems. Until recently, most models of volcanic ground deformation assume deformation occurs in purely elastic rock. However, at large silicic systems heat flow from a hot (~1200 °C) magma chamber can significantly heat surrounding country rock beyond its brittle-ductile transition, becoming viscoelastic. Viscoelastic material surrounding the magma filters and distorts pressure changes within the magma chamber into a lagged, time-dependent geodetic signal and can effectively alter the signal seen on the surface. Along with more realistic rheologies, the inclusion of a wide array of spatially distributed data, allows me to explore alternative source geometries that better describe data and fit our existing knowledge about volcanoes. Currently my work focuses on Long Valley Caldera (Sierra Nevada, CA) because of the existing wealth of data, however the techniques developed here should be useful for other similar systems.

In New Mexico, I am performing pilot GPS surveys of volcanic deformation on the Valles Caldera and the Socorro Magma body. If significant signals are present, it will be necessary to densify surveys and install continuous GPS stations to effectively study time-dependent deformation; including a continuous GPS site over these magmatic sources can be achieved through the eastern extent of the PBO.

## **PERISCOPE: AN OFFSHORE COMPONENT OF EARTHSCOPE FOR SOUTHERN CALIFORNIA**

*Craig Nicholson, David Okaya, Paul Davis and the SCEC Borderland Working Group*

The California Continental Borderland offshore of southern California experienced significant elements of Paleogene subduction, Neogene extension, and major components of the evolving Pacific-North American (NAM) transform system. The Borderland was the locus of Pacific-NAM plate motion for about 70% of its tectonic history, and recent GPS and VLBI data suggest that as much as 20% of the current plate boundary motion may still be located offshore. Understanding the tectonic evolution of the continental margin (USArray), the plate boundary (PBO) and the current tectonic architecture of the San Andreas fault system (e.g., SAFOD), as well as the tectonic history and seismic hazards of southern California necessarily requires a fundamental understanding of the offshore California Borderland. As such, the offshore Borderland should be a major component and a primary target for focused research under EarthScope. We propose to call this offshore component PERISCOPE.

In recognition of the importance and significance of the offshore Continental Borderland, SCEC recently created the SCEC Borderland Working Group. Its purpose is to initiate, foster, and coordinate activities in the California Borderland -- activities that are directly relevant to EarthScope's mission of understanding the active plate boundary deformation, earthquake dynamics and tectonic evolution of southern California. A white paper has been produced by the Borderland Working Group (<http://www.scec.org/borderland>) and a number of Borderland projects have recently begun or are in development. This includes a proposal to NSF Continental Dynamics to conduct an integrated, multi-disciplinary, international study within the offshore Borderland. To fulfill its stated research objectives, however, EarthScope will need to consider how best to expand its USArray and PBO components to include critically needed offshore observatories.

PERISCOPE, as currently envisioned, would include re-examination of existing industry multichannel seismic reflection and well data, temporary (long-term) deployments of OBS instruments, focused multidisciplinary Continental Dynamics studies, and the development and establishment of seafloor and island observatories to monitor seismic, strain, and GPS data in collaboration with other marine disciplines that require similar long-term monitoring in a marine environment.

# PHYSICAL PROPERTY OF THE CHEMICAL HETEROGENEITIES IN THE MID-MANTLE: A STRONG AND SLIGHTLY DIPPING SEISMIC REFLECTOR BENEATH THE MARIANA SUBDUCTION ZONE

*Fenglin Niu Department of Earth Science, Rice University Hitoshi Kawakatsu, Yoshio Fukao  
Earthquake Research Institute, University of Tokyo*

While geochemical studies suggest that distinct chemical reservoirs exist in the lower mantle, seismic studies suggest that the lower mantle is generally less heterogeneous than the upper mantle except for the lowermost several hundred kilometers (D" region). We hereafter use middle mantle to refer the vast portion of the lower mantle that lies above the D" region. The relative homogeneity of the middle mantle may be due to the lack of resolution in current seismological techniques. Only velocity anomalies with size 300 km or larger in the middle mantle and small-scale anomalies in the D" region are resolvable using whole mantle tomographic imaging and waveform modeling, respectively. The situation, however, has been changing in recent years due to the rapid increase in the quality and quantity of seismic data, as well as the development of new analysis techniques. Several recent studies using array data have shown that the middle mantle is not as "boring" as we have thought. Small-scale heterogeneities may be ubiquitous in the middle mantle. Strong seismic reflectors and scatterers have been observed in the middle mantle beneath the western Pacific subduction zones. The depths of these seismic reflectors/scatterers are reported to be at 800 km, 900-1200 km and down to about 1850 km. Differences in S-wave velocity between the reflectors/scatterers and the surrounding mantle could be as high as 4%. Difficulty in detecting these reflectors/scatterers and lack of knowledge on the geometric (lateral extension, dip angles) and seismic properties (sharpness, contrast in P and S wave velocity as well as density) of these reflectors/scatterers have resulted in a poor understanding of the nature of these seismic structures. It is still unclear whether they are related to primordial chemical reservoirs, pieces of subducted oceanic crusts or even parts of a highly heterogeneous global compositional boundary. Full understanding of the mid-mantle reflectors/scatterers could potentially shed light on many unsolved questions in the fields of the mantle convection and geochemistry, as well as the evolution and differentiation of the earth.

We observed a clear later phase approximately 80 s after the direct P-wave in most of individual seismograms recorded by a short-period seismometer network in Japan (J-array) from a cluster of deep earthquakes that occurred at the northern Mariana subduction zone. This phase 1) shows a P-wave particle motion; 2) arrives later from earthquakes with shallower focal depths; 3) has a steeper incident angle than that of P wave; and 4) shows a deviation of a few degrees in the arrival azimuth from that of P wave. We interpret it as an S to P converted wave which takes off downward from the source and is reflected at a velocity discontinuity (reflector) below the earthquakes. Applying an inversion technique to the data set shows that the seismic reflector dips toward southwest by about 20° at 24.25°N 144.75°E 1115 km with a lateral extension at

least 100 x 100 km. The location corresponds to the lower edge of a high-velocity anomaly in global tomographic models. Amplitude and waveform analyses suggest a decrease of S-wave velocity by 2-6% and an increase of density by 2-9% within the reflector. There is almost no difference in P-wave velocity (<1%) between the reflector and the surrounding mantle. The estimated thickness of the reflector is about 12 km. These observations indicate that the observed seismic structure is more likely to be a chemical reservoir rather than a purely thermal anomaly. The seismic reflector might be a piece of subducted oceanic crust, as suggested by a previous study. It also could be related to the break down of the D-phase of dense hydrous magnesium silicates (DHMS) at mid-mantle pressure condition reported by recent mineral physics studies. Both scenarios imply that either mechanical or chemical segregation might occur within the subducted slab at mid-mantle condition.

## **Temporal Variations of Seismogram Similarities: a new approach to the time-varying stress field**

*Fenglin Niu,*

*(713-348-4122, [niu@rice.edu](mailto:niu@rice.edu))*

*Department of Earth Science, Rice University, 6100 Main Street, Houston, TX 77005, USA*

*Paul G. Silver*

*(202-478-8834, [silver@dtm.ciw.edu](mailto:silver@dtm.ciw.edu))*

*Department of Terrestrial Magnetism, Carnegie Institution of Washington, 5241 Broad Branch Road, N.W., Washington, DC 20015, USA*

*Robert M. Nadeau*

*(510-486-7312 [nadeau@seismo.berkeley.edu](mailto:nadeau@seismo.berkeley.edu))*

*Berkeley Seismological Lab., 207 McCone Hall Univ. of California, Berkeley, CA 94720-4760, USA*

A major goal of seismologists is to identify temporal variations in the seismic structure of the crust in response to stress changes near a fault zone. One of the approaches to this problem is to compare waveforms generated by repeat earthquakes, which have nearly the same location and mechanism and produce nearly identical seismograms when recorded at the same station. We have chosen to measure the difference in waveforms of several tight clusters of repeat events that occurred on the Parkfield segment of the San Andreas Fault and recorded by a network of borehole seismometers in the same area (HRSN). An exceptionally well-documented aseismic transient took place on this segment around the beginning of 1993, and we wanted to determine whether it produced observable structural changes in the medium as well. We used two parameters: the lag time,  $\tau(t)$ , and decorrelation index,  $D(t)$ , to characterize the difference between two seismograms at elapsed time,  $t$ . The lag time  $\tau(t)$  is evaluated at the maximum of the cross correlation,  $C_m(t)$ , and the decorrelation index  $D(t)$  is defined as  $1 - C_m(t)$ . We have found a significant change in a particular section of the S-wave coda between two sets of events (1988-1992 and 1993-1997), which appears as a spike in both  $\tau(t)$  and  $D(t)$ . We have run a series of tests which strongly suggests that the observed changes in waveforms are not due to variations in earthquake location (verified by relocating the events from the observed S-P times at different stations) nor due to a uniform change of the background medium. Instead, the likeliest explanation is that there has been a change in the location of distinct scatterer(s) by a few meters.

We utilize a simple procedure for locating spatially those scatterers whose properties have changed in time. For each station, we first construct a differential seismogram  $\Delta s(t)$  by taking the difference of the average of the pre- and post-1993 seismograms. For noise-free seismograms,  $\Delta s(t)$  will consist only of energy from any scatterers whose propagation characteristics (travel time or amplitude) have changed, while an unchanged scatterer will be removed by this procedure. We then performed an  $n$ th-root ( $n=1$ ) stack of the amplitude,  $A(x)$ , of  $\Delta s(t)$  from each station, stacking on the predicted arrival time of a candidate scatterer originating from location  $x$ . This function reaches a maximum about 2 kilometers to the southeast of the cluster and at about 3 km depth. The migration of the scatterer(s) occurred at seismogenic depth and therefore is less likely due to the environmental effects. As the difference is almost absent in the P-wave coda, we infer that the scatterer(s) is probably related to the redistribution of fluid-filled fractures which are more efficient in scattering S-wave energy compared to P. The location and timing of this change in the medium strongly suggests that it is a manifestation of the 1993 Parkfield aseismic transient. As such, it likely represents the stress-induced redistribution of fluids in the crust at seismogenic depths.

# **PRELIMINARY RESULTS ON CRUST AND UPPER MANTLE STRUCTURE BENEATH THE EAST AFRICAN RIFT SYSTEM IN ETHIOPIA, KENYA AND TANZANIA FROM PASSCAL EXPERIMENTS**

*Nyblade, A.A.<sup>1</sup>, M.H. Benoit<sup>1</sup>, M. Tuji<sup>1</sup>, K. Walker<sup>2</sup>, T. Owens<sup>3</sup>, and C. Langston<sup>4</sup>  
1Department of Geosciences, Penn State University, University Park, PA 16802 2Department of Geophysics, Stanford University, Stanford, CA 94305 3Department of Geological Sciences, University of South Carolina, Columbia, SC 29208 4CERI, University of Memphis, Memphis, TN 38152*

We present preliminary results on crust and upper mantle structure beneath the East African Rift System from PASSCAL deployments conducted in Ethiopia and Kenya over the past two years, as well as shear wave splitting results from the 1994-1995 Tanzania PASSCAL experiment. Crustal structure, investigated using receiver functions, is characterized by Moho depths of 40-45 km beneath the Ethiopian Plateau, 30-35 km beneath the Main Ethiopian and Kenyan Rifts, 20-25 km beneath the Afar depression, and 35-42 km beneath unrifted Proterozoic terranes in Kenya. Thus, crustal structure appears to be normal outside of the rift valleys proper. Over 1500 relative P wave travel time residuals have been inverted for upper mantle structure under Ethiopia, and results show a broad region of low velocities extending no deeper than ~350 km. Within the broad region of low P wave velocities, the slowest velocities are found beneath the Afar depression and the western portion of the Ethiopia Plateau. Preliminary resolution tests indicate that there is little evidence for the region of low velocities extending into or through the transition zone, as suggested by many global tomographic images. Tentative results of teleseismic shear-wave splitting analysis on seismograms collected across Tanzania have been obtained by stacking 15 high-quality events per station with a modest range in initial polarization directions. Our analysis includes core-refracted phases in addition to direct S phases from hypocenters deeper than 300 km (to avoid splitting from source-side upper mantle anisotropy). There appears to be a systematic rotation of the fast directions around the Tanzania craton, and the longest delay times (max of 1.0 s) are along the flanks of the craton.

## **SOURCE PROCESS OF THE 2002 DENALI FAULT EARTHQUAKE COMPARED TO OTHER LARGE STRIKE-SLIP EVENTS**

*Arda A. Ozacar, Robert Fromm and Susan L. Beck Southern Arizona Seismic Observatory, Department of Geosciences, University of Arizona, Tucson (arda@geo.arizona.edu; rfr@geo.arizona.edu; beck@geo.arizona.edu) Douglas H. Christensen Geophysical Institute, University of Alaska Fairbanks (doug@giseis.alaska.edu)*

The November 3, 2002 Denali Fault earthquake which is the largest inland event ever recorded in central Alaska, occurred along an arcuate segment of the right-lateral strike-slip Denali Fault. We use first motion P-wave polarities and the inversion of teleseismic P-waveforms to constrain the focal mechanism and rupture history. We find clear evidence for a substantial reverse component at the beginning of the rupture, which can not be explained with a pure strike-slip mechanism. This initial subevent occurred along an asperity 20 km west of the hypocenter and can be attributed to thrusting along the Susitna Glacier Fault. Approximately, 10 sec after the first asperity failed, the rupture propagated unilaterally to the east on a strike-slip fault and released most of the seismic moment along an asperity located 170 km east of the hypocenter, adjacent to the rupture transfer from the Denali Fault to the Toschunda Fault which bifurcates toward the southeast. This earthquake had a duration of ~120 sec and a total rupture length of ~320 km with a maximum slip of 8 m. Correlation with gravity anomalies suggests a relation between moment distribution and physical properties of the subsurface rock units that may support a weaker middle segment marked by fewer aftershocks. Moreover, both asperities coincide with intense gravity gradients possibly reflecting a crustal boundary. We analyzed the aftershock distribution by estimating the number of events, released moment, and b-values within regular spaced bins along the rupture plane. Strong correlation with the obtained asperities and weakness zones are observed, suggesting different aftershock nucleation mechanisms for different segments of the fault. Comparison of this event with similar magnitude November 14, 2001 Kunlun earthquake (Tibet) in terms of rupture length, aftershock distribution, radiated energy, static stress drop, and tectonic setting; implies a stronger seismic coupling along the Denali fault. For a broader approach, large ( $M_w > 7.2$ ) strike-slip earthquakes with well-defined source parameters, are classified on the basis of their location with respect to plate types and boundaries into three categories: interplate, oceanic intraplate and continental intraplate events. Each category is characterized by distinct patterns in terms of source parameters indicating that stresses are high for oceanic intraplate, moderate for continental intraplate and low for interplate events. In this respect, both the Denali and the Kunlun events are exceptional and have an interplate signature. In particular, the Denali Fault is an ancient suture between accreted litho-tectonic terranes which might indicate less strain hardening and cause this non-typical behavior.

# UTAH REGIONAL SEISMIC NETWORK -- EXPLORING POTENTIAL EARTHSCOPE-ANSS SYNERGY

*K.L. Pankow, W.J. Arabasz, S.J. Nava, and J.C. Pechmann*

With the upcoming deployment of EarthScope instrumentation, a genuine need exists for communication and coordination with regional networks of the Advanced National Seismic System (ANSS). The programs of EarthScope and ANSS are complementary. By sharing experience, resources, and knowledge, the goals of both programs will be more easily reached. The purpose of this abstract is twofold: 1) to take the first step of communication in the form of characterizing the resources found at one such regional network -- the Utah Regional Seismic Network (URSN) and 2) to suggest which resources available at regional networks should be considered when implementing EarthScope.

During the past three years there has been a substantial monetary investment by ANSS and the state of Utah to modernize data acquisition, processing, and communication systems found at URSN. The results of this (and previous) investments are 1) a network of 131 stations (62 short-period, 11 broadband, and 69 strong-motion) strategically deployed throughout the Utah study region to best monitor active seismogenic zones and to record weak and strong ground motions in densely populated areas and 2) infrastructure and software improvements so that URSN now operates as a near-real-time earthquake information system, providing Web-based information products. These new developments enhance URSN's long-established role as a state and regional earthquake information center. Also of relevance to EarthScope is the URSN education and outreach program. This program, which has been on-going since 1994, is primarily targeted at Utah's rapidly growing K-12 student body (60% increase expected by 2030). As part of this program, activity packets to support the Utah core curriculum have been developed, teacher workshops led, a travelling exhibit has been developed which visits over 50 schools and libraries annually, and a Web site with earthquake information for the general public has been established and maintained.

With decades of network operational experience in the Utah region, we raise the following three issues that should be considered while deploying EarthScope's USArray and PBO. First, careful attention to the site permit process and environmental sensitivity are a must for working in Utah. Sixty-five percent of the state is owned by the federal government (managed by three different agencies) and 10% is owned by the State of Utah. Second, details and potential challenges regarding sharing data and co-location with existing stations need to be addressed. Any of the 131 URSN-operated stations could be used to supplement the USArray or the flexible array. URSN routinely shares data in real time with neighboring networks through Earthworm modules. Third, given that education and outreach is a large component of the EarthScope program, EarthScope information products could be effectively coordinated with those of existing, well-established URSN education and outreach programs.

# USING A HIGH-RESOLUTION SURFACE WAVE MODEL TO IMAGE LITHOSPHERIC STRUCTURE OF WESTERN EURASIA AND NORTH AFRICA

*Michael E. Pasyanos, William R. Walter*

Over the past few years, we have developed a surface wave model for Western Eurasia and North Africa. We have examined more than 30,000 seismograms and made quality group velocity measurements for about 14,000 Rayleigh wave paths and 7,000 Love wave paths. All of the group velocity measurements were made using the PGSWMFA code. Each period is then tomographically inverted independently using a conjugate gradient method to produce Love and Rayleigh group velocity maps of the region. Short period group velocities are sensitive to slow velocities associated with large sedimentary features. Intermediate periods are sensitive to differences in crustal thickness, such as those between oceanic and continental crust or along orogenic zones. At longer periods we find group velocities reflect the shear velocities of the upper mantle. We are continuing to improve this model by increasing the number of surface wave measurements and making use of more densely-spaced PASSCAL deployments and other regional broadband networks. We have also been experimenting with a number of strategies like variable-resolution tomography and finite frequency tomographic methods in an effort to maximize resolution.

The group velocities can then be used to invert for the shear velocity structure of the lithosphere either alone or in combination with other geophysical data. Because we need to provide inversions for structure at many points, we limit the number of free parameters in our grid search and try to fit the data with simple models of the crust and upper mantle. We estimate structure using an adaptive grid search and constrain the sediments with the model of Laske and Masters (1997). We then solve for the thickness of the crust, the average velocity of the crust, and the velocity of the uppermost mantle layer. The technique is described in detail in Pasyanos and Walter (2002). Major tectonic features of the lithosphere (i.e. sedimentary basins, crustal thickening in orogenic zones, crustal thinning along ridges, contrasts between oceanic and continental crust) are well-resolved in this manner. In most cases, the dispersion results are well-fit by these simple models. Oftentimes, however, these models are simply unable to simultaneously fit the Love and Rayleigh wave group velocities at long periods, suggesting transverse isotropy in the mantle. By allowing for variations in the upper mantle velocities between the vertically propagating shear-wave velocity SV (which affect the Rayleigh wave group velocities) and the horizontally propagating shear-wave velocity SH velocity (which affect the Love wave group velocities), we can successfully fit both of the data sets simultaneously, and also map out the regions of transverse anisotropy in the mantle.

# **AN OVERVIEW OF NORTHERN CORDILLERAN TECTONICS IN THE CONTEXT OF THE LATE MIOCENE TO RECENT OBLIQUE-COLLISION OF THE YAKUTAT MICROPLATE**

*Terry L. Pavlis, Dept. of Geology and Geophysics, University of New Orleans, New Orleans, LA 70148*

The northern Cordillera contains the highest mountains in North America and includes the highest coastal mountain range on earth, yet by "lower 48" standards there are large gaps in our knowledge of this orogenic system. In a broad view of northern Cordilleran active tectonics, all of the major high topographic features above ~58N can be considered local to farfield manifestations of the oblique collision of the Yakutat microplate with North America. The Yakutat microplate originated in mid-Cenozoic time when a composite continental-oceanic block was sliced from the North American margin somewhere between the Pacific northwest and central British Columbia. The microplate was transported laterally along the transform margin during late Neogene time, but had little effect on the topography until ~6-8Ma when a major orogenic welt developed as the microplate was jammed into the subduction-transform transition at the eastern end of the Aleutian trench. Uplift and high latitude combined to generate a glacial landscape well before the widespread onset of northern hemispheric glaciation, and thus, the orogen contains a unique record of an orogen exhumed primarily by glacial processes. As the microplate began to collide with North America, it was subjected to three competing tectonic processes: 1) continued subduction carried the microplate laterally into the subduction-transform transition and carried much of the basement into the subduction zone at the same time as cover was stripped from basement in a fold-thrust belt; 2) partial subduction of basement drove lateral extrusion of southern Alaskan lithosphere toward the westa process that occurred both at a local level within the microplate and at regional scales by rejuvenation of the dextral Denali fault system; and 3) the triangular (map view) shape of the microplate forced lateral (EW) constriction as the microplate was jammed into the corner leading to secondary cross-structures that include refolding of early-formed fold-thrust systems as well as the suture at the top of the thrust stack. The third process is probably primarily responsible for the inconsistent correlation between structure and topography in the orogen, but other processes e.g. extreme focused erosion along glacial valleys and slip-partitioning probably also played a role. Major uncertainties remain on location of the major active structures within an orogen where ~50 km/m.y. of plate interaction are being absorbed, and new studies are badly needed to clarify these problems. Moreover, a basic question of the driving process for the orogen remains poorly resolved because it is unclear if the Yakutat microplate is being driven into the subduction "corner" by the Pacific plate, or if instead, the microplate is being pulled into the mantle by a small subduction zone beneath a short magmatic arc segment represented by the Wrangell Mountain volcanoes. Some of these issues can only be resolved as more information is obtained on structural architecture of the orogen from the surface to mantle depths. Ultimately, resolving these issues has significant implications for broader questions of processes in oblique-collisional orogens, and this orogen can serve as a template for interpretation of the complex Mesozoic interactions that assembled the northern Cordilleran lithosphere.

# **SPATIAL AND TEMPORAL DISTRIBUTIONS OF SHEAR WAVE ANISOTROPY AND ANALYSIS OF REPEATING EARTHQUAKES IN THE KARADERE-DUZCE BRANCH OF THE NORTH ANATOLIAN FAULT**

*Peng, Z. and Ben-Zion, Y., Department of Earth Sciences, University of Southern California, Los Angeles, CA, 90089-0740*

We analyze crustal shear wave anisotropy from seismograms recorded by a PASSCAL seismic network deployed along and around the Karadere-Duzce branch of the North Anatolian fault for about 6 month, starting a week after the August 17, 1999, Mw7.4 Izmit earthquake. On November 12, 1999, the Mw7.2 Duzce earthquake started and propagated eastward from the Karadere-Duzce fault. Our temporary seismic network straddles the eastern end of the August Mw7.4 rupture and the western end of the November Mw7.2 event and recorded about 26000 earthquakes.

We use the technique of Silver and Chan (1991) to estimate the fast polarization direction and delay time associated with shear wave splitting in our data set. Clear evidence of shear wave splitting is found in the records of most stations. Initial results show that stations off the fault generally have fast polarization direction sub-parallel to the regional tectonic stress direction (roughly NW-SE). Stations near the fault show polarization directions that are parallel to the local fault strike (Station FP: about 70 degrees, Station CH: roughly 90 degrees, and Station BV: about 100 degrees from North). This suggests stress-induced cracks aligned by nearby faulting during a major earthquake as a source for the observed anisotropy for these stations. The time delay shows no systematic relationship with either focal depth or hypocentral distance, which indicates that seismic anisotropy in our study area is confined primarily to the top 3 km of the shallow crust.

In an effort to detect temporal changes associated with the occurrence of the Izmit and Duzce earthquakes, we perform analysis of shear wave splitting of repeating earthquakes in our study area. Repeating earthquakes are identified using an equivalency class algorithm (e.g., Aster and Scott, 1993). The similarity measure is based on the mean cross-correlation values of all waveforms between event pairs. The waveform cross-correlation is performed over a time window of 1 sec before and 5 sec after the P arrivals. Our data set can be divided to "fault zone" events that are in the vicinity of the Karadere-Duzce branch of the Izmit rupture zone and the remainder "regional" events (located around Stations CH and BV). Depending on the similarity criteria, approximately 15-40% of events in the fault zone set belong to similar event clusters. The percentage is about 8%-20% for the regional events off the fault.

The analysis done so far does not show clear temporal changes at Station BV near the epicenter of the November 12, 1999 Duzce earthquake. Splitting measurement from 14 repeating earthquakes recorded at Station FP shows slightly changes in both fast polarization direction and delay time before and after the Duzce earthquake. However, the changes are small and are within the error of our estimation method. Updated results will be presented in the meeting.

## **SONIC STIMULATION OF HYDROCARBON PRODUCTION: CALIBRATION OF BOREHOLE TOOLS**

*Wayne D. Pennington (Michigan Tech), Roger M. Turpening (Michigan Tech), and Igor A. Beresnev (Iowa State)*

There has been shown, often by anecdotal evidence, but occasionally by serious studies, that there is a relationship between production of oil and/or gas from hydrocarbon reservoirs and the degree of shaking to which that reservoir has been subjected. Sometimes, that shaking is caused by earthquakes. In order to take advantage of whatever mechanism is responsible, some oil and gas operators have contracted to have artificial shaking of the reservoirs take place, in order to stimulate production. One method of such stimulation involves the placement of a borehole tool in a wellbore.

A project is underway that will measure the output from these tools and provide information that will be useful for simulating the mechanism in the laboratory and for calibrating theoretical studies of the mechanism responsible.

Michigan Technological University (MTU) will conduct experiments at a test site that provides ideal conditions for remote monitoring of the far-field displacements induced by sonic stimulation tools, under closely controlled and repeatable conditions. The test facility is extremely well characterized; the entire geological sequence at the site consists of high velocity formations, ensuring very efficient seismic wave propagation. This test site is intended to become a standard location at which any sonic source can be tested.

In close association with tool manufacturers, theoreticians, laboratory modelers, and others with an interest in sonic stimulation technologies, a set of experiment standards will be designed to provide information on the absolute levels of vibrational energy (frequency, displacement amplitudes, etc) created in the far field by sonic stimulation sources. These techniques will be employed at a test site that is known to be ideal for such purposes. The methodology and results of this test will be provided to the sonic-stimulation community and criticisms and suggestions will be sought, particularly at a meeting held for this purpose. The results will be incorporated into theoretical results (led by Iowa State University) contemporaneously.

The experimental field procedure will be modified, as necessary, to include all source types and deployment conditions (to the extent possible), and repeated. The resulting standard experiment and test site will be made available to the industry at large for calibration of additional source tools. Another set of standards will be developed to provide a scientific methodology to be applied during field demonstrations. Technology transfer is an integral part of all portions of the project.

# THE SEISMIC RESPONSE OF THE SEATTLE SEDIMENTARY BASIN, WASHINGTON STATE, TO TELESEISMS RECORDED ON THE SEATTLE SHIPS ARRAY

*Thomas Pratt, Thomas Brocher, Craig Weaver, Karen Meagher, Thomas Yelin, Robert Norris, Lynn Hultgrien, Elizabeth Barnett*

Between January and May, 2002, we maintained an array of 86 three-component seismometers over the Seattle sedimentary basin to study the amplification of weak ground motions over this major basin. The instruments consisted of 2 Hz, L-22 seismometers recorded on Reftek digital recorders operating continuously at 50 samples per sec. The average horizontal amplitudes of arrivals from three large teleseisms at 88 to 101 degrees epicentral distance (3/3/2002 M7.4 Afghanistan; 3/5/2002 M7.5 Philippines; 3/31/2002 M7.1 Taiwan; 4/26/2002 M7.1 Marianas) have been compared to the average of three bedrock sites east and west of the basin in the 0.1 to 1.0 Hz frequency range. Arrivals in a 100 sec time window beginning at the first S-wave arrival were analyzed, and we required signal-to-noise ratios of 1.6 or greater for inclusion in the analysis. Stations near the center of the basin show amplifications of up to 6 at frequencies of 0.2-0.4 Hz and 0.4-0.8 Hz, and amplifications of as much as 4 in the 0.1-0.2 Hz bandwidth. In east-west profiles, the amplitudes are strongest near the center of the basin but decrease sharply near the edges. In north-south profiles, the amplitudes are largest over the basin and lower over the shallow bedrock of the Seattle uplift, but large amplitudes also occur to the north of the basin and at the north edge of the Tacoma sedimentary basin. These preliminary results indicate that the largest amplifications occur over the Seattle basin, but there is also a correlation between amplitudes and the thickness of the glacial deposits that extend beyond the basin edge. Resonance and impedance effects in the shallow sediments may cause a significant portion of the amplification, but the correlation of large amplitudes with the deep (7-9 km) basin sediments suggests that 3-dimensional effects also play a role.

## THE LAS VEGAS VALLEY SEISMIC RESPONSE PROJECT

*Arthur Rodgers, David McCallen, Shawn Larsen, Larry Hutchings, Hrvoje Tkalčić Lawrence Livermore National Laboratory, L-205, Livermore, CA 94551 Barbara Luke Department of Civil and Environmental Engineering, University of Nevada, Las Vegas, NV 89154 Catherine Snelson, Wanda Taylor Department of Geosciences, University of Nevada, Las Vegas, NV 89154 John Louie and John Anderson Nevada Seismological Laboratory, Mackay School of Mines, The University of Nevada, Reno, NV 89557*

We are engaged in a multidisciplinary, multi-institutional effort to characterize the seismic response of the Las Vegas Basin (LVB) to seismic ground motion. Las Vegas lies above a deep sedimentary basin (maximum depth 5-km) formed by extensional tectonics in the Basin and Range Province. The potential for large earthquakes in the region and possible future nuclear tests at the Nevada Test Site (NTS) expose Las Vegas to seismic risk. Seismologists, computer scientists and engineers at Lawrence Livermore National Laboratory (LLNL), the University of Nevada Reno (UNR) and the University of Nevada Las Vegas (UNLV) are evaluating the response of the basin to seismic ground motion and its effect on structures, with particular emphasis on large structures.

Recordings in Las Vegas of earthquakes and historical nuclear explosions at the Nevada Test Site (NTS) have provided valuable constraints on ground motion in the basin. Site response results show that ground motions in the basin can be amplified by factors of 20 or more relative to sites on Las Vegas Valley's periphery. Site response is strongly correlated with basin depth. Additional broadband data have been recorded to augment the coverage of earlier network data. Ground motions are being synthesized using an empirical convolution (transfer function) methodology. Geotechnical investigations of specific sites using ReMi and SASW are being performed to understand the relationship between ground motions and shallow seismic structure. In particular the presence of thick deposits of unconsolidated alluvial fill and strengthening effects of carbonate cementation. Seismic refraction studies are refining the basin depth model reported by Langenheim et al. (2001) based on gravity and seismic reflection. Preliminary results provide constraints on the fill velocities and are consistent with depth-to-basement model. All these results are being integrated into a community geophysical model of the region for use in finite-difference wave propagation calculations. Observed and simulated ground motions from scenario nuclear tests and earthquakes are being used to predict the response of structures in Las Vegas.

# REFINED FAULT ZONE STRUCTURE AND EARTHQUAKE LOCATIONS AT PARKFIELD, CA

*Steve Roecker, Cliff Thurber, Peter Malin, and Bill Ellsworth*

The Parkfield Area Seismic Observatory (PASO) was a dense telemetered array operated for nearly two years in a 15 km aperture centered on the SAFOD (San Andreas Fault Observatory at Depth) drill site. The main objective of this array was to refine the locations of earthquakes that will serve as potential targets for the drilling and in the process develop a high (for passive seismological techniques) resolution image of the fault zone structure. A particularly challenging aspect of the analysis of this dataset was the known existence of large contrasts in seismic wavespeed in the area that could lead to significant distortion of raypaths and hence exceed the limits of approximate ray tracing techniques. We therefore decided to follow up an initial determination of locations and structure developed using an approximate ray tracer with an application of a finite difference technique to a model containing a finer scale mesh parameterizing the subsurface. Our results show that the main features of the original analysis (earthquakes beneath the trace of the fault and the positions of major contrasts in wavespeed) are robust. At the same time, we determined that shear wave speeds in the upper 2 km of the fault zone were significantly lower than previously estimated, which decreases our estimate of the depth of the main part of the seismogenic zone by several tens of meters.

# USING BOREHOLE FLUID PRESSURE AND STRAIN DATA TO STUDY THE HYDROLOGIC AND MECHANICAL PROPERTIES OF THE NOJIMA FAULT, JAPAN

*Evelyn Roeloffs, U.S. Geological Survey Norio Matsumoto and Hisao Ito, Geological Survey of Japan/AIST*

Following the 1995 M=7.2 Hyogo-ken Nanbu earthquake, the Geological Survey of Japan (GSJ) began collecting borehole fluid pressure and strain data in and near the Nojima fault. We use these data to constrain the hydrologic and mechanical properties of the Nojima fault zone and search for changes in time associated with fault healing.

The GSJ Hirabayashi borehole penetrates the Nojima fault at a depth of 625 m, and is perforated in a shear zone believed to have ruptured in the 1995 earthquake. Interpretation of pumping tests carried out in 1996 and 2000 imply that hydraulic conductivity is high within the plane of the fault, but that fluid cannot flow from the foot walls and hanging walls into the fault zone. The high hydraulic conductivity presumably reflects properties of the fracture zone surrounding the fine-grained fault core. Transmissivity and storage coefficient from both pumping tests are consistent with high vertical hydraulic diffusivity, about  $0.1\text{-}0.5\text{ m}^2/\text{s}$ , although this value is uncertain because the storage coefficient is poorly constrained by the aquifer tests.

We found no evidence that the fault zone permeability decreased between 1996 and 2000, as might have been expected based on the hypothesis that earthquake-induced fractures heal following seismic rupture. In fact, differences between the successive pumping tests indicate that fault zone permeability could have increased slightly between 1996 and 2000. However, the differing results of the two tests could alternatively be explained by changes in a wellbore skin, with no need to invoke changes in fault zone hydrologic properties. Observations in an additional borehole during the pumping tests might have allowed these two possibilities to be distinguished. Phases and amplitudes of earth-tide-induced water-level variations did not change significantly at Hirabayashi from 1996 to 2000, which is also consistent with no detectable decrease of permeability during that time period. Because other studies based on shear wave anisotropy, aftershocks, and fault zone trapped waves did find evidence of fault healing, we believe that the absence of healing in the GSJ Hirabayashi borehole is due to its relatively shallow depth and low bottom-hole temperature (30 degrees C).

A question of interest in Coulomb failure function calculations is whether fault zone pore pressure increases in proportion to compressive stress normal to the fault, or to average stress in the fault zone (as expected based on isotropic poroelasticity). We compared amplitudes and phases of the M2 and O1 earth tide constituents in the water level data from the fault-penetrating Hirabayashi borehole with those of water levels observed in the Ikuha strainmeter borehole, which is 5 km S of Hirabayashi and outside of the fault zone. In the fault-penetrating borehole, the M2 and O1 amplitudes exceed those in the Ikuha borehole by factors of 2 and 1.3, respectively. While the M2 and O1 phases at Ikuha are close to those of areal strain inferred from the 3-component strainmeter in the same borehole, the M2 constituent in the fault-penetrating borehole lags areal strain at Ikuha by 50 degrees. These features imply the Hirabayashi fluid pressure does not respond to mean stress. We attempted to use the 3-component strain data to estimate amplitudes and phases of tidal strain as functions of azimuth, but because ocean-load corrected theoretical tides at Ikuha do not agree with the amplitudes and phases observed by the strainmeter, the areal and shear response coefficients of the strainmeter could not be determined. A further complication is that the wellbore storage effect on the water-level tides introduces uncertainty in the amplitudes and phases of the tidal signals in the fault itself. These factors make it difficult to draw a firm conclusion that the fluid pressure in the Hirabayashi borehole varies with fault-normal strain.

This study illustrates how borehole instrumentation of the type planned for the Earthscope Plate Boundary Observatory can be used to study fault zone properties and highlights some challenges of interpreting borehole strain data in locations subjected to significant ocean loads.

# THE EVOLUTION OF THE SEISMIC-ASEISMIC TRANSITION DURING THE EARTHQUAKE CYCLE: CONSTRAINTS FROM THE TIME-DEPENDENT DEPTH DISTRIBUTIONS OF AFTERSHOCKS

*Frederique Rolandone and Roland Burgmann*

Most studies of the seismic-aseismic transition have focussed on the effect of temperature and/or rock composition and have shown that the maximum depth of seismic activity is well correlated with the spatial variations of these two parameters. However, little has been done to examine how the maximum depth of seismogenic faulting varies locally, at the scale of a fault segment, with time during the earthquake cycle. Geologic observations indicate that the depth of the seismic-aseismic transition varies with strain rate and therefore is also expected to change with time throughout the earthquake cycle. This has strong implications for the mechanics of major fault zones near the base of the seismogenic zone where large earthquakes often nucleate. The maximum depth of seismogenic faulting is interpreted either as the transition from brittle faulting to plastic flow in the continental crust, or as the transition in the frictional sliding process from unstable to stable sliding. The seismic-aseismic transition therefore reflects a fault zone rheology transition or a more distributed transition from brittle to ductile deformation mechanisms. We use seismic data to constrain the depth variations with time of the seismic-aseismic transition throughout the earthquake cycle. We investigate the time-dependent depth distribution of aftershocks following large earthquakes on different segments of strike-slip faults. We apply the double difference method of Waldhauser and Ellsworth (2000) to improve event locations. Distributions of aftershocks in the Mojave desert show that we are able to image temporal changes in the depth of seismicity. The fault segments that ruptured during the 1992 Landers earthquake exhibit different temporal behaviors. For the Johnson Valley and Homestead segments, the depth distribution of aftershocks shows that in the immediate postseismic period the aftershocks are deeper than the background seismicity and the deepest aftershocks become shallower with time. The time period for the shallowing of the deep seismicity differs markedly between these two segments. The characteristics of strain accumulation and release at the bottom of a major fault are still not well defined and understood. We investigate in details the relationship between the temporal change in depth of seismicity and the spatial pattern of the coseismic slip distribution. The analysis of seismic data to resolve the time-dependent depth distribution of the seismic-aseismic transition provides additional constraints on fault zone rheology, which are independent of geodetic data. Together with geodetic measurements, these seismological observations form the basis for developing more sophisticated models for the mechanical evolution of strike-slip shear zones during the earthquake cycle. This study contributes to a better understanding of fault depth extent, and of the stress and strain rate evolution following an earthquake.

## LINGERING STRONG-MOTION INDUCED DAMAGE TO THE EARTH'S CRUST

*Justin L. Rubinstein Gregory C. Beroza Goetz H.R. Bokelmann David P. Schaff*

We use a catalog of 57 repeating earthquake sequences to study the damage to near-surface materials caused by strong ground motion. We believe that near surface damage (cracking) is the most likely cause for velocity reductions that we observe immediately following both the M6.9 Loma Prieta Earthquake and its largest aftershock, the M5.4 Chittenden Earthquake. The strong ground motion during both of these events was strong enough to open cracks near the Earth's surface, the presence of which reduces seismic velocities. Our observations indicate that the phase delays (velocity reductions) accumulate largely near the receiver. The velocity reductions heal with time, following Loma Prieta and Chittenden in a manner similar to the "slow dynamic" healing behavior observed in laboratory studies of nonlinear deformation [TenCate, et al., 2000]. Since the damage left by Loma Prieta had not completely healed by the time Chittenden occurred, it is probable that the local rocks were more susceptible to further damage, allowing the much weaker motions of the smaller Chittenden Earthquake to cause damage comparable in magnitude to that of the Loma Prieta Earthquake.

In this study we verify that nonlinear behavior in strong ground motion is the primary agent that causes the velocity reductions we observe. We compare the magnitude and behavior of the velocity perturbations to the the strong ground motion, the static stress changes, and streamflow changes resulting from Loma Prieta to verify the source of velocity reductions. We also compare the velocity perturbations to the local geology and the proximity of a site to the fault zone.

## OVERVIEW OF NATIONAL SEISMOLOGICAL NETWORK, NEPAL

*S. Sapkota and S. Rajaure National Seismological Centre, Nepal Department of Mines and Geology*

Nepal Himalaya occupies nearly one-third length of the total Himalayan arc. The seismicity in this region is attributed to the collision of Indian Plate with Eurasian Plate. The Nepal-Himalaya has experienced devastating historical earthquakes such as M<sub>w</sub>~8-8.5 of 1255 and 1934 A.D.

Department of Mines and Geology started monitoring of earthquakes installing one short period vertical component seismometer in Phulchoki hill in 1978 in technical collaboration with Laboratoire De Geophysique (LDG) France. In 1985 four more stations were added in Central Nepal. In 1994 the existing seismic network was upgraded and 12 seismic stations were installed in Centre+East Nepal and five stations were installed in Western Nepal under the National Seismological Centre (NSC), in technical collaboration with Department Analyse Surveillance Environnement (DASE), France. In 1998 four more stations were added in the western Nepal in Karnali area and the total number of seismic stations operating in the whole territory of Nepal is 21. The stations are distributed in Lesser Himalaya and Sub Himalaya of Nepal.

A three layered velocity model with P wave velocities of 5.6, 6.5 and 8.1 km/sec and corresponding S wave velocities of 3.2, 3.7 and 4.6 km/sec with interfaces at 23 km and 55 km depth (Pandey, 1985) is used in routine processing. The network can detect local magnitude as low as 2 for the events occurring within the network. The technical and seismic alert system allows quick response for any technical defects and threshold magnitude

The waveform signals are processed in Kathmandu Centre (Centre+East) and Birendranagar (West) Centre for localization and determination of other parameters. The bulletin is produced in GSE 2.0 format. The seismic bulletin is sent to DASE-France, USGS-USA and ISC-England

The geological, geophysical and geodetic data show stress and strain accumulation in the mid- crustal ramp in the interseismic period (Pandey et al, 1995). The seismic activity is characterised by a narrow zone of very intense microseismic activity that can be traced all along the Himalaya of Nepal which follow approximately the topographic front of the Higher Himalaya. Most of the events lie between MCT and MBT in plan ranging in depth from 10 to 20 km. This network is providing basic data for research on Himalayan Seismotectonics and for seismic hazard assessment.

## EXPECTED PERFORMANCE OF THE PROPOSED PBO NETWORK

*David A. Schmidt, Jessica R. Murray, and Paul Segall*

With the recent funding approval of Earthscope, the scientific community is poised to begin the installation phase of the proposed Plate Boundary Observatory (PBO). GPS and strainmeters will soon be distributed across the western United States as a backbone array with an additional clustering of instruments along the plate boundary and at other target regions. Prior to the placement of instruments, it is important to evaluate the network performance as a function of station geometry, instrument density, and instrument ensemble (strainmeter versus CGPS) given the scientific objectives and budgetary constraints. We are currently evaluating the proposed network in order to offer recommendations on how best to optimize the network. As a first step of this endeavor, we will present results from numerical simulations that assess the ability of the proposed PBO network to resolve fault and volcanic source processes.

The proposed network geometry is evaluated through a series of numerical simulations based on the scientific objectives of the PBO initiative. Three characteristic events are simulated: an aseismic transient on the central San Andreas fault, a silent earthquake on the Cascadia subduction interface, and a propagating dike at a regional volcanic center. Simulations are performed for different source dimensions, amplitudes, and durations. For example, the Parkfield simulations of an aseismic transient use a circular source model whose slip profile is Gaussian in shape. Slip on the fault accumulates with time in the form of an error function  $\text{erf}(t)$ . Source parameters are varied so as to simulate events with magnitudes from Mw 4 to 6.5 and durations from 0.1 to 3 years. Rupture dimensions and slip amplitudes are chosen such that all simulations have an average stress drop of less than 10 MPa. A similar methodology is used for the Cascadia simulations; however slip propagates northward from central Oregon along the base of the subduction interface. For the simulations of a propagating dike, the dike opens at an initial depth of 5 km and propagates towards the surface. Maximum opening, length, and duration are varied as in the fault simulations.

We will present results that describe the PBO network performance as a function of the magnitude and duration of the event for each of the three scenarios and provide insight on the expected level of resolution. The Extended Network Inversion Filter (ENIF) is used to infer the original source parameters from synthetic time series data given the proposed station distribution. For each scenario, synthetic GPS data are created that include a white noise error source with a standard deviation of 0.002 m and a random walk component of 0.0013 m/sqrt(yr). The ENIF is an implementation of a Kalman filter that is well suited to extract a time-dependent signal from noisy data and is efficient at analyzing large time-series data sets. Resolution of the source process is evaluated by comparing the synthetic input model with the inferred source model determined by the ENIF. Our results provide a baseline expectation of the network performance.

## TEMPORAL AND SPATIAL VARIATIONS IN THE LIMITS OF THE SEISMOGENIC ZONE, COSTA RICA

*S.Y. Schwartz and H.R. DeShon, Earth Sciences and IGPP, Univ. of California, Santa Cruz  
A.V. Newman, Earth and Environmental Sciences, Los Alamos National Laboratory, Los Alamos, NM S.L. Bilek, Dept. of Geological Sciences, University of Michigan*

The part of the plate boundary at subduction zones capable of generating seismic moment release (exhibiting frictional stick-slip behavior) is fairly restricted in depth and variable along strike. Factors that control the localization of seismic moment release are just beginning to be understood through integrated studies of seismicity, seafloor bathymetry, geodesy, fluxes of heat and fluid and frictional behavior of material in the laboratory. Future drilling to seismogenic depths is being proposed by IODP with the new riser vessel and promises to greatly improve our understanding of convergent margin seismogenic zones. In preparation for drilling into the Central America convergent margin, we have tried to characterize seismogenic zone behavior near the proposed drill site and north, beneath the Nicoya Peninsula, Costa Rica.

Beneath the Nicoya Peninsula we find an abrupt transition in the updip limit of microseismicity from 20 to 10 km where the origin of subducting oceanic crust changes from East Pacific Rise (EPR) to Cocos-Nazca Spreading Center (CNS). Thermal measurements on the incoming plate suggest that the temperature of the crust (colder EPR and warmer CNS) may control the seismogenic up-dip limit along the Nicoya portion of the Middle America Trench. The reason for the thermal variations is presently unknown, however, it is clear that conditions required for the transition from stable sliding to stick-slip behavior can vary over a very short distance. Variability in the updip limit of the seismogenic zone near the Osa Peninsula, Costa Rica is also supported by comparisons of the mainshock and aftershock characteristics of two recent underthrusting earthquakes on 8/20/99 (Mw 6.9) and 6/16/02 (Mw 6.4). The majority of the 1999 event aftershocks occur between 10 km and 30-35 km depth along a quasi-planar surface dipping at  $\sim 20^\circ$ . The aftershock area of the 1999 event is believed to represent rupture of bathymetric highs within the subducting Quepos Plateau that acted as asperities. We suggest that limiting conditions controlling the transition between stable sliding and stick-slip behavior may change over the seismic cycle and that the subduction of highly disrupted seafloor in the vicinity of the 1999 mainshock has established a set of conditions which presently limit the seismogenic zone to be between 10-35 km below sealevel. A shallowing of the seismogenic zone appears to occur south of the 1999 mainshock as seen in the characteristics of the 6/16/02 earthquake that ruptured this portion of the plate interface

Our evolving image of the seismogenic zone is one in which updip and downdip limits vary as a function of time within an earthquake cycle and reflect temporal changes in critical parameters influencing the transition from stick-slip to stable sliding behavior.

## POST-EARTHQUAKE DEFORMATION FROM INSAR AND STRAINMETERS CORRELATED TO PORE-PRESSURE TRANSIENTS

*Paul Segall (Stanford University), Sigurjón Jónsson (Harvard University), Rikke Pedersen (Nordic Volcanological Institute), Kristjan Agustsson (Iceland Meteorological Office,), Grímur Björnsson (National Energy Authority)*

Despite considerable effort, it has proven difficult to distinguish between competing models of postseismic deformation based on direct field observations. We present unique measurements consisting of satellite radar interferograms, borehole strainmeters, and water level changes in geothermal wells following two magnitude 6.4 earthquakes in the South Iceland Seismic Zone (6/17/2000 and 6/21/2000).

The deformation recorded in the interferograms cannot be easily explained by either afterslip or visco-elastic relaxation but are consistent with poro-elastic rebound in the first one to two months following the earthquakes. This interpretation is confirmed by direct measurements which show rapid (1-2 month) recovery of the earthquake induced water level changes. In contrast, the duration of the aftershock sequence is roughly 3.5 years, suggesting that pore-fluid flow does not control aftershock duration. However, because the displacements detected by InSAR are dominated by pore-pressure changes in the shallow crust, we cannot rule out a longer pore-pressure transient at the depth of the aftershocks. The aftershock duration, however, is consistent with models of seismicity rate variations based on rate and state dependent friction.

A borehole dilatometer located 3 km from the first rupture recorded a 10 microstrain coseismic compression followed by a roughly one month long strain relaxation (dilation). For a fault suddenly introduced into a poroelastic medium the postseismic volume strain is predicted to increase as the induced pore pressure gradients relax. That is the post-seismic strain is predicted to be compression. Because there is no fluid exchange with the dilatometer, the strain measured by the strainmeter is not in the same as the strain in the surrounding rock, when pore-fluid flow occurs. The instrumental strain is related to the strain within the rock far from the borehole and the local change in fluid pressure. For two-dimensional dislocations the strain in the rock becomes more compressive, however, the predicted strain-meter response is time-invariant. We are currently exploring whether shallow drainage can explain the observed strainmeter response.

## **ARE DEEP EARTHQUAKES BENEATH THE HIGH HIMALAYA IN THE CRUST OR IN THE MANTLE?**

*Anne F. Sheehan, University of Colorado at Boulder, Francis T. Wu, SUNY Binghamton, Gaspar Monsalve, Frederick Blume, Vera Schulte-Pelkum, Tom de la Torre, Roger Bilham, University of Colorado at Boulder, M. R. Pandey, Sudhir Rajaure, Soma Nath Sapkota, Department of Mines and Geology, Kathmandu, Nepal, H.B. Liu, Institute of Geology and Geophysics, Chinese Academy of Sciences*

In 2001-2002, the University of Colorado at Boulder and SUNY Binghamton, in collaboration with the Department of Mines and Geology of Nepal and the Institute of Geology and Geophysics of the Chinese Academy of Sciences, operated 29 broadband seismic stations throughout eastern Nepal and southern Tibet. The stations were deployed roughly equally (subject to logistic constraints) throughout a 300 km by 300 km region. The objectives of this Himalayan Nepal Tibet PASSCAL Seismic Experiment (HIMNT) are to study the mountain building processes of the Himalaya through both earthquake source and crust and mantle structure imaging. We seek to determine the geometry of fault ramps, where seismic events with characteristic focal mechanism concentrate, and whether the decollement can be detected through seismicity or material differences. Using teleseismic data we expect also to map features in the upper mantle. Recent work by Jackson and McKenzie has suggested that the strength of the lithosphere resides within the crust, rather than in the mantle, and our studies of the deep continental earthquakes in the region provide a test of this hypothesis. Hundreds of local earthquakes recorded by the HIMNT experiment have been picked and located. The local earthquakes are studied to determine possible major dislocation surfaces and the internal structure and rheology of the orogen. Many earthquakes are found along the proposed mid-crustal ramp beneath the region of maximum relief along the Himalayan Front. We find clusters of deep earthquakes near the crust-mantle boundary both beneath southern Nepal and southern Tibet. The southern Tibet events are particularly deep for continental earthquakes, with many on the order of 85 km depth. We have performed teleseismic receiver function analysis of the HIMNT data and have estimates of crustal thickness throughout our study area. The combination of local crustal thickness estimates from teleseismic receiver functions with hypocentral determination of earthquakes within the same region allows detailed evaluation of depth of earthquakes relative to the crust-mantle boundary. Velocity analysis is performed to examine the sensitivity of earthquake hypocenters and receiver function crustal thickness estimates to the velocity model used. Full waveform moment tensor inversion of local earthquakes greater than magnitude 4.0 is performed to examine the earthquake size and style of faulting, and provides an additional constraint on hypocentral depth. A double-difference algorithm is utilized to examine the relative locations of events. Surface wave analysis is ongoing to examine lateral variations in mantle velocity structure and to better understand the sense and style of subduction and lithospheric deformation beneath this segment of the Himalayan arc.

## **DOWNGOING SLAB SEISMICITY IN JAPAN EXAMINED THROUGH HIGH PRECISION EARTHQUAKE HYPOCENTERS**

*David R. Shelly and Gregory C. Beroza (Dept. of Geophysics, Stanford University, CA; dsheilly@pangea.stanford.edu), Satoshi Ide (Dept. of Earth and Planetary Science, University of Tokyo, Japan)*

Seismicity has great potential to tell us about the mechanisms and processes active in subduction zones. Current catalog locations of this seismicity, however, often err by many kilometers, obscuring important details. We present earthquake hypocenter relocation results from subduction regions in Japan, obtained by applying the double-difference relocation algorithm (Waldhauser and Ellsworth, 2000) to catalog phase data from the Japan Meteorological Agency (JMA) for the period of 1994-2000. We examine several diverse slices of subduction zone seismicity in Japan, including a region in Kyushu and one in the central Nankai trough region. We also analyze sections showing the double seismic zone in central Honshu, the Tohoku district of northern Honshu, and Hokkaido.

Results show an increase in the organization of seismicity compared with catalog locations. In particular, we find that the seismogenic planes narrow by up to 50% in cross-section after relocation. In places, however, they retain substantial apparent width. Relocated hypocenters from central Honshu (35 degrees latitude) northern Honshu (39 degrees latitude) and Hokkaido show significantly narrower and more distinct planes of seismicity for both the upper and lower planes of the double seismic zone compared with catalog locations. In each of these regions, we find seismicity in the core of the downgoing plate, between the two prominent planes of seismicity. That is, there is more to the intermediate-depth seismicity than the double seismic zones. Specifically, relocations from these regions show a general increase in seismicity where the dip of the slab changes, including increased seismicity between the planes of the double seismic zones. This suggests plate bending may be important in generating these earthquakes.

## **A REAL-TIME SEISMIC NETWORK FOR K-12 SCIENCE EDUCATION IN NEVADA**

*Ken Smith and Diane DePolo Nevada Seismological Laboratory, University of Nevada Reno, Reno, NV 89557 ken@seismo.unr.edu; diane@seismo.unr.edu Catherine M. Snelson, Shelley A. Zaragoza, and Jenelle Hopkins Department of Geoscience, University of Nevada Las Vegas, Las Vegas, NV 89154-4010 csnelson@unlv.edu; szagos@physics.unlv.edu; jhopkins@interact.ccsd.net*

We are establishing an innovative K-12 based seismic network in Nevada schools providing a platform for involving K-12 science educators and students, academic education professionals, and the earth science research community in an "authentic" research program to promote science education in the classroom. Twenty-two stations have been funded by the Department of Energy (3 for Las Vegas) and by the Nevada Public Agency Insurance Pool (19 in rural Nevada counties; Wayne Carlson Director NPAIP) under the auspices of the Nevada Earthquake Safety Council. Bishop Manogue Catholic High School in Reno has also purchased their own seismograph system and other residential stations are operating in the northern Nevada area on commercial wide-band Internet connections. Currently eight stations are generating live data feeds to the Nevada Seismological Laboratory and to IRIS Data Management Center in Seattle ([http://www.iris.washington.edu/bud\\_stuff/dmc/bud\\_monitor.html](http://www.iris.washington.edu/bud_stuff/dmc/bud_monitor.html) - IRIS network code EQ). Several other stations have been installed and are in the process of coming on on-line. These data are used to more effectively locate regional earthquakes and add to the growing ground motion database for the region.

The network of low-cost seismographs equipped with robust PC based Internet communications and interactive waveform display software links Nevada science classrooms in real-time to the Nevada regional seismic network. The platform will provide a basis for innovative approaches to training educators in earth science and modern Internet and data acquisition technologies to inspire young people in science. School PC's are already in place on the Internet and can, in most cases, be used for basic data acquisition system. As a result, there is a significant cost savings in equipment purchases and installation logistics. In this model of a low cost K-12/research program, students and educators participate in operating the systems at the school level and interact with researchers to maintain a quality real-time network. As part of the program, curriculum materials that meet Nevada State Standards have been developed under the Department of Energy funded component of the program in Las Vegas by Jenelle Hopkins (Las Vegas Science Teacher through UNLV Master's Degree Program). Since K-12 becomes an integral part of the research program, the researchers have a natural vested interest in K-12 earth science education. The more effective researchers are in informing students and educators of the scientific objectives being addressed the better the research component, and we hope this dynamic will result in a meaningful relationship between K-12 and the research community.

## COORDINATES FROM THE NATIONAL CORS NETWORK

*R. Snay, W. Dillinger, J. Marshall, M. Chin, T. Soler, M. Cline, R. Foote, M. Eckl*

The U.S. National Geodetic Survey (NGS) computes positional coordinates daily for more than 350 permanent ground-based GPS stations that comprise the National Continuously Operating Reference Stations (CORS) network. Each daily solution involves the use of a recent 24-hour data set, freely available by the Internet. These quality control activities are designed to detect significant deviations from adopted positional coordinates and/or velocities, whereupon the adopted coordinates and velocities may be updated. Such coordinate changes were applied, for example, to several CORS located in Alaska in association with the magnitude 7.9 Denali earthquake of 3 November 2002. These daily solutions are combined and submitted since early 2002 as weekly densification solutions for the North American Reference Frame (NAREF) Working Group.

In addition, NGS annually estimates positional coordinates and velocities for stations in the National CORS network using several years of pertinent GPS data. NGS will update previously adopted positional coordinates and velocities if the new estimates differ from the adopted values by pre-specified tolerances. The most recent "multi-year" product uses every third day of data available from 1994 through 2001 for 461 National CORS and other globally distributed sites. From this product, we have identified roughly 45 sites having at least three years of data whose estimated velocities relative to the North American tectonic plate are less than 1mm/yr horizontally and 2mm/yr vertically.

## **CHARACTERIZING THE LAS VEGAS BASIN FOR STRONG GROUND MOTIONS: PAST, PRESENT, AND FUTURE ACTIVE SOURCE EXPERIMENTS**

*Catherine M. Snelson, Shelley A. Zaragoza, and Darlene J. McEwan, Department of Geoscience, University of Nevada Las Vegas, 4505 Maryland Pkwy, MS 4010, Las Vegas, NV 89154-4010, 702-895-2916, csnelson@unlv.edu*

The Las Vegas Valley is located in the southern Basin and Range, which has undergone a significant amount of extension that continues today. This extension has resulted in a series of normal faults as well as strike-slip faults that cut across the region. In the Las Vegas Valley, these faults have contributed greatly to the original geometry of the basin. The cities of Las Vegas, North Las Vegas, and Henderson sit atop this fault-bounded basin, which has been shown to have varying amplification factors (e.g., Su et al., 1998). Recent paleoseismic studies have illuminated that several normal faults in the Las Vegas region have Quaternary offsets and have the potential to produce an earthquake of M6.5 to 7.0 (Slemmons et al., 2001). A gravity inversion, which combined gravity, seismic reflection, and aeromagnetic data indicate that there are a series of sub-basins exist beneath the unconsolidated basin fill, with the deepest sub-basin occurring 5 km west of the fault block bounding the eastern edge of the basin and the basin depth ranging from 2 km in the west-northwest to 5 km in the east-northeast (Langenheim et al., 2001). An estimation of a M 6.9 earthquake in or near the basin may produce about \$11 billion in damage and a large number of deaths/injuries (Perry and O'Donnell, 2001). As a result, there is an increased effort to characterize the valley for strong ground motions. A multidisciplinary group of seismologists and engineers from the University of Nevada Las Vegas (UNLV), the University of Nevada Reno, and Lawrence Livermore National Laboratory have come together to study the Valley and its potential response to strong ground motion for both test readiness and earthquakes.

As part of this project, two refraction surveys were acquired in 2002 using quarry blasts around the valley and a chemical blast from NTS as sources. UNLV with assistance from the University of Texas at El Paso (UTEP), students from UNLV, UTEP, and Stanford, volunteers from the community and several students from Centennial High school deployed 400+ portable seismic recorders ("Texans") throughout the valley. Shot point locations were located at three quarries in the valley, one to the north, one to the east and one to the southwest and a chemical blast at the Nevada Test Site. The profiles cross the Las Vegas Valley Shear zone, several of the active Quaternary faults, and a prominent NW/SE trending step in the basin floor across which the basement drops from 2 to 5 km in depth. The primary questions we have set out to answer are: 1). What is the geometry and velocity structure of the Las Vegas basin? In order to characterize the basin sufficiently it is important to know the velocity structure within the entire basin, and this is best estimated by collecting seismic refraction data. This new information can help identify areas where strong ground shaking is going to be greatest. 2). Can we identify existing faults and address their significance for seismic risk? Integrating these new data with the existing data can identify the geometry of existing faults. 3). Can we identify of any sub-basins within the larger basin, thereby testing the model produced from the gravity inversion? In addition, the sub-basins could be areas where there is increase amplification and focusing of energy.

Preliminary analyses of the newly acquired seismic refraction data indicate that the basin has an average P-wave velocity of about 4.5 km/s and the basin depth is consistent with the estimated basin depths ranging from 2 to 5 km deep. Both tomographic inversion and forward modeling techniques are being used to analyze these data. Unfortunately these data were contaminated with a large amount of cultural noise and can only provide first order results. As a result, we will acquire two additional seismic refraction profiles across the Valley using controlled-sources in August 2003. These new data will be added to the tomography to produce a 3-D velocity model of the basin. In addition, "Legacy" refraction data that has been digitized will add a deeper crustal component to the model and proprietary industry reflection profiles will be interpreted and tied with the velocity model. All of these data will be integrated into a community model, which is being produced by the Las Vegas Basin Seismic Response working group to further assess the site response of the basin.

## MAPPING THE MANTLE LITHOSPHERE FOR DIAMOND POTENTIAL

*Snyder DB Geological Survey of Canada, Ottawa Bostock MG Dept. of Earth & Ocean Sciences, University of British Columbia, Canada Lockhart GD BHP-Billiton, BHP Diamonds, Inc., Canada*

Diamond deposits are typically identified in four stages: (1) regional targeting in which a region's potential is assessed, often by grid till sampling for indicator minerals or global seismology; (2) kimberlite detection by till sampling and high resolution aeromagnetic surveys; (3) deposit delineation in which drill hole core sampling determines a specific deposit's volume and lithology; and (4) evaluation of a deposit's worth and its feasibility to be mined. The diamond exploration industry needs discriminating tools to reduce risks at all of these stages. Seismic techniques can provide 3-D maps of key physical properties in the mantle to 700 km depth to help accomplish stage one.

Four years of recording global earthquakes using a broadband seismometers located near the Ekati diamond mine can be analyzed by several independent techniques to reveal information about layered structures within the mantle of the central Slave craton. Variations with earthquake azimuth in the arrival of SKS phases can be most easily modeled by assuming two distinct layers of anisotropy (seismic fabric or grain) within the lithosphere. The lower layer probably lies in the mantle and the anisotropy aligns with both North American plate motion and the strike of mantle structures identified by previous conductivity and geochemical analyses, at ~N50°E. The upper layer is more varied and hypothesized to result from regional fold structures in the upper crust; that are distinct from the mantle trends.

Deconvolution of P- and S-waves from several earthquakes located at the same general azimuth reveals discontinuities in seismic wave velocities or density below each seismic station. Traditionally, the sharp increase in both velocity and density at the Moho (roughly base of the crust) is the most prominent of these discontinuities. Its depth varies between 36 and 42 km near Ekati. Unusually, equally prominent discontinuities at 85-100 and 140-150 km depth indicate a layer of low velocity between these depths. These depths coincide with a very prominent regional conductor identified by recent magneto-telluric studies (A. Menzel-Jones) and an ultra-depleted harzburgite layer identified from studies of garnets extracted from xenoliths in kimberlite core (W. Griffin). The 95- and 145-km discontinuities are not typical of cratons globally; similar features are observed beneath the Yellowknife area and are there interpreted as a relic Proterozoic subduction or underthrust zone. One of these subduction zones may extend NW into the Ekati area or Ekati may be underlain by an older (2.6Ga) convergent zone. Another discontinuity is recognized globally and throughout the Slave craton at about 410 km depth. Beneath Ekati this feature is especially shallow (400 km) and thus may provide clues about the thermal state of the mantle at this depth, the hypothesized source region for Ekati kimberlites.

The seismic results aid us in constructing a NW-SE cross section of the Slave craton from the surface to 700 km depths and relate it to surface geology and other geophysical and petrological constraints on mantle composition. Continuing recording of earthquakes at 18 stations will enable other techniques and provide 3-D structure as well.

## **NORTH EURASIA GPS DEFORMATION ARRAY (NEDA)**

*G.M. Steblov and M.G. Kogan*

Since 1997, NEDA Permanent GPS Network is operated by Russian GPS Data Acquisition and Analysis Center (RDAAC Geophys. Service Russ. Acad. Sci.). This network provides precise observations over the vast expanse of North Eurasia. All stations of NEDA have been classified as global IGS stations. The daily data download is fully automated with latency of < 1 hour. There is a good progress with converting NEDA to a high-rate (1-Hz) sampling rate mode in order to support observations of rapid ionospheric processes and of LEO occultations. As a result of five years of operation of NEDA, realization of the Eurasian reference frame is significantly stronger, because several stations of this network sample the largest cratonic regions such as Siberian and East European cratons. NEDA also allowed us to map an enigmatic Eurasia – North America plate boundary in northeast Asia and to decipher the deformation pattern across this boundary at the Cherskiy Range in east Siberia, in Kamchatka, and in the Sakhalin Island. This study was performed as a joint project of RDAAC with Lamont-Doherty Earth Observatory, MIT, and University of California Berkeley. Majority (all in the near future) of NEDA stations are equipped with meteorological sensors; such systems allow us to measure precisely the water vapor in the troposphere. The estimates that we performed so far for 2001-2002, demonstrate a remarkable consistency among stations over Siberia, with distinct seasonal patterns and latitudinal dependence. International GPS Service (IGS), Incorporated Research Institutions for Seismology (IRIS), and Jet Propulsion Laboratory (JPL), played a key role in providing GPS systems and various support for the NEDA network.

## **CHARACTERISTIC EARTHQUAKES AS POSSIBLE ARTIFACTS: APPLICATION TO NEW MADRID**

*Seth Stein, Department of Geological Sciences, Northwestern University, Evanston IL 60208; (847)-491-5265; seth@earth.northwestern.edu Andrew Newman, EES-9, MS D462, Los Alamos National Laboratory Los Alamos, NM 87545; (505)-665-3570 anewman@lanl.gov*

In many areas, the largest earthquakes - termed characteristic - appear more common than expected from the log-linear frequency-magnitude relation observed for smaller earthquakes. Whether this effect is real or apparent is an interesting question. Apparent differences might arise from several possible situations.

One possibility might arise where the length of the earthquake history is comparable to the mean recurrence time of large earthquakes predicted by a Gutenberg-Richter distribution. Apparent characteristic earthquakes can occur if earthquake recurrence intervals are distributed about the mean for that magnitude range, because sampling bias makes those with shorter intervals more likely to be observed than those with longer ones (fractions of earthquakes cannot be observed). A second possibility is suggested by the fact that characteristic earthquakes are often inferred because paleoseismic data are discordant with instrumental or historical data. Hence apparent characteristic earthquakes would occur if paleoseismic data overestimate earthquake magnitudes or underestimate earthquake recurrence.

Both effects may be operating in the New Madrid Zone. Numerical simulations suggest that because the 2000 year paleoseismic record is comparable to the recurrence time expected for  $M > 7$  earthquakes, there is a significant probability of observing apparent characteristic earthquakes. Moreover, paleoliquification data appear to overestimate paleoearthquake magnitudes, in part because these data were calibrated by assuming the 1811-12 earthquakes were magnitude 8.3 events, whereas more recent analysis finds that these earthquakes were low  $M$  7.

## **DEFINITION OF THE SILVER CREEK FAULT AND EVERGREEN BASIN FROM ACTIVE-SOURCE SEISMIC REFLECTION IMAGING, SAN JOSE, CALIFORNIA**

*W.J. Stephenson, R.A. Williams, J.K. Odum, C.M. Wentworth, R.T. Hanson, and R.C. Jachens*

Preliminary interpretation of 20 km of P-wave seismic reflection data provides new information on the configuration of the basement surface, the nature of the sedimentary basin fill and the location of the Silver Creek Fault (SCF) adjacent to and within the elongate, northwest-trending Evergreen Basin (EB) located in San Jose, California. These data, which were acquired as part of a larger project to understand seismic hazards in the Santa Clara Valley, were focused on determining fault locations, basin shape, and seismic velocity structure that could affect earthquake ground motions. The 40-km long by 8-km wide EB has been defined previously by gravity modeling and seismic tomography. We acquired two seismic profiles using a 240-channel recording system with 5-m receiver and 10-m source intervals. Profile 1, which follows the Guadalupe River northwestward just west of the western edge of the EB, reveals a moderately undulating basement surface overlain by about 400 m of well-layered Pleistocene and possibly Pliocene sedimentary deposits. Basement paleotopography is indicated by undulations of up to 50 m of relief over about 200 m lateral distance, with overlying beds truncated against the basement highs.

Profile 2 trends northeastward and crosses the EB. A 2-km-long, and as deep as 450-m basement reflection on the western end of this profile shows 100 m of local relief and dips gently eastward before appearing to terminate abruptly in the vicinity of the previously inferred trace of the SCF. A steep gravity gradient and a groundwater boundary inferred from InSAR are the only previous constraints on the location of the SCF here as the fault has no instrumentally-recorded seismicity. We interpret this basement reflection termination to be the location of the SCF. To the east, the sedimentary fill appears to thicken abruptly as indicated by the generally flat-lying layered reflections extending to at least 1.5 km depth. The SCF is poorly constrained but appears to dip steeply to the east, as indicated by the series of westward terminations of reflections just east of the fault. Bedding in a 500-m wide zone above the easternmost basement reflection is tilted and deformed, relative to reflections outside the SCF zone, but the presence of faulting is unclear. The trace of the InSAR boundary directly overlies the eastern tip of the basement reflection termination, and it also overlies the zone of more concentrated deformation, but it is not clearly associated with faulted near-surface sediments at this preliminary stage of analysis.

## VALIDATION OF A SCHEMATIC MODEL FOR STABLE CONTINENTAL REGION EARTHQUAKES

*Pradeep Talwani, Robert Trenkamp, Abhijit Gangopadhyay, and Inmaculada Dura-Gomez*

According to a schematic model proposed to explain Stable Continental Region (SCR) earthquakes (Talwani and Gangopadhyay, 2000) and preliminary results of 2-D modeling (Gangopadhyay et al., 2002), earthquakes occur in failed rifts at sites of local stress concentrators in response to plate tectonic forces. These local stress concentrators can be in the form of intersecting faults, fault bends, buried plutons and/or stress pillows. We test this model with multidisciplinary data from the Middleton Place Summerville Seismic Zone (MPSSZ) near Charleston, S.C. The earthquakes occur in a 20 x 30 sq.km zone and are concentrated near the intersection of the NNE trending Woodstock fault and the NW trending Ashley River fault. They occur on the northeast periphery of a buried pluton. A validation of the model was provided by the results of GPS surveys. Results of reoccupation of GPS sites in and outside MPSSZ in 1993, 1997, and 2000 suggest that the strain is accumulating in the region of active seismicity (MPSSZ, ~600 sq. km) at a rate of  $\sim 10^{-7}$ /year. Outside the MPSSZ in an area of ~5000 sq. km it is accumulating at  $\sim 10^{-8}$ /year and outside that it reverts back to  $10^{-9}$ /year consistent with other observations for the North American plate. These observations support the idea of localized stress build up and seismicity. The strain rates in MPSSZ are consistent with recurrence rates for M 7 inferred from paleoseismology. The strain rates outside MPSSZ,  $10^{-8}$ /year, are consistent with recurrence rates derived from b-values, suggesting that in SCR settings recurrence rates obtained from paleoseismology should be used in hazard calculations.

# MODELING SOURCE PARAMETERS AND LOCATING REGIONAL EARTHQUAKES WITH BROADBAND WAVEFORM DATA

*Ying Tan, Lupei Zhu, Don Helmberger*

Retrieving source parameters including mechanism, depth, location and origin time of small earthquakes ( $M_w \leq 4.5$ ) has to rely on local and regional seismic data. Although real-time systems built on dense seismic networks are being developed to monitor local seismic activity for rapid notification and damage assessment in recent years (e.g. Trinet, Southern California), a period of transition is expected in many areas in the world where a combination of relatively sparse short-period stations with only a few broadband instruments will be the only means of obtaining accurate locations of small seismic events. Most of these areas are extremely important in view of tectonics and geodynamics. We propose a new method of retrieving complete source parameters for small events using regional broadband waveforms from a few stations (1-2) plus available short period polarity data. We conduct a comprehensive test of the method on the Tibet Plateau. We present our work in two parts:

(1). Calibration of the Tibet Plateau: Fitting first P, S arrivals and surface waves on broadband recordings of 60 earthquakes recorded by a one-year PASSCAL deployment (1991.7-1992.7) is used to develop a two-layered crustal model and re-tune ISC locations and origin times of the events in a least-square sense. These three component records are then used to determine the source mechanism and depth of the events following the  $\chi^2$  cut and paste method discussed by Zhu et al (1999). A big advantage of this method is that it allows Pnl and surface waves to shift differently, compensating imperfections of Green's functions and providing path-dependent timing corrections for major arrivals. (2). Testing two station solutions: Recordings from two permanent broadband stations, Lhasa and Tunl, are used to determine the mechanism and depth of 18 recorded events out of 60. Quality of the estimates can be assessed from quality of the data, the compatibility of Pnl and surface waves, and also the variation of estimated focal mechanisms as a function of depth. Estimated mechanisms and depths of 12 events, which we give an  $A_j$  mark, compare very well with those obtained using the whole array in (1). Taking the estimated mechanism, depth, 1-D crustal model plus path-dependent timing corrections, we conduct a grid search, based on waveform matching at the two stations, for a new location for each event in a relatively large area. The size of the area depends on expected level of uncertainty in ISC location of the event. This new type of relocation process moves 19 events from their original ISC locations towards locations determined by the well-distributed PASSCAL array in (1), with improvements from 27km to 8km.

# **FINE-SCALE STRUCTURE OF THE CORE-MANTLE BOUNDARY FROM FARM AND PASSCAL DATA**

*Michael S. Thorne and Edward J. Garnero Department of Geological Sciences, Arizona State University, Tempe AZ 85287*

Anomalous boundary layer structure at the Core Mantle Boundary (CMB) is investigated using a global set of broadband SKS and SPdKS waves from the IRIS/GSN FARM archives and past PASSCAL experiments. SPdKS is an SKS wave that intersects the CMB at the critical angle for ScP, thus initiating short segments of diffracted P-waves (Pd) along the CMB at the core entry and exit locations. The wave shape and timing of anomalous SPdKS data are analyzed relative to SKS, with some SPdKS data showing significant delays and broadening compared to SKS. Anomalous SPdKS data are modeled with 3 classes of models: (1) mantle-side ultra-low velocity zones (ULVZ), (2) core-side rigidity zones (CRZ), and (3) core mantle transition zones (CMTZ). For ULVZ structures, P and S velocity reductions with dVs: dVp ratios of 1:1 and 3:1 are explored, where 3:1 is appropriate for a partial melt scenario. Our detailed analyses of SPdKS anomalies suggest strong variations at the CMB at shorter length scales (< 10 – 100 km) than resolved in current tomographic inversions. We produce maps of inferred boundary layer structure, and show regional maps displaying the fine-scale heterogeneity of these inferred structures.

## **NEWLY DETECTED DEFORMATION IN YELLOWSTONE'S UPPER GEYSER BASIN**

*Anahita A. Tikku - Ocean Research Institute, University of Tokyo Japan David C. McAdoo - NOAA Laboratory for Satellite Altimetry Mark Schenewerk - Give 'em an Inch*

We present evidence for oscillatory vertical motions of up to 10 cm, and corroborative fluctuations in gravity of up to 15 microGals occurring with varying periodicities of several hours to tens of hours in the southern end of the Upper Geyser Basin within the Yellowstone caldera. Deformation on this timescale has been previously undetected. The vertical ground motion is roughly three orders of magnitude larger than the historic and ongoing overall inflation and deflation rates within the caldera. Furthermore the crustal deformation appears to be similar in amplitude over a large areal extent, up to 800 m, with negligible horizontal motion. Simple models of the observed deformation indicate pressure fluctuations at depths of > 2 km in the hydrothermal-magmatic system with concomitant volume changes of  $\sim 0.00085 \text{ km}^3$ . These fluctuations are most likely due to variable injection of gas or brine from a deep magma reservoir and/or dynamic fluid circulation in the deep hydrothermal system. Two possible mechanisms of how fluid circulation could create pressure fluctuations are by self-sealing via mineral deposition or volumetric expansion and contraction of the crust. Our observations indicate a very robust hydrothermal-magmatic system.

## **SEISMIC IMAGING OF THE DOWN-GOING INDIAN LITHOSPHERE BENEATH CENTRAL TIBET**

*Frederik Tilmann\*, James Ni, and the INDEPTH Seismic Team Department of Physics, New Mexico State University, Las Cruces, NM 88003-8001 \*Now at: Department of Earth Sciences, Cambridge University, Cambridge CB3 0EZ, UK*

A tomographic image of the upper mantle beneath central Tibet from INDEPTH data has revealed a sub-vertical high velocity zone from 100 to 400 kilometers depth, located beneath central Tibet. We interpret this zone to be down-going Indian lithosphere. The additional Indian lithosphere discovered in this study accounts for most of the shortening in the mantle since the collision at ~50 Ma. Down-going lithospheric material inevitably drags neighboring asthenospheric material along. Combined with apparent southward-directed subduction along the northern margin of the plateau, which would likewise induce a downward flow, a deficit of asthenosphere would result, which must be counter-balanced by a focused upward-directed return flow. Such an upward flow provides an explanation for the low velocity body imaged beneath northern Tibet, and provides a mechanism for heating the crust and eroding the remaining lithosphere beneath northern Tibet.

## **ANALYSIS OF BROADBAND TELESEISMIC DATA IN LAS VEGAS VALLEY**

*Hrvoje Tkalčić and Arthur Rodgers Lawrence Livermore National Laboratory, L-206, Livermore, CA 94551 Catherine Snelson and Darlene McEwan Department of Civil and Environmental Engineering and Department of Geosciences, University of Nevada, Las Vegas, NV 89154*

Las Vegas is situated in a broad sedimentary basin in the Basin and Range Province. A model of the depth to basement was derived from gravity data. We are using newly acquired broadband seismic data to evaluate the basin model and estimate velocities of sedimentary fill. We collected data of recently recorded teleseismic events, to determine basin structure, site response and crustal structure.

Delay times of teleseismic P-waves show variation of up to 0.5 seconds across relatively short distances (15 km or less), providing some valuable information on basin shape and thickness. Teleseismic P-waves have good signal-to-noise for low frequencies (0.05-0.2 Hz) and this complements site response measured from regional earthquakes and explosions. Preliminary results for site response estimates from the teleseismic data show a good agreement with site response estimates inferred from the regional data. Furthermore, the measured amplitudes and P and S-wave energies for the recorded data have a potential to provide additional constraints in modeling the basin shape and structure.

Receiver functions will help constrain crustal thickness and shear velocities as part of a larger effort to build a regional three-dimensional model. This work is in progress.

## **HIGH SEISMICITY RATE IN BHUTAN BASED ON RESULTS FROM A LOCAL EARTHQUAKE SEISMIC NETWORK**

*A. Velasco, K. C. Miller, L. S. Hollister, D. Hernandez*

The Kingdom of Bhutan lies east of Nepal and south of Tibet in the Himalayas. We report preliminary results from a five-station network deployed as a pilot experiment to examine seismicity patterns and lithospheric structure in central and western Bhutan. The seismic stations, comprised of equipment from the PASSCAL instrument pool, were installed in January of 2002 in cooperation with the Geological Survey of Bhutan. The first six months of data have been processed and a preliminary catalog of local and regional events has been developed. Over six months, the network recorded over 1600 events, of which 642 events were regional/local events. The preliminary locations are not well constrained for events outside the aperture of the network, and preliminary magnitude estimates show significant microseismicity in the region, and some clustering of events. We will be working to improve these locations by obtaining supplemental data from seismic other seismic stations. From this work, we will attempt to identify the locations of seismogenic structures in the region. Further analysis will allow for lithospheric studies, including velocity model development and receiver function and shear-wave splitting analysis. With these new results, we hope to gain insight into the processes of crustal-scale deformation for this region of the Himalayas.

# **ANOMALOUS FAULT ZONE WEAKNESS FROM GEODETIC AND SEISMIC MEASURES; A CASE STUDY BETWEEN THE LANDERS AND HECTOR MINE RUPTURES**

*John E. Vidale, Yuri Fialko, Yong-Gang Li, Peter Shearer, Duncan Agnew, and David Sandwell, UCLA (vidale@ucla.edu), UCSD, USC*

Several very recent results suggest weakness, damage, and healing on the network of faults criss-crossing the Mojave desert in the area of the 1992 Landers and 1999 Hector Mine earthquakes. An examination with InSAR of anomalous gradients in the region within tens of km of the Hector Mine rupture shows concentrated shear and normal strain on several unbroken fault traces that occurred coseismically. The area around the Landers ruptures shows similar anomalous strains. In addition, the Landers and Hector Mines fault planes in places have distinct low-velocity zones (LVZ's), probably extending across the seismogenic depth range. Finally, the LVZ's recover some of their strength in the years after fault breakage and also after strong shaking, presumably restrengthening toward their condition prior to the recent earthquakes.

These hints suggest intermittently weak fault zones, reduced in velocity by 10-40%, and reduced in modulus by roughly 50%, which extend to 5 km depth or deeper. The geodetically inferred compliant zone appears to be about a km wide, whereas LVZs measured from fault-zone-guided waves are about 100 m wide. Intuitively, we expect that we are seeing a gradational rather than discrete weak zone, with the greatest weakness at the fault trace, and a reduction of weakness with depth. It is also possible that the low compliance seen with InSAR may be partly due to weakening from strong shaking.

We plan to conduct a pilot EarthScope study to systematically map the structural cross-section of the Calico, Rodman, and/or Pinto Mountain fault zones. All of these faults were observed with InSAR to anomalously strain in the Hector Mine earthquake. A combination of explosions recorded into profiles and fan-geometry seismic lines, passive monitoring for deeper structure, and exploration of geodetic observations would test and extend models of active faults. The spatial extent of fault weakness, and the loss and recouping of strength across the earthquake cycle are critical ingredients in our understanding of fault mechanics.

## **EARTHQUAKE APPARENT STRESS SCALING**

*William R. Walter, Kevin Mayeda, Rengin Gok, Jennifer O'Boyle and Stan Ruppert Earth Sciences Division Lawrence Livermore National Laboratory*

There is currently a disagreement within the geophysical community on the way earthquake energy scales with magnitude. One set of recent papers finds evidence that energy release per seismic moment (apparent stress) is constant (e.g. Choy and Boatwright, 1995; McGarr, 1999; Ide and Beroza, 2001). Another set of recent papers finds the apparent stress increases with magnitude (e.g. Kanamori et al., 1993, Abercrombie, 1995; Mayeda and Walter, 1996; Izutani and Kanamori, 2001). The resolution of this issue is complicated by the difficulty of accurately accounting for and determining the seismic energy radiated by earthquakes over a wide range of event sizes in a consistent manner. We have begun a project to reexamine this issue by analyzing aftershock sequences in the Western U.S. and Turkey using two different techniques. First we examine the observed regional S-wave spectra by fitting with a parametric model (Walter and Taylor, 2002) with and without variable stress drop scaling. Because the aftershock sequences have common stations and paths we can examine the S-wave spectra of events by size to determine what type of apparent stress scaling, if any, is most consistent with the data. Second we use regional coda envelope techniques (e.g. Mayeda and Walter, 1996; Mayeda et al., 2003) on the same events to directly measure energy and moment. The coda techniques corrects for path and site effects using an empirical Green function technique and independent calibration with surface wave derived moments. Our hope is that by carefully analyzing a very large number of events in a consistent manner using two different techniques we can start to resolve this apparent stress scaling issue.

This work was performed under the auspices of the U.S. Department of Energy by the University of California, Lawrence Livermore National Laboratory under Contract No. W-7405-Eng-48.

# SYSTEMATIC DETERMINATION OF EARTHQUAKE FAULT PLANES FROM A DIRECTIVITY ANALYSIS OF LONG-PERIOD SPECTRA

*Linda M. Warren and Peter M. Shearer*

Earthquake focal mechanisms resolve two possible fault planes. If the earthquake has a predominantly unilateral rupture, the pulse width will vary depending on the angle from the rupture direction, allowing the actual slip plane to be determined from a directivity analysis. We have developed a method to estimate the amount of pulse broadening from the spectrum and apply it to a long-period database of large, globally-distributed earthquakes between 1988 and 2000. We select vertical-component P waves at epicentral distances of 20-98 degrees. We compute the spectrum from a 64-s-long window around each P wave arrival. Each spectrum is the product of source, receiver, and propagation response functions as well as local source- and receiver-side effects. We correct each spectrum for the known instrument response, an average source model, and a 1D Q model. Since there are multiple receivers for each source and multiple sources for each receiver, we can approximate the source- and receiver-side terms by stacking the appropriate P log spectra. The resulting source-specific response functions include any remaining source spectrum and the effect of near-source attenuation in the upper mantle; the receiver stacks include the site response and near-receiver Q structure. We remove the appropriate source- and receiver-side stacks for each path, leaving effects from directivity and lateral variations in attenuation. We find that the directivity signal dominates. The spectrum is also affected by depth phases and core reflections. We model the effect of the later arrivals by making stick seismograms with the predicted arrival times and relative amplitudes of P, pP, sP, PcP, pPcP, and sPcP, and computing and analyzing the spectra in the same manner as for our observations. For shallow earthquakes, the signal predicted for the interference of other phases is of approximately the same size as our observed signal and, for many events, can be matched to the observed azimuthal variations by changing the earthquake depth. For deeper earthquakes, the depth phases arrive later relative to the direct arrival and we exclude records for which the depth phases arrive within the signal window. This depth constraint restricts our analysis to 66 earthquakes deeper than 200 km depth that are recorded at 25 or more stations. For each of these earthquakes, we plot our pulse-width estimates on the focal sphere along with the Harvard CMT solution. To determine the preferred slip plane for each earthquake, we test all possible rupture vectors that lie on one of the nodal planes by fitting a cosine curve to the pulse-broadening estimates. We take the plane containing the best-fitting rupture vector as the fault plane and use bootstrap resampling of the pulse-broadening measurements to estimate our confidence that this plane is the fault plane. In about 40% of the cases, one of the two nodal planes produces a much better fit to the data and can be identified as the true fault plane. Our results show good agreement with the known rupture directions and slip planes of recent earthquakes. The remaining earthquakes either have insufficient focal sphere coverage to determine if they are directive, are not directive, have a rupture direction near the intersection of the two nodal planes, or have complex rupture histories that interfere with determining the rupture direction.

## **AUTOMATED ANALYSIS OF SEISMIC DATA QUALITY AT THE DMC**

*Bruce R. Weertman Incorporated Research Institutions for Seismology, Data Management Center*

Real-time data that flows into the DMC is stored in a file system named BUD (Buffer for Uniform Data). We will present progress made on a new software system under development at the DMC for assessing the quality of waveform data flowing through the BUD. The system, named QUACK - Quality Analysis Control Kit, features a modular design that allows third parties to write software plug-ins that measure custom quality parameters. Currently two groups, (ISTI and the NEIC) are developing QUACK plug-ins for measuring power spectral density and timing accuracy. We will demonstrate two operational plug-ins, developed at the DMC, for measuring signal mean, variance and data availability. While initially implemented at the DMC, QUACK is portable and should be useful to other groups such as PASSCAL, GSN Data Collection Centers, FDSN Data Centers and regional networks

## REGIONAL LG ATTENUATION FOR THE CONTINENTAL UNITED STATES

*R.L. Wesson, D.E. McNamara, H. Benz and A. Frankel*

We have gathered nearly 4000 Lg paths from regional earthquakes, recorded at existing United States Seismograph Network (USNSN) and Advanced National Seismograph Network (ANSS) broadband stations at distances of 150 to 3000 km. Fourier amplitude spectra of Lg phases (windowed from 3.7-3.0km/s), recorded at high frequencies (0.5-16Hz), are used to determine regional frequency-dependent attenuation relationships across the continental US. We use SVD to simultaneously invert for Lg amplitudes to improve the regional estimation of Lg Q. Results from this study compare favorably with results from previous individual regional Lg Q studies and are valuable parameters for the US National Hazard map.

## **CRUST AND UPPER MANTLE SHEAR-WAVE STRUCTURE OF THE COLORADO PLATEAU, RIO GRANDE RIFT AND GREAT PLAINS**

*Michael West(1), James Ni(1), Scott Baldrige(2), Dave Wilson(3), Wei Gao(4), Rick Aster(3), Steve Grand(4), Steve Semken(5) (1) New Mexico State University, Department of Physics, Las Cruces, NM 88003 (2) Los Alamos National Laboratory, EES-1, Los Alamos, New Mexico 87545 (3) New Mexico Institute of Mining and Technology, Socorro, NM 87801 (4) The University of Texas, Department of Geological Sciences, Austin, TX 78712 (5) Dine College, Division of Natural Sciences, Shiprock, NM 87420*

We present images of the lithosphere and upper mantle shear velocity structure of the southwestern U.S. based on data from the LA RISTRA project—a two year broadband experiment using PASSCAL instrumentation. Rayleigh wave phase velocities are used to map the crust and upper mantle shear velocity structure to ~350 km depth across the 950 km array. Interstation rayleigh wave phase velocities are measured using 54 instruments distributed along a 950 km array. To minimize phase velocity errors, we find it is beneficial to include events which lie further from the great circle path than traditionally considered (up to 15 degrees). The range of backazimuths helps minimize the effects of multipathing. Independent receiver function results are used to constrain the depth of the sediment layer and crustal thickness. Phase velocities are then inverted for shear velocity structure of both the crust and mantle to a depth of ~350 km across the transect. The resulting velocity model reveals a unique crustal structure for each tectonic province. The region surrounding the Rio Grande rift is seismically slow throughout the crust, while the edge of the Great Plains has a thick fast lower crust. In the mantle, we find a sharp transition from the 200 km thick continental lithosphere of the Great Plains, to 45-55 km beneath the Rio Grande rift, thickening again beneath the Colorado Plateau to 120-150 km. The upper mantle signature of the rift is roughly twice the width of its surface morphology. An asthenospheric low velocity channel, likely the result of warm mantle infill behind the sinking Farallon plate, underlies the region west of the Great Plains and extends to 300 km depth. Buoyant forces associated with this channel are sufficient to support much of the high elevation of the rift and plateau. No evidence for a deep mantle source is found beneath the rift, implying that rifting is a response to lithospheric strain and is not driven by active mantle upwelling. Velocities 55-90 km beneath the rift axis are 10% slower than beneath the Great Plains, consistent with small amounts of partial melt. Low velocities extend to 200-300 km depth on either side of the rift but not directly beneath it, forming an “inverted-U” shape. This feature may reflect mantle that has cooled through passive upwelling, in a subadiabatic environment, in response to rifting and possible small-scale convection driven by variations in lithospheric thickness.

## **VERTICAL AND HORIZONTAL VELOCITY RESULTS FROM GPS IN RELATION TO MAPPED STRUCTURES, SOUTHERN TAIWAN**

*David V. Wiltschko, Center for Tectonophysics, Texas A&M University, College Station, TX; Jih-Hao Hung, Institute of Geophysics, National Central University, Chung-Li, Taiwan, ROC; Peng Fang and Yehuda Bock, Institute of Geophysics and Planetary Physics, Scripps Institution of Oceanography, University of California, San Diego, San Diego, CA.*

We have collected GPS data from the southern portion of the Taiwan fold and thrust belt in order to assess the kinematics of this fold and thrust belt on a structure-by-structure basis. Our data set includes over 1700 site-sessions at 145 sites in campaign mode and 14 local permanent sites.

The magnitude of the horizontal component of velocity ( $V_h$ ) systematically decreases from east to west with respect to cratonic Eurasia. As has been found by others, the azimuth of  $V_h$  rotates counterclockwise in going toward the southwest. Not all variations in velocity are associated with mapped major faults. The Central Range and Coast Range are converging across the Longitudinal Valley. The vertical component of velocity ( $V_v$ ) follows a different pattern. To the east of the Slate Belt-Western Foothills boundary, the orogen appears to be uplifting at a uniform rate, although not rigidly. To the west,  $V_v$  values appear to be controlled by local fault dip. Nearby thrust fault dip is a good predictor of surface velocity inclination. Within the Western Foothills  $V_v$  is highly variable in contrast to the slow spatial variation in horizontal velocity. Except for the plate boundary (Longitudinal Valley), strain rates are highest in the frontal fold and thrust belt. Significantly, all structures in the fold and thrust belt appear to be active, although some more than others. Strain rates are modest over the Central Range and extensional in nature in the southern Central Range. In addition, some strain nets straddling the Slate Belt - Western Foothills boundary indicate oblique extension. The strain pattern is consistent with model results which show that the hinterland deforms as a unit with over-all decrease in deformation toward the foreland.

We interpret these results to indicate that the depth of involvement of the deformation in the orogen deepens to the east (as would be expected) but changes character and perhaps deformation mechanism across the Slate Belt - Western Foothills boundary. Rocks moving by both folding and motion on thrust faults have a larger influence on surface motions from GPS in the west. The Slate Belt - Western Foothills boundary appears to mark a fundamental transition in present surface motions across Taiwan.

# RELOCATION OF HYPOCENTERS AND LOCAL EARTHQUAKE TOMOGRAPHY IN TAIWAN

*Francis T. Wu, SUNY Binghamton C.S. Chang, Y.M. Wu, Central Weather Bureau, Taiwan  
Harley Benz, USGS Antonio Villasenor, Utrecht*

The aftershocks of the 1999 Mw=7.6 Chi-Chi earthquake in Central Taiwan as well as the high level of ambient seismic activities provide a rich source of data for mapping seismicity and for local earthquake tomography. Using the double-difference method (Waldhauser and Ellsworth, 2000) ML>2 earthquakes under the island and parts of the eastern offshore area covered by the Taiwan seismic network were relocated. Phase and event locations in the Central Weather Bureau (Taiwan) catalog are used as input. While the seismicity under northern Taiwan suggest duplex plate structures in the Ryukyu subduction zone, offshore of southeast Taiwan, between the Hengchun Peninsular and the two volcanic islands, nearly vertical Benioff zone can be discerned. In Central Taiwan active upper crustal seismicity under the Western Foothills is juxtaposed with a nearly aseismic Central Range to its east. But a well-organized, steep west-dipping zone in the lower crust (20-35 km), next to the aseismic Central Range, shows that brittle deformation occurs in the lower crust as well. Coupled with focal mechanisms of the larger events determined by Kao et al. (2000) the dominant modes of deformation in the subduction zones and Central Taiwan can be mapped.

Using the local earthquakes as sources we have imaged the crustal and mantle structures under the island. By including the aftershocks of the Chi-Chi earthquake up to the end of 2002 the crustal structures under the Central part of the island are better illuminated. Employing a tomographic inversion code of Benz (Benz et al., ), with block size of 5 km x 5 km x 2 km, the subduction zones and the some details of the crustal structures emerge. The northern subduction zone is imaged generally as a high velocity zone but there are several overlapping structures. The Central Range is seen as a relatively high velocity zone at upper crustal depth (down to 16 km) and below that depth the velocities are low compared to those under the Western Foothills. The relative low can be seen down a maximum depth of about 52 km west of Hualian – indicating the maximum depth of the crust. The root is noticeably asymmetric, with a very steep boundary on the east and relatively gentle slope on the west.

The seismicity and tomographic images provide key constraints for the interpretation of the tectonics of Taiwan. The steep, west-dipping lower crust seismic zone, for example, is evidently associated with a high angle thrust that is responsible for the creation of the crustal root.

## References

Kao, H., Liu, Y.H., W.T. Liang, and Chen, W.P. 2002. Source parameters of regional earthquakes in Taiwan: 1999-2000 including the Chi-Chi earthquake sequence, *Terrestrial Atmosphere Ocean*, 13, 279-298.

Waldhauser, F. and Ellsworth W.L. 2000. A double-difference earthquake location algorithm: Method and application to the northern Hayward fault, *Bulletin Seismological Society of America*, 90, 1353-1368.

## RESULTS FROM LONG-BASE STRAIN MEASUREMENTS IN LOS ANGELES, CALIFORNIA AND YUCCA MOUNTAIN, NEVADA

*Frank. K. Wyatt, Stephen Dockett, and Duncan Carr Agnew Institute of Geophysics and Planetary Physics Scripps Institution of Oceanography University of California, San Diego*

We have recently increased the number of long-base strainmeters in the United States significantly, by constructing two new instruments. One is a 558-m laser strainmeter (GVS) in Los Angeles, built as part of the Southern California Integrated GPS Network (SCIGN), with backing from the Keck Foundation, Caltrans, and the City of Glendale. The other is a 405-m strainmeter (YMS) in the south adit of the Exploratory Studies Facility at Yucca Mountain, Nevada, constructed as part of the Yucca Mountain site characterization project with support from the Department of Energy. Both installations complement continuous GPS measurements in the surrounding area, by providing much

greater sensitivity to deformation at relatively short periods (hours to months). Both instruments include automated servo systems, web-access remote control, optical anchors, two-stage thermostatted optical tables, and a new design of stabilized laser.

The GVS instrument is in Verdugo Canyon by the side of the Glendale freeway, about 5 km south of the outcrop of the Sierra Madre thrust zone, in a region of posited NS compression: the strainmeter azimuth is N 14 deg E. The YMS instrument is mounted on the side of the tunnel, about 1200 m in from the south portal, with an azimuth of N 91 deg E; for this installation, the anchors extend horizontally rather than (as usual) vertically.

The YMS instrument began operation on August 29, 2002, and the GVS instrument eight days later. Both have run essentially continuously since that time (though with one major outage at GVS because of a storm knocking out the local power grid), and given good records of the short-term strain variations, despite some initial problems (unexpected misbehavior in copies of our standard electronics).

Both instruments provide good records of the tides, which agree with theoretical predictions to roughly 20%, the difference being most likely caused by the substantial topography around GVS and above YMS. Both instruments have also given good records of large earthquakes, including the Denali (Alaska) event in late 2002. The long-term strain rates, though not well-defined with the limited length of data available, are comparable to what is expected from geodetic measurements, and do not show any initial transients. We have seen two effects at these instruments not found in previous records. At GVS the south end, whose anchored monument is on shallow fill (about 3 m) shows very large thermoelastic signals, which, along with most of the meteorological effects, are removed by the anchoring to 20 m depth--though some residual remains, we suspect a genuine contribution from the motions of the nearby freeway (we do not have any difficulty with traffic-induced signals). The strain recorded at YMS shows a large correlation with changes in air pressure, something not found in surface installations; this appears likely to be strains induced by pressure changes on the tunnels.

In keeping with SCIGN data policy, all data from the GVS system are publically available, with a latency comparable to other SCIGN data. The YMS data, after being approved for Quality Assurance, are being deposited with the DOE/YMP Document Control Center.

# **MANTLE EARTHQUAKES BENEATH THE HIMALAYAN-TIBETAN COLLISION ZONE AND RHEOLOGY OF THE CONTINENTAL LITHOSPHERE**

*Zhaohui Yang and Wang-Ping Chen*

Recently, there is a renewed surge of interests regarding the mechanical strength of lithospheric mantle beneath continents – an issue that has far-reaching implications for understanding continental dynamics. For two decades, one of the key evidence for a strong lithospheric mantle is the occurrence of intra-continental earthquakes in the mantle, originally discovered beneath southern Tibet in 1981. To a large extent, recent debate on this issue hinges on whether both focal depths and crustal thickness are well enough determined in the same region to resolve if earthquakes near the Moho indeed occurred in the mantle. Here we present a significant amount of new data and a comprehensive compilation of focal depths, fault plane solutions, and crustal thickness in and around the Himalayan-Tibetan collision zone to show that there are a number of mantle earthquakes, reaching a body-wave magnitude of 6, beneath the western Himalayan syntaxis, the western Kunlun, and southern Tibet (near Xigaze). Frequent occurrence of intra-continental earthquakes in the mantle is strong, in situ, evidence that the lithospheric mantle is strong enough to accumulate elastic strain under geological strain rates.

## DRIP DRAG?

*George Zandt, Hersh Gilbert Department of Geosciences, University of Arizona, Tucson, AZ, USA  
Thomas J. Owens Department of Geological Sciences, University of South Carolina, Columbia, SC, USA*

The Miocene-Pliocene delamination of the southern Sierra Nevada batholith lower crust residuum and its sinking through the upper mantle provides an opportunity to investigate how a mantle downwelling (drip) viscously interacts (drag) with the overlying crust. Xenolith data, volcanism patterns, and seismic mantle tomography are combined to hypothesize a S- to SW-displacement of the delamination-induced drip by the background mantle flow. If this idea is correct, we would expect to observe a complex crust-mantle interaction zone along the drip drag track to the northeast of the current drip location at about 36.3N and 119.3W.

In 1997 a 24-station broadband array was deployed for 9-months in the southern Sierras between about 36N and 37.3N latitudes (CU-PASSCAL project, PI: Craig Jones). We used 34 teleseismic events ( $M > 6$ ) recorded by the array to generate a migrated stacked receiver function image to 100-km depth. The image reveals a heterogeneous and anisotropic structure in the crust-mantle depth range, but with three regions of distinctly different character. Directly to the east of the drip, a very high-amplitude Moho is observed with crustal thickness of 35 km beneath the Owens Valley and dipping westward to 45 km beneath the Sierra-Great Valley boundary. The amplitude of the Moho conversion diminishes westward and is absent beneath the portion of the current drip location that is imaged with the available data coverage. This area of diminished amplitude, or absent, Moho constitutes the second characteristic region. The third region is located NE of the drip and is characterized by a flat 48-km-deep converter beneath the Sierra Nevada. At the eastern edge of this region, the northward continuation of the bright Owens Valley Moho is observed at 35 km depth dipping westward beneath the Sierra Nevada to a depth of about 40 km before losing amplitude and vanishing. This Moho and the deeper 48-km discontinuity overlap over a narrow zone. By comparing the same images constructed separately with events from the SE and events from the SW, the 48-km discontinuity and portions of the bright Moho are shown to be anisotropic with NE-SW oriented fast direction.

We interpret this complex pattern of heterogeneous and anisotropic structures as a manifestation of the viscous coupling between a S-SW migrating drip and the overlying crust. The downward pull of the drip may explain the westward thickening of the Moho as well as the dynamic depression of the topography that dominates over the isostatic Airy effect. The strong coupling along the path of the drip drag thickens and disrupts the crust-mantle boundary and diminishes and eventually eliminates the Moho converter above the drip. The 48-km converter, located only to the NE of the drip, is interpreted to be a new Moho ( $< 3$  Ma) established by magmatic underplating associated with asthenospheric upwelling in the wake of the migrating drip. The NE-SW orientation of seismic anisotropy associated with the 48-km discontinuity and portions of the older, shallower Moho may be due to viscous shear with the drip and the SW-directed mantle wind. We conclude by suggesting that the drip drag effect may eventually reconcile a number of apparently disparate volcanic, tectonic, and geomorphic features of the southern Sierra Nevada and adjacent regions.

## **NETWORK INSTALLATION IN THE YANQING-HUAILAI BASIN, CHINA AND PRELIMINARY STUDY OF NATURAL AND MAN-INDUCED EVENTS**

*Rong-mao Zhou[1], Yun-tai Chen, Zhi-xian Yang[2], Chris Hayward[1], Mary Templeton[3], Brian Stump[1], Xiang-wei Yu, Shi-yu Bai and Xiang-tong Xu[2] ( [1] Southern Methodist University, Dallas, TX 75275-0395; [2] Institute of Geophysics, China Seismological Bureau, Beijing 100081, P. R. China; [3] IRIS-Passcal Seismological Instrumentation Center, Socorro, NM 87801 )*

The cooperative project "A comparative study of natural and man-induced seismicity in the Yanqing-Huailai basin and the Haicheng area " is being carried out by Southern Methodist University and Institute of Geophysics, China Seismological Bureau, China. IRIS PASSCAL Seismological Instrumentation Center provided STS-2 broadband seismometers and the new Quanterra Q330 digitizer and PB14 Baler recording systems. The geographic focus of this investigation is in the Yanqing-Huailai Basin around Beijing. In Fall 2002, an initial 5 stations deployment was deployed by people from all three institutions and in Spring 2003 another five stations were installed by the group at IGCSB. The data from the first 5 stations has been collected and exchanged among SMU, IGCSB and IRIS. Some local, regional and teleseismic events from natural earthquakes and man-induced sources have been well recorded and identified. Study of the seismic waves from these sources will provide a mechanism for understanding the local propagation path effects and constraints upon the dynamics of the source mechanism.

## **THE SAN ANDREAS FAULT OBSERVATORY AT DEPTH (SAFOD): TESTING FUNDAMENTAL THEORIES OF EARTHQUAKE MECHANICS**

*Mark D. Zoback (Dept. of Geophysics, Stanford University, Stanford, CA) Stephen Hickman and William Ellsworth (US Geological Survey, Menlo Park, CA)*

In the SAFOD experiment we propose to drill into the San Andreas fault at a site characterized by creep and regularly repeating small earthquakes near Parkfield, CA. The SAFOD experiment has two complementary sets of scientific objectives. First, we seek to constrain, through direct sampling and measurement, the many hypotheses that currently exist about the composition, state (stress, pore pressure, temperature, etc) and on-going physical and chemical processes in an active, plate-bounding fault zone. The second set of scientific objectives are related to establishment of a long-term observatory directly within the active fault to study the processes associated with initiation, propagation and arrest of seismic (and aseismic) rupture.

In addition to drilling through the fault zone and making a broad suite of geophysical measurements, we will sample a continuous profile of fault-zone rocks and fluids and measure stress and pore pressure conditions within the SAFOD borehole. In this manner, we will compare and contrast the state of stress, fluid pressure and mechanical properties within the currently active San Andreas fault zone with that of the adjacent crust. After the sampling and downhole measurements phases of the experiment, we will deploy a suite of seismic, strain, pore pressure and temperature monitoring equipment in the fault zone. We will then use these instruments to monitor directly the process of strain accumulation and release during the cycle of repeating microearthquakes and episodic fault creep as well as monitor any changes in pore pressure and temperature that might occur through time. We will also have the capability to directly observe the earthquake nucleation process in the very near field and address a number of outstanding questions about the dynamics of earthquake rupture.

In the summer of 2002, a 2-km deep pilot hole was drilled at the SAFOD site to test geologic models of the area and its suitability as a site for the SAFOD experiment and make initial measurements of stress, temperature and other parameters. At the completion of drilling, an array of seismometers was installed in the pilot hole from 1 to 2 km depth to precisely locate microearthquakes that will be targeted with SAFOD. The results of these experiments will be reviewed, especially in regard to their significance with respect to the scientific objectives of the main SAFOD drilling project.

## **Development of a New Broadband Optical Seismometer**

*Mark Zumberge and Jonathan Berger*

*Scripps Institution of Oceanography, University of California, San Diego*

*Erhard Wielandt*

*Institute of Geophysics, Stuttgart University, Stuttgart, Germany*

The mainstay observatory-class seismometers used by global networks for the past two decades are no longer manufactured and there is no other commercially available product of sufficient quality on the market today. For such quality instruments, the development risk is high, the development time long, and the market small and apparently not sufficient to provide commercial viability.

To meet the instrumentation requirements of global seismology, we have designed and built a prototype sensor that uses optical fiber interferometry to record the motion of an inertial mass. The use of optical fiber interferometry rather than traditional electronic displacement transducers affords significant advantages. Features of this broadband optical seismometer include:

- A linear, high-resolution displacement sensor;
- Displacement measurement referenced to the wavelength of light, providing continuous calibration;
- Increased dynamic range;
- Increased bandwidth;
- No electronics in the sensor — only optical fiber connection to the seismometer — eliminating heat from electronics in the sensor package and noise pickup from connecting electrical cables;

Smaller package — our design will be applicable to both vault and borehole installations and should be relatively easy to manufacture.

